Study of Sufficient Capacity Design in Next-Generation Optical Networks

by

Anjali Sharma

17104263

DEPARTMENT OF ELECTRICAL ENGINEERING

INDIAN INSTITUTE OF TECHNOLOGY KANPUR

January, 2023

Study of Sufficient Capacity Design in Next-Generation Optical Networks

A Thesis Submitted

In Partial Fulfillment of the Requirements

For the Degree of

Doctor of Philosophy

by

Anjali Sharma

17104263

under the guidance of

Dr. Yatindra Nath Singh

DEPARTMENT OF ELECTRICAL ENGINEERING

INDIAN INSTITUTE OF TECHNOLOGY KANPUR

January, 2023

CERTIFICATE

It is certified that the work contained in the thesis entitled "***Study of Sufficient Capacity Design in Next-Generation Optical Networks***" by ***Anjali Sharma*** has been carried out under my supervision and this work has not been submitted elsewhere for a degree.

12th **January, 2023**

(Dr. Yatindra Nath Singh)

Thesis Supervisor

Professor

Department of Electrical Engineering

Indian Institute of Technology Kanpur

Uttar Pradesh - 208016

India

DECLARATION

This is to certify that the thesis titled **Study of Sufficient Capacity Design in Next-Generation Optical Networks** has been authored by me. It presents the research conducted by me under the supervision of **Dr. Yatindra Nath Singh**.

To the best of my knowledge, it is an original work, both in terms of research content and narrative, and has not been submitted elsewhere, in part or in full, for a degree. Further, due credit has been attributed to the relevant state-of-the-art and collaborations (if any) with appropriate citations and acknowledgements, in line with established norms and practices.

12/01/2023

January, 2023

Signature

(Name: Anjali Sharma)

Programme: PhD

Department: Electrical Engineering

Indian Institute of Technology Kanpur

Uttar Pradesh - 208016

India

Synopsis

Name of Student: **Anjali Sharma** Roll Number: **17104263**

Degree for which submitted: **Ph.D.** Department: **Electrical Engineering**

Thesis Title: **Study of Sufficient Capacity Design in Next-Generation Optical Networks**

Name of thesis supervisor: **Dr. Yatindra Nath Singh**

Month and year of submission: **January, 2023**

Optical Networks, using Optical fibers as transmission medium, form the backbone of the World's communication infrastructure. The advantages of low attenuation, availability of colossal bandwidth and low cost-per-bit make it an ideal medium for communication networks. The Optical Fiber Networks (terrestrial and undersea) carry over 99% of Internet traffic and have always been known as a "Just Sufficient Capacity Network". A country's economy depends heavily on digital infrastructure, which in turn is dependent on the state of its optical network infrastructure. Consequently, the communication traffic in the core optical networks is increasing by 30-60% yearly. To match this exponential growth, efficient utilization of the available resources in the optical networks is critical. The other solution is to upgrade the network capacity by adding spatial dimensions. The upgrade of the network could be performed over a period of time to manage the costs without compromising the Quality of Service. Two possible technologies have been studied extensively over the last decade to push the capacity bounds of core optical fiber networks: Elastic Optical Networks and Space Division Multiplexed-Elastic Optical Networks.
The flexible spectrum grid, adaptive modulation formats, and Bandwidth Variable Transponders and switches enable 'Elastic Optical Networks'. The highlight of this technology is that the assigned optical channels are tailored according to the bandwidth requirement, leading to efficient usage of the available capacity. While providing spectral resources (subchannels) to the connection requests, Routing and Spectrum Assignment (RSA) must be performed with minimal resources. A few constraints on RSA are spectrum continuity

over path and contiguity over links. But stringent compliance of these constraints and the dynamic nature of the connection requests' arrival and departure leaves the available resources in a fragmented state. Sometimes, the resources are available, yet some of the incoming connection requests cannot use them due to non-compliance of the RSA constraints. This brings inefficiencies and unfair spectrum utilization even with the sufficiently available capacity. Effective fragmentation management techniques are to be used to mitigate the problem.

In the first work of the thesis, in **Chapter 2**, we propose a Vectored Fragmentation Metric (VFM), a network-wide measure, to find the fragmentation state of the spectrum accurately. The proposed metric utilizes both RSA constraints as independent contributing parameters. We study this metric for changing network traffic dynamics and present our findings using simulations. The fragmentation in the network spectrum is directly affected by the arrival rates of the connection requests, service times, heterogeneity in bandwidth demands and spectral resource utilization. The proposed VFM metric can also recognize the no fragmentation and relative fragmentation values appropriately. By using these parameters as variables, we establish the usefulness of the proposed metric as an appropriate fragmentation indicator.

In **Chapter 3**, we compare the proposed metric, VFM, with the existing fragmentation metrics in a fragmentation management scenario. We use a threshold-based defragmentation strategy to mitigate the severe long-term effects of fragmentation. The defragmentation is triggered using a pro-reactive approach, i.e., when the metrics cross the threshold values, or a connection is blocked. When a connection is blocked, the threshold levels are also updated before the defragmentation. This approach ensures that the spectrum with minimum fragmentation is maintained throughout the simulation. One observation is that the Adapted-VFM with proposed defragmentation scheduling uses a considerable fraction of the total simulation time. If the Fragmentation-Aware technique can control the blocking of the connections at lower traffic load, then it should be used to have a less complex system.

In **Chapter 4**, to avoid the time-consuming defragmentation process, we propose a penalty-based Fragmentation-aware RSA, where a penalty is imposed on the links if they cannot provide resources due to fragmentation. When a connection request arrives in the network, it searches for the least cost route and the required number of resources in a first-fit manner. Sometimes, the arriving connection request cannot find the needed spectral resources. The penalty proportional to the difference between Required Spectrum Slices and Available Spectrum Slices is levied on the links of the least-cost route. Future connection requests are expected to avoid these links with increased costs. We do not try to mitigate fragmentation but prevent it altogether, leading to a simpler operation. The proposed techniques have better connection request admissions and network resource utilization.

The EONs with 12.5 GHz sub-channels can contribute a 30% increase in the usable capacity after the deployment of relevant technology supporting equipment at the network nodes. But to further push the capacity bounds, using spatial dimension parameters is inevitable. In the second half of the thesis, we study the resource provisioning flexibilities in the spectrum extended to the spatial domain in Space-Division Multiplexed- Elastic Optical Networks (SDM-EON). SDM-EON can be enabled by either Multiple-fiber, Multicore Fiber (MCF), or Multi-mode Fiber. MCF technology is most promising because the transmission bandwidth can be multiple of the number of cores within a single fiber cladding diameter, fitting into the existing systems' spatial footprint. The MCF may have crosstalk impairments subject to the inter-core spacing and coupling between the cores. The resource provisioning problem becomes the Routing, Core and Spectrum Assignment (RCSA) issue for these networks.

In **Chapter 5**, we provide adaptive accommodation to connection requests considering all the impairments and route selection parameters: Link length, Fragmentation, Crosstalk and Spectral Resource Utilization in the links of the SDM-EON. The links' costs depend on the combination of all the parameters and their weights. The RCSA adaptively becomes a particular parameter-oriented as per the spectrum state. It ensures that whatever impairment might affect future performance should be dealt with first by increasing the weights of the relevant parameter. The blocking performance and network resource utilization are far better than the particular impairment-aware resource provisioning. But the network utilization is still limited to $60-65\%$ due to crosstalk considerations, leading to unusable capacity. At least one core's equivalent spectral resources become unusable.

In **Chapter 6**, we leverage the capacity loss due to crosstalk-aware methods in SDM-EON by marking them as redundant/spare resources to be used in case of any network link failure. The proposed work provides resilient resource provisioning with crosstalk considerations. We divide the available spatial resources (Cores) into Protected, Unprotected, and Dedicated Spare Core groups. The Dedicated Spare Core groups are connected to form protection cycles to provide the backup path. The proposed link protection method performs better than the robust Link-Disjoint Path Protection. Introducing resilience in the provisioning makes it a more reliable and efficient network system. Extensive simulations and substantial performance evaluation metrics support the findings for all the proposed works.

Finally, we summarize the thesis in the last chapter with emphasis on all the findings and their impacts. We also discuss the problems for further investigation.

Acknowledgment

Words often fail to express one's inner feelings of gratitude to their mentors and supporters. This journey of the Doctor of Philosophy could not have materialized without the constant support and kind words of people around me. Foremost, I am thankful and indebted to my thesis supervisor *Dr. Yatindra Nath Singh* for his valuable advice, constant encouragement, sincere support and patience. The discussions about research topics, different technologies, the universe, history, stories and sometimes movies encouraged me to appreciate life's little nuances and subtlety of logic.

I want to express my warm regards to *Dr. Shilpi Gupta*, *Dr. Rajshekhar Gannavarpu* and *Dr. Adrish Banerjee* for their kind inputs at various stages of the research work in Departmental Review Committee meetings and Seminars. I would also like to express my gratitude to *Dr. Pradeep Kumar K.* and again to *Dr. Yatindra Nath Singh* for laying down the foundations of the research through their courses. I would also like to thank all the instructors during TA duties and tutorship for their kind support. I want to thank the Department of Electrical Engineering, IIT Kanpur and the Ministry of Human Resource Development (MHRD) for providing financial support to pursue my PhD program.

I owe thanks to *Prof. Rachna Asthana* for her guidance and support. I owe great gratitude to my school teachers *Mrs. Kiran*, *Mr. Chetan Jain*, and *Mr. Anil Kapoor* for making Maths and Science so interesting for us. I wholeheartedly thank you all.

I want to acknowledge the administrative staff in the department, *Mr. G.P. Mishra*, *Ms Anuradha Pandey*, *Ms Chhavi Srivastava* and *Mr Ramkripal*, for making reimbursements, leave-related and other critical things easier for us.

I want to thank all the ACES 301 and 401 colleagues who helped create a good environment suitable for research activity. I thank and appreciate *Dr. Varsha Lohani*, for her help, support and suggestions in different collaborative works. A special thanks to *Dr. Pallavi Athe*, *Dr. Kumar Gaurav*, *Dr. V Sateeshkrishna Dhuli*, *Dr. Amit Vishwakarma* and *Rameshwar Nath Tripathi* for being kind and encouraging seniors when I joined the lab. I extend my gratitude to my peers in lab *Rashmi Kushwaha* and *Rahul Bhattacharyya* for enriching my research exposure. I am also thankful to *Baljinder Singh Heera*, *Ajeet Singh Shekhawat*, *Nagendra K Singh* and *Sobir Ali* for inspiring and fruitful discussions during different collaborative research works.

I extend my sincere thanks to other colleagues *Rahul Prakash Singh*, *Kumari Akansha*, *Amit Pandit*, *Akhilesh Patel*, *Paresh Upadhyay*, *Gunjan Bharti*, *Kunal Agham*, *Nidhi Singh*, *Suraj Kalakoti*, and *Ruchi Srivastava* for their cheerful and warm company. I thank the thesis proofreaders amongst you, but all errors remain mine. Thanks to all of you, the lab environment has always been positive, encouraging and driven towards excellence.

I sincerely thank all the GH-1 staff for making my stay at IIT Kanpur much more convenient and comfortable.

I want to express my sincere gratitude towards *Aditi*, *Moon Moon Bordeori*, *Shreyasi Som* and my other friends for being a constant pillar of support, for being patient with me and for keeping me grounded during my journey at IITK. I thank *Manas* for his kindness while listening to all my grumbles and disappointments and celebrating my little successes. Last but most importantly, I owe all I have achieved to my parents, my brother *Ashish*, who thinks my books' stack makes an excellent headrest, and *Simba*. I thank them for their unconditional love, utmost care, continuous support, and wholehearted blessings throughout my life. I would not be where I am without you people.

January, 2023

Anjali Sharma

Contents

List of Figures

List of Tables

List of Symbols

Symbol	Description
CW	Sub-channel bandwidth
$G(N,L)$	Graphs having N number of nodes and
	L number of bidirectional links
$G(V,E)$	Graphs having V number of vertices and
	E number of bidirectional edges
M	Modulation level
α	Contiguity Fragmentation
β	Continuity Fragmentation
β	propagation constant
κ	coupling coefficient
ω_{tr}	core pitch
BW_r	Required bandwidth
S_r	Required number of spectrum slices
C_l	Cost of the l^{th} link
D_l	Normalized length of the link l
FR_l	Fragmentation parameter of the link l
h	power-coupling coefficient
r_0	bend radius
RU_l	Resource utilization of the link l.
XT_l	Crosstalk parameter of the link l

Symbol	Description
w_h	Weight of the link length parameter
w_f	Weight of the fragmentation parameter
w_u	Weight of the link resource utilization parameter
w_{xt}	Weight of the crosstalk parameter

List of Abbreviations

Abbreviation	Description
AON	**A**ll-**O**ptical **N**etwork
AoI	**A**ge **o**f **I**nformation
APS	**A**utomatic **P**rotection **S**witching
AVFM	**A**dapted **V**ectored **F**ragmentation **M**etric
AW-DRA	**A**daptive **W**eights-based **D**ynamic **R**esource **A**ssignment
BV-OXC	**B**andwidth **V**ariable- **O**ptical Cross-**C**onnect
BVT	**B**andwidth **V**ariable **T**ransponder
DSC	**D**edicated **S**pare **C**ore **G**roups
DWDM	**D**ense **W**avelength **D**ivision **M**ultiplexing
EDFA	**E**rbium **D**oped **F**iber **A**mplifier
EON	**E**lastic **O**ptical **N**etwork
FIPP	**F**ailure **I**ndependent **P**ath **P**rotecting **p**-cycles
FM	**F**ragmentation **M**etric
ICT	**I**nformation and **C**communication **T**echnology
ILP	**I**nteger **L**inear **P**rogram
IXT	**I**nter-Core **C**ross**T**alk
LDP	**L**ink **D**isjoint **P**ath
MCF	**M**ulti **C**ore **F**iber
MGON	**M**ixed **G**rid **O**ptical **N**etwork
NGON	**N**ext **G**eneration **O**ptical **N**etwork

Abbreviation	Description
O-OFDM	**O**ptical- **O**rthogonal **F**requency **D**ivision **M**ultiplexing
OTN	**O**ptical **T**ransport **N**etwork
OXC	**O**ptical **C**ross **C**onnect
PDM	**P**olarization **D**ivision **M**ultiplexing
PWCE	**P**rotection **W**orking **C**apacity **E**nvelope
PWCE	**P**rotected **W**orking **C**apacity **E**nvelope
PWCG	**P**rotected **W**orking **C**ore **G**roups
QoS	**Q**uality of **S**ervice
RBESA	**R**outing and **B**est **E**ffort **S**pectrum **A**ssignment
RCSA	**R**outing, **C**ore, and **S**pectrum **A**ssignment
RMCSA	**R**outing **M**odulation **C**ore and **S**pectrum **A**ssignment
RSA	**R**outing and **S**pectrum **A**ssignment
RSA	**R**outing, **S**pace and **S**pectrum **A**ssignment
ROADM	**R**econfigurable **O**ptical **A**dd/**D**rop **M**ultiplexer
SBPP	**S**hared **B**ackup **P**ath **P**rotection
SDM	**S**pace **D**ivision **M**ultiplexed
SDN	**S**oftware **D**efined **N**etwork
SE	**S**pectral **E**fficiency
SF	**S**pectral **F**ragmentation
SpF	**Sp**atial **F**ragmentation
SSE	**S**patial **S**pectral **E**fficiency
TLBO	**T**eaching **L**earning **B**ased **O**ptimization
UPWCG	**U**nprotected **W**orking **C**ore **G**roups
VFM	**V**ectored **F**ragmentation **M**etric
WDM	**W**avelength **D**ivision **M**ultiplexed
XTA	Crosstalk **A**ware

Dedicated to My Parents,

Ranjana and Anil Kumar Sharma

Chapter 1

Introduction

> As the area of light expands, so does the perimeter of darkness - *Albert Einstein*

Human beings' ability to communicate in verbal, non-verbal, visual and written modes sets them apart from all other genera on our planet. Isn't it marvellous to see two people sitting at opposite ends of the world and communicating within a fraction of a second? We have come a long way from Stone Age to the Age of Information. The "art of sending messages" or simply "communication" comprises of passing some information between the sender and receiver. The sender and receiver could be separated by distance, time, or even generations. The journey from the stone inscriptions, cave paintings, fire signals, drum beatings, and paper letters to telephone calls, electronic mails, instant messages, and cloud-based services has resulted from sheer human persistence to communicate effectively and efficiently.

The Renaissance contributed much to the ideas that were more inclined toward what humans could do for themselves. The Industrial Revolution and the Age of Information resulted from deep scientific insights during the Renaissance. The optical telegraph in 1794 by the Chappe Brothers, the electric telegraph in 1837 by the inventors Sir William Fothergill Cooke and Sir Charles Wheatstone, and the wireless telegraphy in 1894 by Marconi are some important inventions that came out of all the revolutionary ideas. The telegraph was initially used to control railroad traffic and broadcast news and messages. New variants and devices, like the telephone, kept appearing in different parts of the world, leading to the telegraph's continuous evolution and the Age of Information.

Age of Information (AoI) started in the 1950s with the primary objective of using Information Technology (IT) in economic developments. The developments of transistors led to the onset of AoI and formed the backbone to support computing and communications technologies. Other than electronics and devices, in the initial years of AoI, using electromagnetic waves of high frequencies as the carrier waves for the information was researched extensively. The most famous communication technologies at that time were Microwave and optical communication systems having carrier frequencies in the $1 - 100$ GHz and $10^4 - 10^9$ GHz regions of the electromagnetic spectrum, respectively. Of the two, optical communication systems mostly carry the signal over a guided optical fiber medium. They have evolved tremendously and currently carry more than 99% of the world's Internet traffic on land terrains and undersea. In the next section, we present a brief overview of the evolution of optical communication networks, followed by design issues in managing and using such large-scale networks.

1.1 Evolution of Optical Fiber Communication Networks

Over five decades of the evolution of telecommunication networks, the transportation capacity of the transmission medium has grown from a few Mbps to a humongous Pbps per fiber-km. There are three known generations of legacy telecommunication networks. First-generation network links were copper-based and used microwave technology. The transmission and switching of the information signal were in the electronic domain. Second-generation networks used optical fibers in place of copper and microwave links. The data transmission was in the optical domain, but the switching required optical-electronic-optical conversions. At that time, using optical fibers in communication networks required the mitigation of fiber-associated losses. The repeaters were placed every 10 km to mitigate the fiber losses and maintain the signal. In 1970, three Corning scientists achieved the feat of reducing fiber losses below 20 dB/km in 630 nm wavelength transmission region,

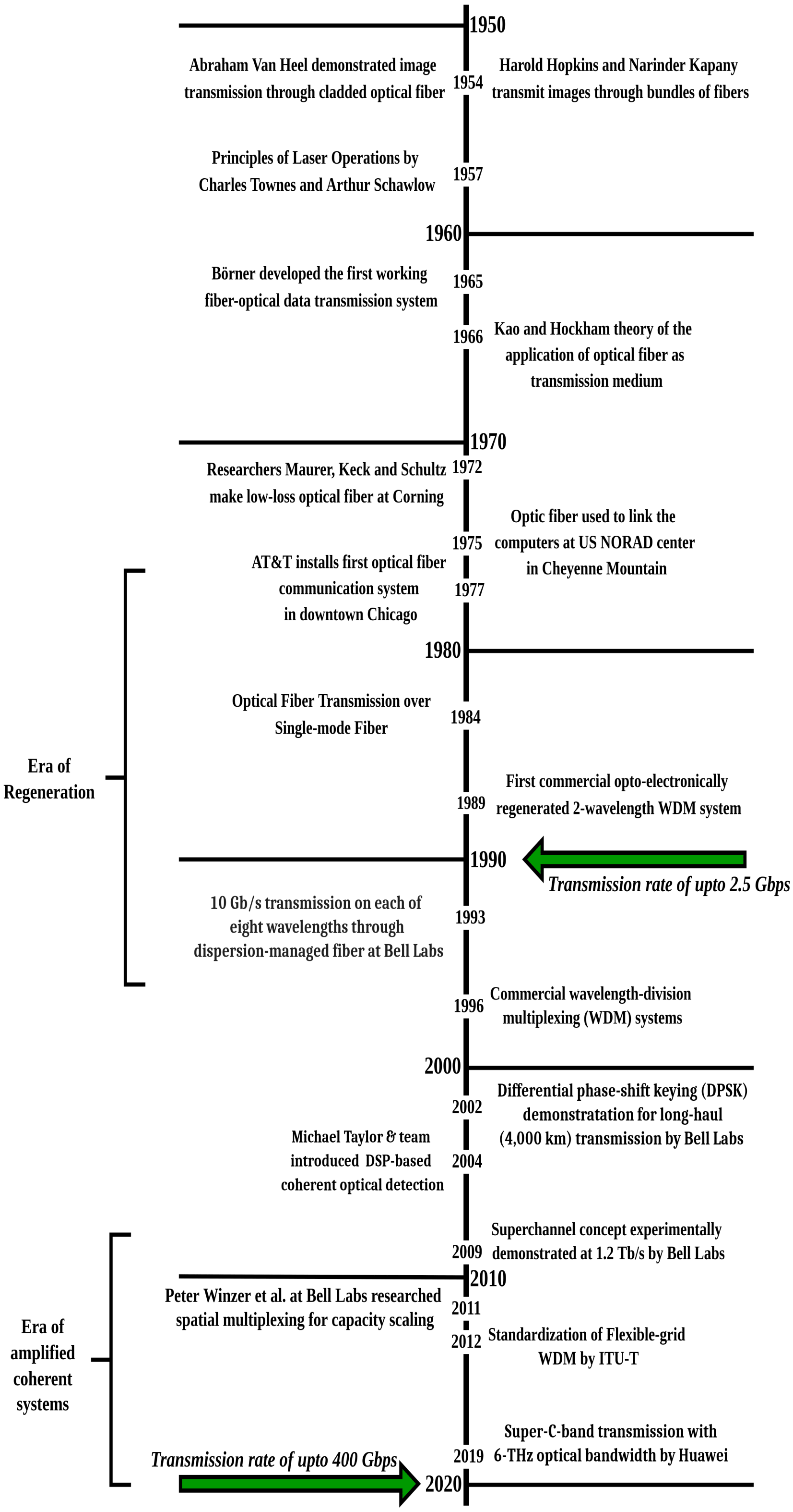

Figure 1.1: Some of the Key Milestones in the evolution of Optical Network Technologies, [1]-[13]

[4]. In 1979, a Japanese group further reduced the losses to 0.2 dB/km in the 1550 nm wavelength transmission region, [5]. Current optical network technologies are the scion of the third-generation legacy networks. The transmission and switching are in the optical domain with 1550 nm systems, making it an All-Optical Network (AON). The repeater spacing was further pushed to 50 km, which then made the Optic Fiber Communication systems economically viable.

The fourth-generation networks used concepts like Wavelength Division Multiplexing (WDM), Erbium Doped Fiber Amplifiers (EDFA), and Reconfigurable Optical Add/Drop Multiplexers (ROADM) for further more efficient use of available resources and reduction in cost per bit. WDM technology ensured that existing fiber could have more capacity with viable network applications and could be used more efficiently without laying more fibers. Statistical multiplexing, where the resources are used as per need, was used to achieve the objective, as mentioned before. The 1980s was the decade of extensive research in WDM technologies, starting with a simple two-wavelength WDM system, [6]. In WDM, the data is transmitted over multiple wavelengths (lightpaths [1]) in an optical fiber medium. WDM facilitated joining multiple wavelengths before transmission using Multiplexers (Mux) and then separating them at receiving end using Demultiplexers (DeMux). During the 1990s, the WDM technology was researched together with periodic amplification and periodic dispersion compensation to boost the usable capacity and increase the regenerator spacing.

In the 1990s decade, WDM technology was a boon for the telecom industry, and the demand and supply for related systems resonated. The popularity of the Internet and the world wide web further fuelled the bandwidth requirement, hence more demand for WDM technology systems, creating a telecom bubble. The two market crashes and the subsequent "Telecom Bubble Burst" in the 2000-2009 decade were not good for the telecommunications industry. The supply was more than the demand, and the research and development of such systems were slow and not very promising.

During market plunges in the 2000s, economic considerations required repeater placements to be further reduced without compromising on the quality of transmission. Coherent de-

[1] lightpaths, routes, paths terms are used synonymously

tection of amplitude and phase at receiving end constituted the primary research goals in the fifth generation of optical networks. Further, the availability of coherent designs led to the investigation of adaptive modulation formats in which the messages are encoded in amplitude and phase of the signal. Coherent detection, adaptive modulation formats, and digital signal processing techniques helped achieve distortionless operations and more spectral efficiency, that is, more information in a given capacity. *Spectral efficiency* can be formally defined as the amount of information transmitted per second in 1-Hz bandwidth. Optical networks have significantly evolved from spectral efficiency of 0.05 bit/s/Hz to 10 bit/s/Hz. Currently, a maximum spectral efficiency of 16 bit/s/Hz can be achieved using Polarization-Division Multiplexing (PDM). The available bandwidth, which is actually usable in a silica optical fiber is 100nm in the 1550nm region. It adds up to an available capacity of 12.5 THz. Together with PDM, the maximum optical channel rate is 199.4 Tbps. This capacity was considered sufficient not long ago, but the recent paradigm shift in Internet-driven applications tells a different story.

1.2 Towards Sufficient Capacity using Next Generation Optical Networks

So far, the Core Optical networks have been considered a "Just Enough Capacity Networks". Ever since 2010, the crippling dependence of the World economy and communication on the Internet has led to more capacity demand. To further push the capacity, one option is to keep improving the spectral efficiency, and the other is to deploy more fibers in the network. These two possibilities have been researched extensively in the last decade. They are called Next Generation Optical Networks, as most of their enabling technologies are in experimental or lab setup stages. The first technology needs the upgradation of network nodes to support a flexible-grid optical network. It allows the tailoring of optical channels as per the connection request's requirements, which results in considerably decreased wastage of spectral resources. The second technology needs the upgradation of optical fiber links, which can linearly increase the available capacity. However, there are some associated non-linearities which limit the functional capacity. These two technologies are briefly explained in Figure 1.2. A detailed explanation is covered in the following sections.

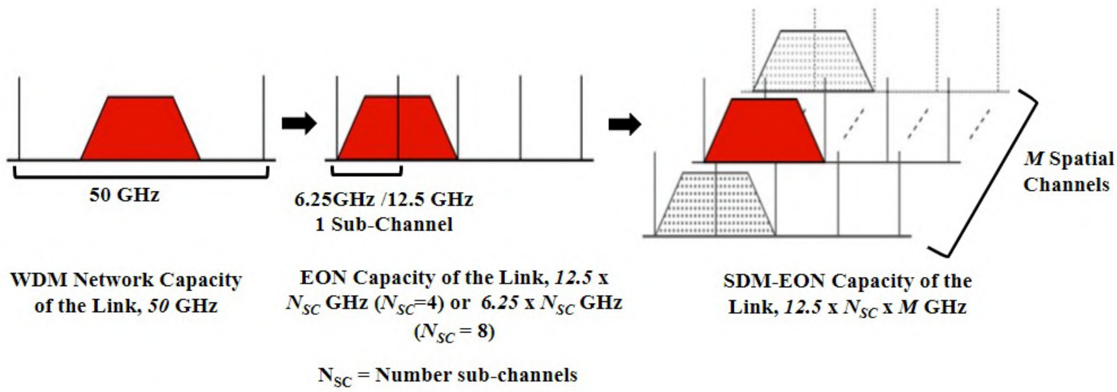

Figure 1.2: Spectrum Usage over an optical link in (a) Traditional Fixed-Grid with 50 GHz width of a grid, (b) Flexible-Grid having sub-carriers of 12.5 GHz/ 6.25 GHz width, and (c) Flexible-Grid extended to Spatial dimension, with a theoretical capacity of M x Total capacity of EON.

1.2.1 Elastic Optical Networks

The increasing demand of bandwidth is now fast outstripping service providers' best efforts to supply it. When service providers aimed to go beyond 100 Gbps and up to 400 Gbps transmission rates, it became challenging to fit such spectrally broad requirements in a 50 GHz ITU-T grid using standard modulation formats. The higher modulation formats can support limited distance transmission. Also, traditional WDM- optical networks have large spacing between adjacent channels (50 GHz or 100 GHz) specified by International Telecommunication Union (ITU-T) standards. If there is a low-traffic demand, after resource allocation, most of the channel space lies vacant. There is considerable wastage of spectral resources. The removal of this particular limitation can lead to improvements in efficiency, bit rate, and energy saving. Then came the Flexible-Grid concept, in which the spectrum needs are met by concatenating multiple closely spaced sub-channels. It provides the advantages of efficient spectrum utilization and minimum regenerations (multiple modulation formats). ITU-T G.694.1 recommendation provides a spectral grid for DWDM applications [11]. The second and third editions of the same recommendation include definitions for a flexible DWDM grid. The ongoing advancements in device technologies present optical networks as a large pool of shareable resources. The Bandwidth Variable Transponders (BVT) and Bandwidth Variable Optical Cross-connect Switch (BV-OXC) enable flexibility in bandwidth allocation by which it is possible to accommodate variable bandwidth connection requests. The fine granularity of such sub-channels can provide high spectral efficiency. The feature that truly makes it an Elastic Optical Network (EON) is the flexibility to adjust the allocated bandwidth in real time. This thesis uses the terms Elastic Optical Networks and Flexible Optical Networks synonymously.

The main characteristics of EONs are Bandwidth Segmentation, Bandwidth Aggregation, and Mixed and Reach-based accommodation. Using Segmentation characteristics, EON provides a fractional bandwidth connection to an optical path between a node pair. If only partial bandwidth is required, EON can provide enough bandwidth using a sub-channel without excessive wastage. To meet the increasing traffic demands beyond a specific limit, EON enables the aggregation of multiple sub-channels, which are multiplexed to provide a super-wavelength channel. Additionally, overlapping sub-channels using the Optical-Orthogonal Frequency Division Multiplexed (O-OFDM) system could improve spectral efficiency. The optical signal could deteriorate over long distances, so using higher modulation formats for spectral efficiency may not be necessary. The appropriate sub-channels and modulation formats can be allocated to ensure the most optimum utilization of resources in EON.

Resource provisioning is a crucial research domain in EON, as it should judiciously use the available spectral resources. The EON is generally represented by a Graph having a few nodes, and the optical fiber links connecting the nodes. When a connection request arrives in the network at a node, a communication path to another node need to be setup using the available network link resources. The resources in the EON links are the spectrum slices/slots (SS) or sub-channels allocated to incoming connection requests. Before resource assignment, the required bandwidth (BW_r) is calculated in terms of required number of spectrum slices (S_r) using the modulation level (M) and the sub-channel bandwidth (CW),

$$S_r = \frac{BW_r}{CW * M} \tag{1.1}$$

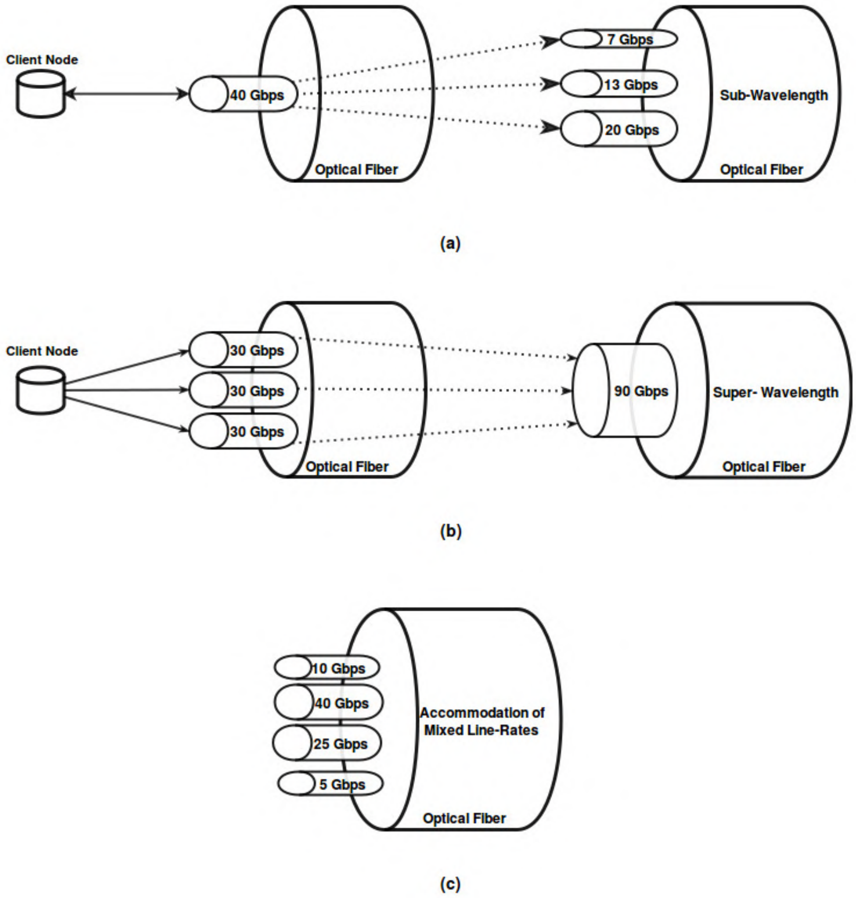

Figure 1.3: Some main characteristics of Elastic Optical Networks (a)Bandwidth Segmentation (b)Bandwidth Aggregation (c) Accommodation of Mixed Line Rate.

Routing and Spectrum Assignment (RSA) techniques are used to find a suitable path over network links for a connection request between two endpoints (nodes). Appropriate modulation level is selected as per the total length of the selected path. Then, the RSA finds the available S_r in a contiguous (the spectrum slices share boundaries) and continuous manner (same spectrum index range) throughout the end-to-end path. Consider the scenario as shown in Figure 1.4 (a)-(c). If the spectrum slices satisfying the constraints are available, the connection request is provisioned and set up as in Figure 1.4(b). However, in Figure 1.4(c), a connection request for two slices from node N1 to node N4 cannot be set up. More than two slices are available in each of the individual links, i.e., A, B, and C, and still, due to spectrum assignment constraints, the request cannot be satisfied.

When the connection requests arrive and depart in a highly dynamic manner, and there is

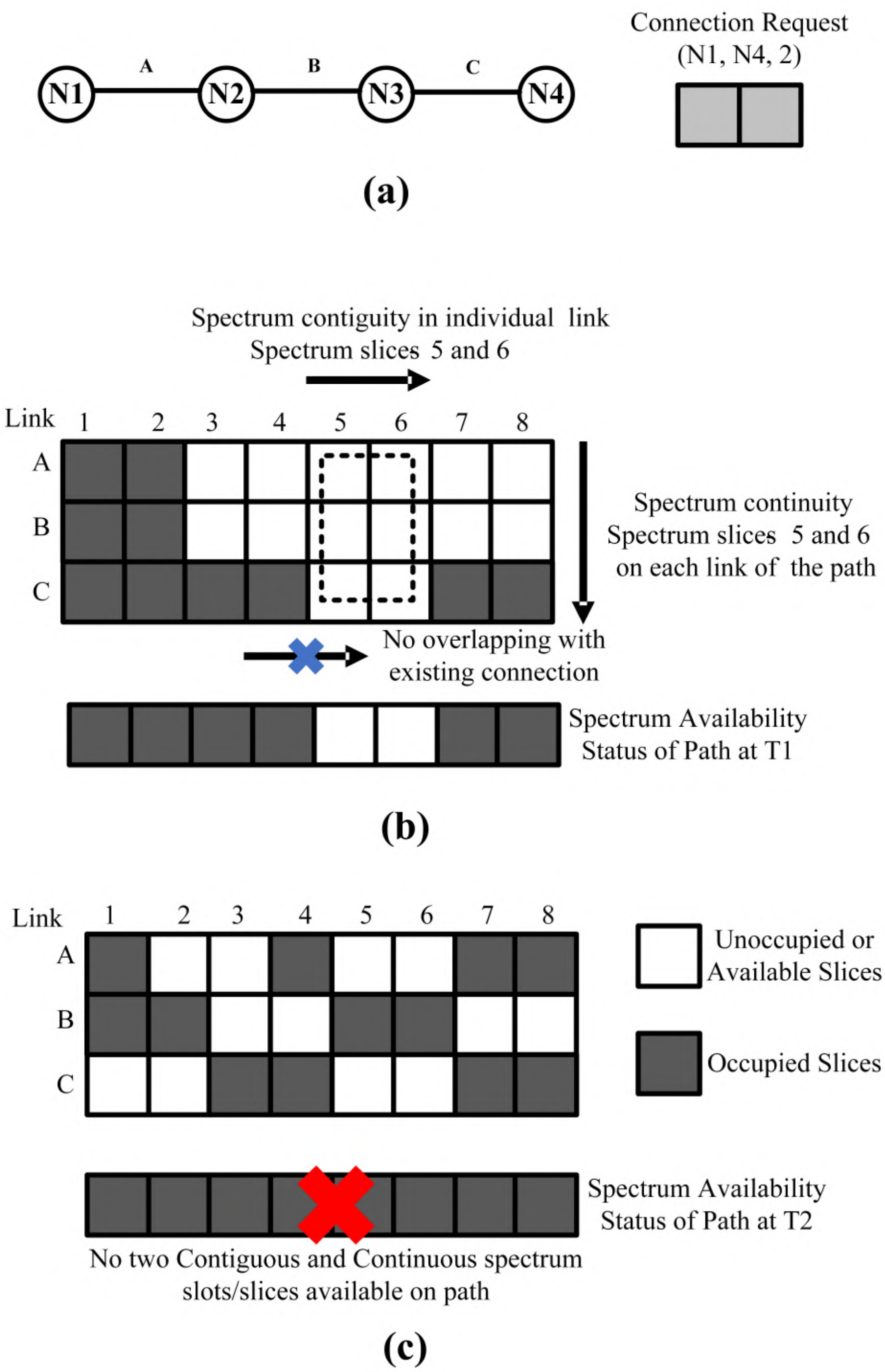

Figure 1.4: (a) A connection request between N1 and N4 with two SS requirement. (b) Spectrum scenario at time T1, and the slot on the path complying with the continuity constraint, (c) Non- availability of slices for the same connection request at another time T2 due to Fragmentation.

a strict imposition of spectrum assignment constraints, there arises an inefficiency called Spectrum Fragmentation. Fragmentation is due to the non-availability of the available spectrum slices as per the routing constraints in the links of candidate paths. The Frag-

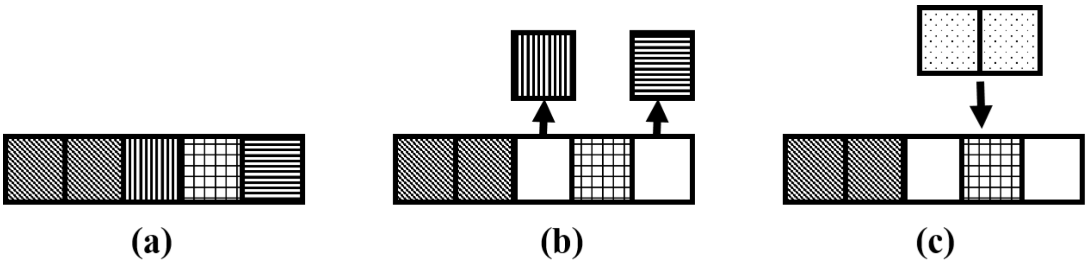

Figure 1.5: (a) Connection requests occupying spectrum resources at a time t_1, then (b) two connection requests depart at t_2, two spectrum slices become available. (c) A new connection request with two spectrum slice requirements arrives at t_3 but cannot be accommodated as available resources are not contiguous.

mentation degrades the network performance resulting in an increased blocking probability of connection requests. It also leads to unfairness towards the connection requests with higher SS requirements, as the connections with fewer SS requirements are more likely to find resources. In Figure 1.5(c), we can see that a connection request with two spectral resource requirements could not be fulfilled in the fragmented spectrum scenario. However, if a single spectral resource is required, two connections could be accommodated simultaneously. The time to find spectral resources also increases in a fragmented scenario, and there is no surety of whether connection requests will be provisioned.

To better understand the problem and find the remedial approaches for Fragmentation, studying the factors causing or affecting Fragmentation in the network spectrum is imperative. A brief literature survey of Spectrum Fragmentation and its management in RSA is given in table 1.

EON's characteristics make it a capacity-rich and robust system for future optical networks, and gradual deployment of EON requires the upgradation of WDM nodes (source, sink or transit). A projected traffic forecast is used to decide on the migrating nodes cost-efficiently. A multi-step network upgrade approach should be structured and interoperable with existing node technology. The upgradation steps would lead to Mixed-Grid Optical Network (MGON), where a few nodes are flexible-grid, and others are fixed-grid compliant. The nodes for the upgradation are selected to increase network efficiency while

Table 1.1: Literature Survey of Design Issues in EON

Issues/Aspects	Design Parameter	Techniques and Findings	Ref
Routing and Spectral Assignment	Route Selection	Accommodate the connection requests as per the fragmentation status of the links in the selected path	[33],[34],[35] and [36]
	Spectral Resource Assignment	Spectral resources selection as per constraints. Computation complexity increases with the dedicated techniques (Exact Fit, First-Last-Exact Fit)	[46], [47], [48]
Analytical Modeling of Spectrum Fragmentation	Unfairness in resource provisioning	Single channel and super-channel provisioning to evaluate the Fragmentation in the single-link spectrum. Superchannel requests' blocking is more in both analytical and simulation model	[27, 28]
Fragmentation Metrics	Link-Level	These metrics tend to ignore small fragments and cannot differentiate between various spectrum scenarios in individual links.	External [42], Shannon entropy [42], Access Blocking probability [42], Utilization Entropy [43], High-slot mark [43] and Spectrum Compactness [44]
	Path-Level	Uses Wasted-Unused-Free Ratio of the spectrum slices to inform about the loss of the effective number of spectrum slices due to fragmentation	[49]
	Network Level	Link consecutiveness aspect in all the links consolidated to decide on a network's fragmentation level.	[50]
Fragmentation Management	Fragmentation-Aware Approaches	Employed before the onset of the Fragmentation. Operational and computation cost is low.	Spectrum partitioning [29], Multipath [30], Multigraph [42]
	Defragmentation:	Reorganization of active or selective connections in a fragmented state. Rearrangement is of the current path or occupied spectral resources. Computationally complex.	Proactive and Reactive defragmentation[39], [40], ([41])[26], [42], [37], [44],

maintaining the Quality of Service (QoS) until the next migration step.

Another way to increase the capacity is to activate already deployed dark optical fibers. However, it may increase the overall cost linearly because of the added costs of amplifiers, transceivers and power consumption. Migrating to EON first, then enabling the Spatial dimension should be recommended as it will take less time to upgrade a node than digging and replacing the fibers buried deep into the ground or subsea.

1.2.2 Space Division Multiplexed- Elastic Optical Networks

SDM-EON can lead to a significant capacity increase using suitable spatial channels, i.e., core-based, mode-based or both. The spatial dimension can be exploited in resource provisioning to increase the upper bounds of the capacity of the optical networks. SDM-EON can simultaneously set up several connection requests in the same fiber and spectral range by using different cores or modes. The SDM-enabling fibers have multiple cores or support multiple modes. EONs, having a flexible grid, can itself provide up to 30% additional capacity itself, [67]. The flexibility in spectral and spatial domains can increase the optical fiber cable capacity manifolds. An optical network with bundles of single-core fibers or multiple fibers (MF), Multi-Core fibers (MCF), and Multi-Mode fibers (MMF) enables the usage of spatial dimension [17]. The cross-section of the multiple and multi-core fibers is shown in Figure 1.6. The spatial parameter to choose for a particular application is limited by fiber length, transmission reach and other impairment factors.

The subsea optical network cables currently use up to thirty-six fiber pairs, which makes it MF-SDM. The owners use a fraction of these fiber pairs, and the rest are leased to generate revenue from the infrastructure. The usage of MF-SDM leads to a linear increase in the number of optical components, and from an energy consideration perspective, it might not be an efficient technique. Multi-mode Fibers with a single core (MMF) have been researched since the early 1980s, however, they have a short transmission reach because the spatial parameters become coupled and lead to signal degradation over longer distances. Additional signal processing techniques at the receiver end need to be employed to remove the signal degradations in MMF-SDM. It is still a cheaper and more energy-efficient SDM technology option than MF-SDM.

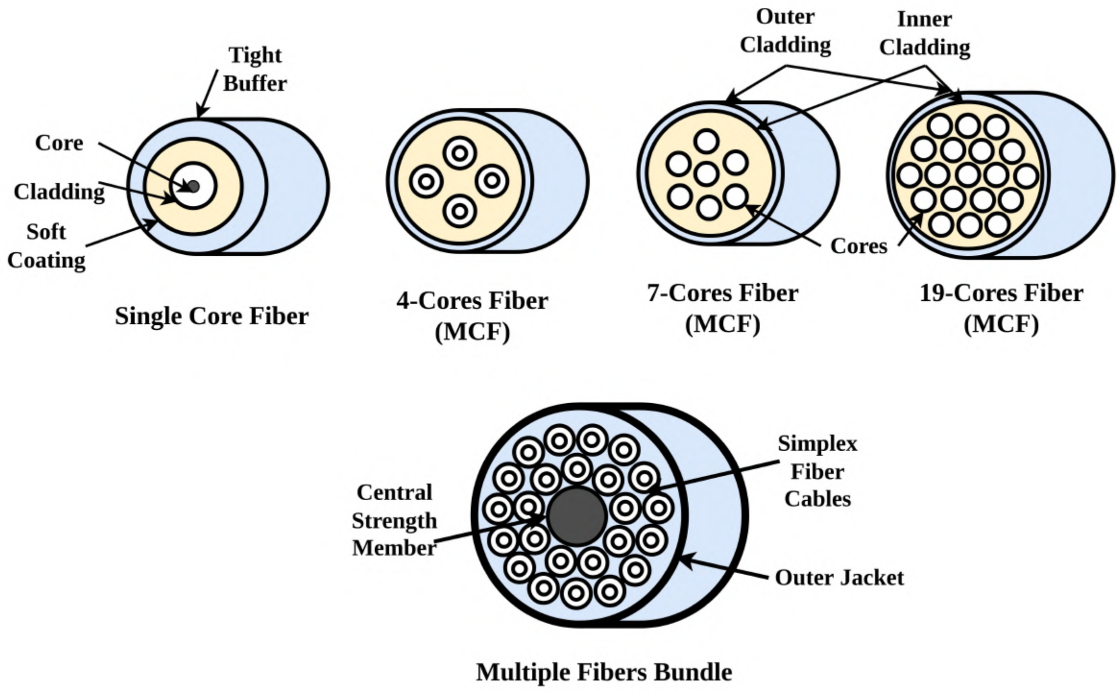

Figure 1.6: Various Optical Fiber Types

Multi-core Fibers (MCF) have several distinct cores sharing a common cladding, and the cores are coupled variably. The MCF can have Coupled Cores, Uncoupled Cores or Weakly Coupled Cores, depending on the power-coupling coefficients, core positioning and pitch, and the cladding dimension. In weakly coupled and uncoupled MCF, the cores are placed sufficiently apart to minimise inter-core interactions, and the available capacity is almost proportional to the number of cores in the MCF. The coupled MCF has a smaller core pitch, leading to a strong interaction between the signals in the adjacent cores. These interactions are called Inter-Core Crosstalk (IXT), which gets accumulated over distance and gives a deteriorated signal at the receiver side. The IXT is the ratio of the optical power leaked from the adjacent core towards the core under observation and the actual optical power levels in the core under observation. The formula of the IXT in a core is as follows.

$$IXT = \frac{n - n.exp(-(n+1).2.h.L)}{1 + n.exp(-(n+1).2.h.L)} \tag{1.2}$$

$$h = \frac{2.\kappa^2.r_0}{\beta.\omega_{tr}} \tag{1.3}$$

Here, L is the length of the link l, h is the power-coupling coefficient, κ is the coupling coefficient, r_0 is the bend radius, β is the propagation constant and ω_{tr} is the core pitch, and n is the number of cores adjacent to the core under consideration [17].

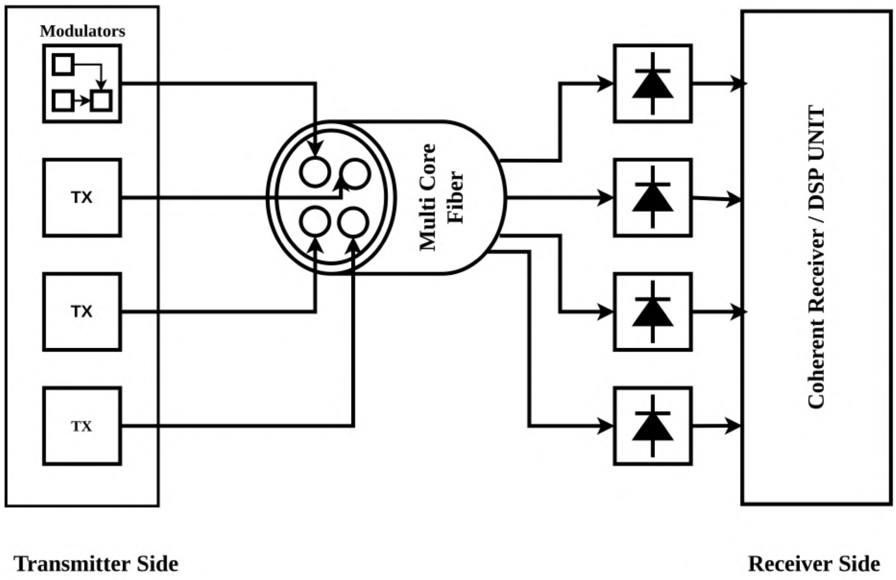

Figure 1.7: Basic Schematics of the MCF-based SDM optical network system

Most of the recent research and developments in MCF designs have been directed towards putting more cores within the given cladding dimension to increase the capacity of a single MCF while minimizing the crosstalk values. The basic schematics of a MCF-based system is shown in Figure 1.7. To achieve the objective, heterogenous cores, trench-assisted cores, increasing the dimension of cladding, and circular design of core arrangements to increase the core pitch have been proposed. Each of the proposed techniques has some pros and cons. It is observed that increasing the cladding diameter may lead to an increase in the probability of fiber link failure and a decrease in fiber splicing accuracy [18]. Also, the heterogeneous core can face inconsistencies and flaws in the fabrication process. Most of the studies and experiments on the remedies mentioned above, have been limited to simulations and lab testbeds.

To summarise the above discussion, weakly coupled or uncoupled MCFs can be a better approach for small-scale deployment and testing of the MCF-enabled backbone optical networks. In 2019, a 6.29 km long Multi-core fiber testbed was deployed in L'Aquila, Italy, under the INCIPICT project. The MCFs used in the testbed were Randomly Coupled 4-Core Fiber, an Uncoupled 4-Core Fiber and an Uncoupled 8-Core Fiber [19]. The installation was successful without significant attenuation and Crosstalks in the deployed fibers.

In coupled SDM-EON, weakly or strongly-coupled, Crosstalk-aware resource provisioning

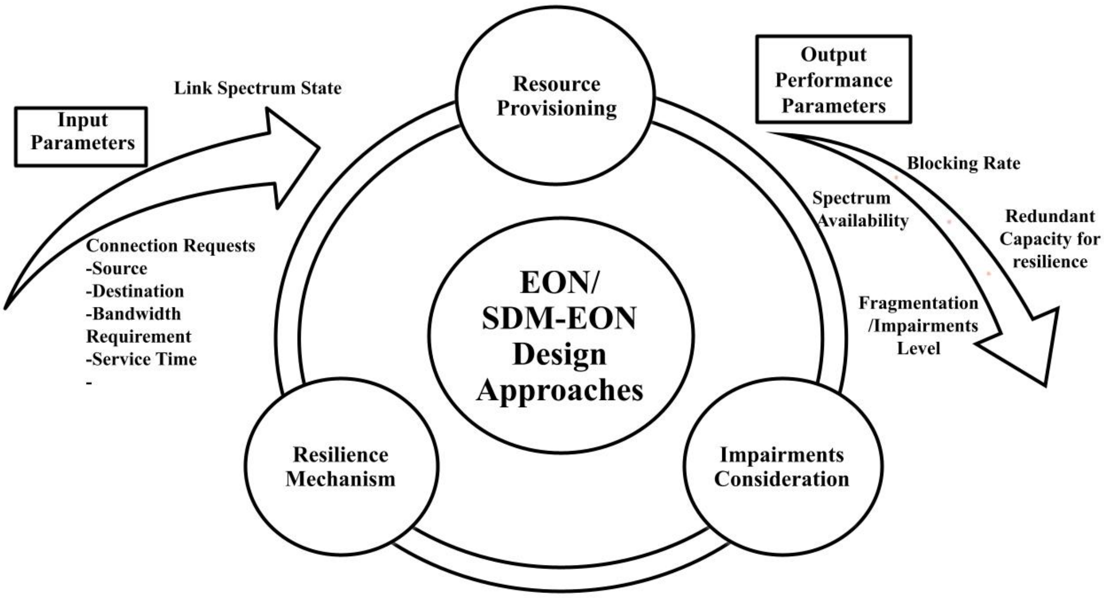

Figure 1.8: Network Design Approaches in EON and SDM-EON

with appropriate modulation formats is needed. The adaptive modulation formats facilitate coherent long-distance transmission by avoiding signal degradation and obtain better spectral efficiency. The resources in SDM-EON are the spatial parameters (cores) and the spectral parameters (spectrum slices/slots). The resources allocated to the connection requests arriving in the MCF-based SDM-EON are the spectrum slices in one of the cores of the MCF link in the network. Hence, the resource provisioning is three-dimensional in SDM-EON, i.e., route, core and spectral slots. A suitable route, core, and modulation format are selected to find the appropriate spectrum slices, making it a Routing, Modulation, Core and Spectrum Assignment (RMCSA) problem. Just like in EON, some constraints are associated with the RMCSA problem: Spectrum Contiguity in the links, Spectrum continuity in the links of the paths, and Space/ Core continuity in the cores of the links of the selected path. Crosstalk constraint could also be added if the used MCF has coupling among the cores (weak or strong). The awareness about crosstalk could be used at any sub-problem stage of the RMCSA. For example, after finding the shortest path and modulation format, the core with the least crosstalk value is selected. Then the first-fit spectrum allocation is performed in the selected core. The other way is to make first-fit core selection and then crosstalk-aware best-fit spectrum allocation. The computational complexity associated with them vary and both of them have been investigated extensively in literature.

In SDM-EON, the crosstalk-aware (XA) provisioning could lead to severe spectral Fragmentation. The XA techniques, require the spectrum slices to be occupied in such a way, that the same spectrum slices in the adjacent cores are not occupied. This leads to spectral fragmentation in the adjacent cores. The crosstalk awareness reduces the available capacity by a significant amount. A solution to this problem is to employ crosstalk threshold-based provisioning. Such techniques allow crosstalk in the cores up to some tolerable levels. Then, Fragmentation in the adjacent cores can be significantly reduced. Several research works have also supported the usage of wasted capacity due to crosstalk in providing resilience to connection requests. In that sense, they are not wasted but are redundantly kept aside and used if any failure occurs. Designing resilience schemes is another one of the most critical research areas in core optical networks. Especially in SDM-EON, the resilience schemes are much needed as it carries humongous capacity in every MCF link.

The core optical transport networks carry a huge amount of bandwidth. Any component failure, even for a few milliseconds, could be detrimental to the Services' quality, impacting the Service Provider's revenue gain. Two main categories of resilience schemes are protection and restoration, employed to avert losses due to failure. In protection techniques, the resources are pre-planned and reserved in advance, which reduces the backup resources search time, and provides timely reconfiguration of failed connections. In restoration techniques, the backup resources are calculated on the fly, and reconfiguring the failed connections can take longer. Sometimes, it is not possible at all to find the backup resources. Thus, protection techniques are more reliable than restoration techniques but at the cost of redundant resources. The redundant resources used in protection techniques could be dedicated to a particular route/lightpath or shared among multiple routes. Shar-

Table 1.2: Literature Survey of Design Issues in SDM-EON

Issues/Aspects	Design Parameter	Techniques and Findings	Ref
Fiber Design	Reducing Crosstalks and increasing the number of cores	7-cores and trench-assisted crosstalk-controlled 19-cores in hexagonal layout, 37-cores in circular layout crosstalk reduced by an increase in the core pitch	[17],[18]
Node Design	Spectral and Spatial Switching Granularity	Independent Switching for where each Spectral slice and cores are individual switching entity. In Joint Switching, all spatial dimensions are a single entity to be switched together. In fractional Joint Switching, the spatial entities are divided into groups, and the groups are switched together. The space complexity of Independent switching is highest.	[69]
Resource Provisioning	Crosstalk and Fragmentation Considerations	Crosstalk removal by using DSP techniques at th receiver side, Core prioritization while allocating resources, dynamic path selection by using crosstalk information, three-dimensional fragmentation metrics to find the crosstalk severity in the selected paths, Crosstalk-aware defragmentation, Fragmentation aware routing and then Crosstalk-aware Core and Spectrum Allocation.	[70],[71], [72], [73], [74], [75], [76], [77]
Resilience Techniques	Link and Path Protection	Dedicated path protection, shared path protection and link-protecting pre-configured cycles are used together with crosstalk and energy-efficient considerations	[81], [82], [83], [84],[85]

ing resources allows some respite from redundancy, but there is the condition of sharing among link disjoint routes for reliable restoration.

The major challenges in the Next Generation Optical Networks are to provision the resources in most efficient manner, both spectrally and spatially, and to maintain the QoS. The growing traffic rate requires the network algorithms to be computationally less complex and provide the most optimum solutions in the minimum possible time. Our proposed works in this thesis have been centered around these objective.

1.3 Motivation and Objectives

Optical Networks are the key elements of the Global Information and communication infrastructure. It is required to strengthen the core optical networks by deploying the Next Generation technologies to keep up with the increasing bandwidth demand trends. The most economical way is to use the existing bandwidth resources efficiently and selectively upgradation of the network elements as per the need. Two technologies, EONs and Spatial dimension enabled-EONs, have been discussed extensively over the last decade. These networks use the flexibility of the spectrum grid to provide almost the exact bandwidth required by the connection requests, hence not leading to any wastage. The adaptive modulation formats also contribute to the spectral efficiency of this.

When introduced at the network component level, all these features cause several constraints to be followed during the assignment of the resources to dynamically arriving and departing connection requests. Spectral Fragmentation is one such outcome of the stringent constraints. The addition of spatial dimension increases the capacity in multiples of the added space dimensions. The number of space dimensions, fibers, cores or modes depends on the impairment characteristics and the physical dimension of the fiber cladding. So, this tradeoff between the number of spatial dimensions and their related impairments adds more constraints to the resource allocation schemes. The motivation of this thesis lies in improving the existing resource provisioning techniques by introducing new metrics and the independent sub-resources (route, space and spectrum) assignments. The thesis's objective is to provide resources to any connection request arriving in the network using computationally efficient and simple techniques if resources are available by utilizing the real-time link spectrum status information and mitigating the performance degradation parameters. To fulfil the thesis aim, we carried out the following investigations with the objectives:

- To find a network-level fragmentation metric that combines the Fragmentation caused by the RSA constraints.
- To use the network-level fragmentation metric to trigger the reliable fragmentation management approaches in a cost-efficient way, the cost being the time complexities.
- The fragmentation management can still be costly above some traffic load values. Finding fragmentation-aware methods that can support maximum traffic admissibility before defragmentation is unavoidable.
- To study how much additional capacity can be gained by enabling the spatial dimension in EON, i.e., SDM-EON, and using the resource provisioning techniques to tackle the associated issues.
- To investigate the usefulness of the dynamic path finding using adaptive costs of the network links, where the costs are dependent on the Crosstalk, Fragmentation, fair resource distribution and suitable modulation formats.
- To utilize the wasted capacity due to impairment mitigation in resilient dynamic resource provisioning in SDM-EON.

1.4 Thesis Organization

The thesis is organized as follows: In Chapter 2, we study and analyse a network-level Vectored Fragmentation Metric using different traffic scenarios and related parameters as evaluation criteria. We discuss the basic requirements of the metric and its ability to identify the Fragmentation in the network.

In Chapter 3, we use the proposed Vectored Fragmentation Metric to perform fragmentation management using a Pro-Reactive defragmentation approach. A defragmentation approach is a computation-wise costly process, but it is one of the most effective techniques to mitigate the effects of Fragmentation. We use a green-field approach in the proposed work, where all the active connections are rearranged during defragmentation to create a tightly-packed spectrum scenario.

In Chapter 4, we propose a fragmentation-aware, penalty-based resource provisioning technique. In this work, Fragmentation is not controlled or managed. The cost of the fragmented links is increased or penalized in proportion to the fragmentation level. It ensures that incoming connection requests use the least-cost or least fragmented paths. It further improves the admissibility of connection requests for a particular traffic load range.

In Chapter 5, we move to resource provisioning in Multicore Fiber based Space Division Multiplexed-Elastic Optical Networks, which have spectral and spatial fragmentation issues. In our study, the objective of spectral and spatial Fragmentation are orthogonal to each other. There is a requirement for high spatial Fragmentation to mitigate the deterioration due to inter-core crosstalks and low spectral Fragmentation to mitigate the unavailability of spectral resources as per routing constraints. In our proposed work, we use dynamically changing costs of the link to find the least cost path for any connection request. The link parameters affecting the cost of the links are assigned some weights, and the weights vary adaptively over time as per the link spectrum state. Our proposed technique uses a Teaching-Learning based optimization method to converge on the appropriate weights of the parameters.

In Chapter 6, we have added an extra layer of resiliency to the resource provisioning technique of SDM-EON. The crosstalk effects limit the excess capacity gain obtained in MCF-enabled SDM-EON. Our proposed technique uses the crosstalk-affected cores as the Dedicated Spare Core groups, which protect a few Working Core groups. The core-granularity-based protected working core envelopes are used to accommodate connection requests, which are inherently protected by pre-configured structures. The pre-configured structures provide faster and capacity-efficient link protection against single failures.

Finally, we conclude the thesis with critical insights into the work and future scope of the work, which are worth investigating.

Chapter 2

Study and Analysis of Vectored Fragmentation Metric

> The recipe of research is easy- Ask questions, then some more questions. Research is all about asking questions!
>
> *A piece of conversation with Prof. Yatindra Nath Singh*

In this chapter[1], we propose and investigate a two-dimensional *Vectored Fragmentation Metric (VFM)* for EON. The Path-based fragmentation metrics are computationally time consuming, and the Link-based fragmentation metrics do not consider the continuity constraint related fragmentation. Using VFM, we want to consider the fragmentation associated with both contiguity and continuity constraint. This chapter presents a qualitative and quantitative assessment of the VFM. In the quantitative assessment, different dynamic traffic parameters are considered to study the behaviour of the VFM. The dynamicity of the traffic is characterized by the average arrival rate (λ), average holding time (μ), and maximum bandwidth demand by the connection requests.

[1]This chapter is based on the previously published work: Anjali Sharma, Varsha Lohani, and Yatindra Nath Singh, "A Vectored Fragmentation Metric for Elastic Optical Networks," ***Photonic Network Comunications***, 2022

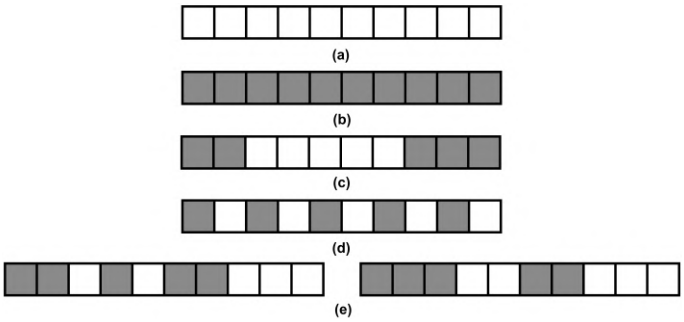

Figure 2.1: Types of fragmentation cases.

2.1 Proposed Vectored Fragmentation Metric (VFM)

The blocking of a connection request can happen due to the unavailability of contiguous bandwidth slices in one or more links forming the path over which connection is to be set up. It will happen due to improperly managed RSA, leading to fragmentation in the link and network spectrum. While considering a metric to quantify fragmentation level in the spectrum, we would like to have a single metric that can represent the fragmentation level considering both contiguity and continuity aspects.

Based on earlier studies, we enumerate as follows a few cases which a useful fragmentation metric should be able to identify (Figure 2.1), [38].

a. All slices are free (no fragmentation)

b. All slices are busy (no fragmentation)

c. Free slices are contiguous (no fragmentation)

d. All free slices are unusable (absolute fragmentation)

e. Same number of free slices can exist with varying number and sizes of fragments in the different spectrum scenarios but may have different level of fragmentation (relative fragmentation). For example in Figure 2.1(e), both link spectrum scenarios has five free slices but obviously the first one is more fragmented than the second one.

We formulate a vectored fragmentation metric that provides a single absolute value for the fragmentation level while taking care of all the above scenarios. The proposed metric considers the fragmentation in individual links (α-component) and also the fragmentation over some paths (β-component). For the α-component, we find maximum contiguous Spectrum Slices (SS) over individual links. For the β-component, we find the maximum number of continuously available links for each spectrum slice. Operationally, we can assume a centralized network controller that interacts with all the nodes to gather all the links' status and set up the paths for the arriving connection demands. As it has the entire links' status, it is expected to make better decisions [51]. The central controller can determine the VFM using the individual links' status and continuity of available slices across the specified paths.

We can define α- and β-components as follows:

- **α-component** is covering the fragmentation due to non-contiguity of total available SS in individual links across the whole network, and
- **β-component** is the fragmentation on spectrum indices due to non-continuity of available SS on the links of the representative paths in the network.

2.1.1 Formulation of metric

VFM is the fragmentation indicator that is denoted using ν. It is the resultant of α- and β- components. For the α- component, the maximum contiguous SS in a link are taken up against the total available SS in the link. Ideally, if all the available SS form a single contiguous slot collection, there is no fragmentation. Multiple SS scattered in the link spectrum in a dis-contiguous manner are the main cause of fragmentation. An important assumption considered in using the metric is that at least one spectrum slice is available in the network spectrum/ links of the network. Also, the β- component checks continuity of all SS individually on the links of the path, i.e., the component decides on the non-continuity aspect of fragmentation from individual slice indices' point of view. Multiple selective paths are used to check the continuity of each slice index over all the links in each path. Minimum number of paths are chosen so that minimum link repetition is there and the status of almost all the path flows are covered. Then, the continuity of links for all the spectrum slice indices (available in at least one of the links on the path) is used.

The maximum number of continuous hops where SS (of a particular index) are available is taken against the total available (unused) hops/links for that spectrum slice over the whole path. The individual components (α and β) and the fragmentation indicator (ν) is defined as follows (equations 4.1 - 4.2).

$$\alpha = \frac{1}{|EL|} . \sum_{i=1}^{EL} \frac{CG_i}{SS_i} \tag{2.1}$$

$$\beta = \frac{1}{|P|} . \sum_{i=1}^{P} \frac{1}{E_i} \sum_{j=1}^{E_i} \frac{CN_j^i}{AS_j^i} \tag{2.2}$$

$$VFM = \nu = \sqrt{\alpha^2 + \beta^2} \tag{2.3}$$

Here L is the set of links in the network, and EL is the set of links with at least one empty (available) spectrum slice. The SS_i is the total number of available SS in the i^{th} link, and CG_i is the maximum number of contiguous SS available on the i^{th} link. P is the set of multiple paths covering all the links in the network, specified for the path continuity aspect, and H_p is the number of hops on p^{th} path in set P. E_i is the total number of spectrum slice indices in the network spectrum with at least one empty spectrum slice anywhere on the i^{th} path. Next, AS_j^i is the number of hops where slices on j^{th} index are free in the i^{th} path, and CN_j^i is the maximum number of continuous hops with available j^{th} SS in i^{th} multi-hop path. TSS is the total number of SS in the network (includes both available and occupied).

This formulation calculates the fragmentation level in the network spectrum using the available SS. If there are no available SS, then no fragmentation exists. We emphasize choosing selective paths out of all possible path combinations for $\beta-$component as it ensures that we get a network-wide β-component with less computational overhead. The $\beta-$component is not specific to any particular connection request, but the selected paths represent continuity information of many paths.

A few paths out of candidate paths CP [2] are given priority for inclusion in P used in β-component calculation following a Path Preference Policy (PPP). The PPP selects the paths from CP that are most prone to fragmentation (longest) while covering all the

[2] Paths between all source-destination pairs

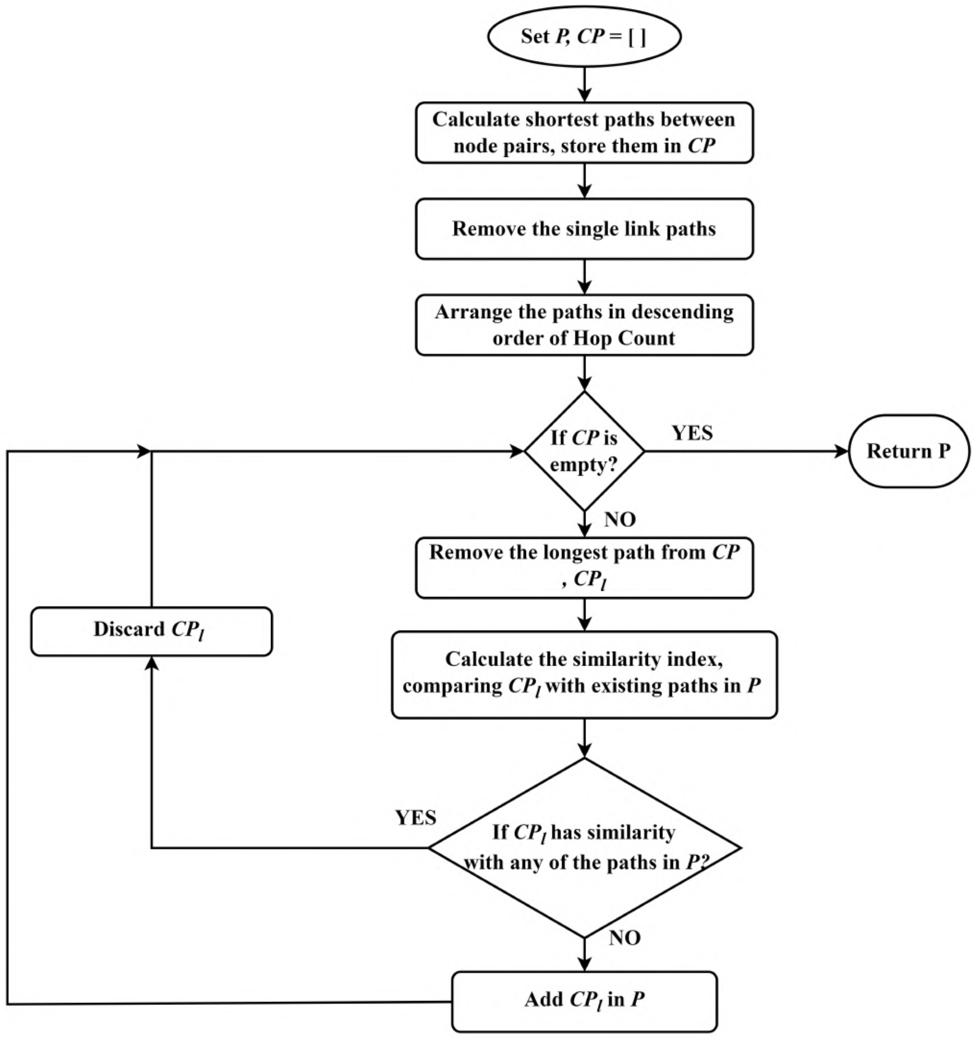

Figure 2.2: Flowchart of Path Preference Policy for candidate paths in β-component's calculation

links. PPP uses a path similarity index to check the repetition of the candidate path from CP with the already selected P paths to reduce the calculation overhead.

- PPP starts the path selection with the longest paths, more vulnerable to degradation due to fragmentation.
- Repetition of the link indicates the common links in path 'p' when compared with the links in paths already in P. PPP should choose the path with a minimum or no repetition of the path flow.

As per our understanding, instead of using all the possible path combinations, CP, we try to use a few longest paths, which are essentially the most actively used routes, and are most prone to fragmentation and contribute maximum to β-component at an abstract level. The PPP's flowchart is shown in Figure 2.2.

The maximum and minimum values of the α and β components can be found using the worst and best case scenarios. If TSS is the total number of SS and H_p is the number of hops in the selected paths, the range of α-component is $[\frac{2}{TSS}, 1]$. The range of β-component is $[\frac{2}{H_p}, 1]$, if H_p is even, and $[\frac{2H_p}{H_p^2-1}, 1]$, if H_p is odd.

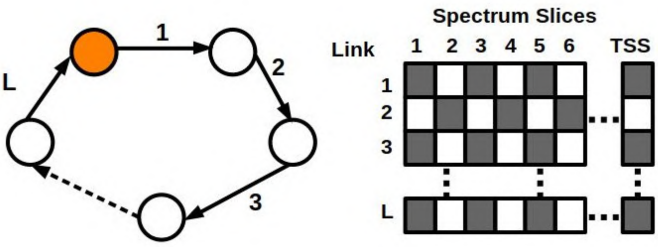

Figure 2.3: Worst case fragmentation scenario in a network with TSS, the total number of SS in each link.

The lower limit of the range is calculated by considering a worst-case scenario as shown in Figure 2.3. In the worst-case scenario, each link in the network exhibits Figure 2.1 case (d)'s spectrum status, with slices available alternatively in a link as well as in a path. As shown in the Figure 2.3, a single available slice is the maximum contiguous slot size in each of the links and also in the path(s). This scenario has only half of the available resources. We also get a highly fragmented scenario over a path if the maximum continuous slice over a single path is 1 for a spectrum index *'i'*, even if half of the resources on that path are available. If such a case exists for all the spectrum slice indices, we get a worst-case scenario for the α and the β. The best-case scenario is when all the available SS resources are available continuously and contiguously.

2.1.2 Example of fragmentation level calculation

In Figure 2.4, we have a 4-nodes 5-links network, with its network spectrum status. All the white blocks represent empty or available SS. In this spectrum scenario, the occupancy level is 50%.

In the example, for the calculation of α-component, the average ratio of maximum contiguous slot size to total available SS over all the links is considered. The CP contains

A→B (1), A→B→D→C (1-4-5), A→B→D (1-4), B→D→C→A (4-5-3), B→D→C (4-5), B→D (4), C→A (3), C→B (3-1), C→B→D (2-4), D→C→A (5-3), D→C→B (5-2), D→C (5). Let us assume that the PPP selects A→B→D→C (1-4-5), and B→D→C→A (4-5-3) to be used in β-component calculation covering all of the source-destination pairs' path flows, hence $|P| = 2$. For the example, we calculate the fragmentation level using VFM and a Link-based External Fragmentation Metric (L-EFM) only.

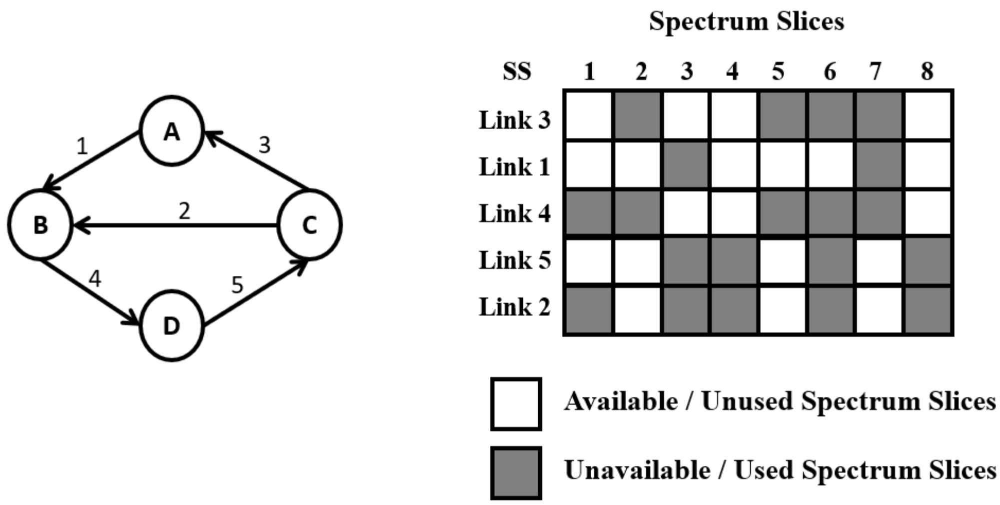

Figure 2.4: An example for calculation of vectored- fragmentation metric with 50 % occupancy.

The L-EFM considers the largest contiguous slot's size (CG_i) and total available SS (SS_i) in links, $i \in L$, to decide the fragmentation level [42]. It is the most basic metric with less complexity. It also tends to ignore fragmentation due to smaller fragments present in the spectrum. The L-EFM formulation is given in equation 4.5.

$$L - EFM = 1 - \frac{1}{L}\sum_{i=1}^{L}\frac{CG_i}{SS_i} \tag{2.4}$$

The α-component, β-component, ν, and other normalized version of VFM are calculated next:

$$\alpha = \frac{1}{5}.(\frac{2}{4} + \frac{3}{6} + \frac{2}{3} + \frac{2}{4} + \frac{1}{3}) = 0.5 \tag{2.5}$$

$$\beta = \frac{1}{2}(\frac{1}{8}(\frac{1}{2}+\frac{1}{2}+\frac{1}{1}+\frac{2}{2}+\frac{1}{2}+\frac{1}{1}+\frac{1}{1}+\frac{2}{2})+\frac{1}{7}(\frac{2}{2}+\frac{1}{1}+\frac{1}{2}+\frac{1}{2}+\frac{1}{1}+\frac{1}{1}+\frac{1}{2})) = 0.7991 \quad (2.6)$$

$$\nu = \sqrt{\alpha^2+\beta^2} = \sqrt{0.5^2+0.7991^2} = 0.9426346 \quad (2.7)$$

$$VFM_{min} = \nu_{min} = \sqrt{\alpha_{min}^2+\beta_{min}^2} = 0.79056 \quad (2.8)$$

$$NVFM = \nu_{norm} = \frac{\nu-\nu_{min}}{\nu_{max}-\nu_{min}} = \frac{0.9426-0.79056}{1.414-0.79056} = 0.243928 \quad (2.9)$$

$$AVFM = 1-\nu_{norm} = 0.756 \quad (2.10)$$

In this example, the network spectrum occupancy is 50%, which means that half of the total SS is used. L-EFM for this network is 0.5. The α and β components to compute VFM are 0.5 and 0.7991 respectively. The ν or the VFM value is 0.9426346 . Normalized Vectored Fragmentation Metric (NVFM), ν_{norm} is 0.243928. If the ν_{norm} is closer to 1, then fragmentation in the network spectrum is not significant. In this example, a moderate fragmentation is present in the spectrum. While comparing the VFM with other link-based fragmentation metrics, we use the Adapted form of VFM (AVFM), i.e., $(1-\nu_{norm})$. Using AVFM ensures that the same meaning as L-EFM is conveyed effectively; a low metric value means a lower level of fragmentation and vice versa. The AVFM value, in this network, is 0.756 (1- NVFM).

The network spectrum utilization and its relationship with fragmentation level in the system could be an interesting finding. However, a direct relationship between the two is improbable because the occupied spectrum's arrangement also plays a part. The fragmentation level can vary for the same network spectrum utilization values when observed in steady-state conditions in the real-time traffic scenario.

We compare theoretical aspects of the VFM and the other metrics reported in the literature. The comparison allows us to put vectored fragmentation metric in perspective. The comparison is based on some of the essential characteristics as well as the complexity of the metrics. Table 2.1 compares link-based metric, path-based metric, and the vectored metric using some key features such as the ability to identify fragmentation scenarios and the time complexity. The VFM can outperform link-based metrics for fragmentation estimation at the network level with an additional computation cost but still less than the

Table 2.1: Comparison of fragmentation metrics

Characteristics	***Link- based***	***Path- based***	***Vectored***
Identifies fully fragmented scenario (Figure 2.1(d))	No	No	Yes
Identifies zero fragmentation scenario (Figure 2.1a,b,c))	Yes	Yes	Yes
Differentiates between fragmentation scenarios Figure 2.1(e))	Some of them	Yes	Yes
Time Complexity	Lowest among others $\mathcal{O}(S.L)$ [38]	High $\mathcal{O}(S.L)$-$\mathcal{O}(S.L.G)$ [38]	Moderate $\mathcal{O}(2.S.L)$
General Observations	1. Ignores small fragments 2. Can be relative or absolute 3. Covers only contiguity aspect 4. Defines fragmentation aspect in terms of spectrum compactness as well 5. External, Entropy-based, Compaction-based, Highest-slot mark, Access-blocking probability	1. Specific to a path of the connection request 2. Can be relative or absolute 3. Covers contiguity and continuity aspect specific to connection request 4. Calculates fragmentation in all path combinations for better accuracy but increasing computational complexity 5. Wasted-Unusable-Free Ratio metric	1. Covers all available spectrum slices 2. Absolute 3. Can covers both contiguity and continuity aspect independently. 4. Calculates fragmentation in selective path combinations for better accuracy and reduced computational complexity.

S is the total number of spectrum slices, L is the total number of Links, and G is the total number of permissible granularity of connection requests.

cost of the path-based fragmentation metric.

We conducted simulation study of adapted form of the vectored fragmentation metric (AVFM).

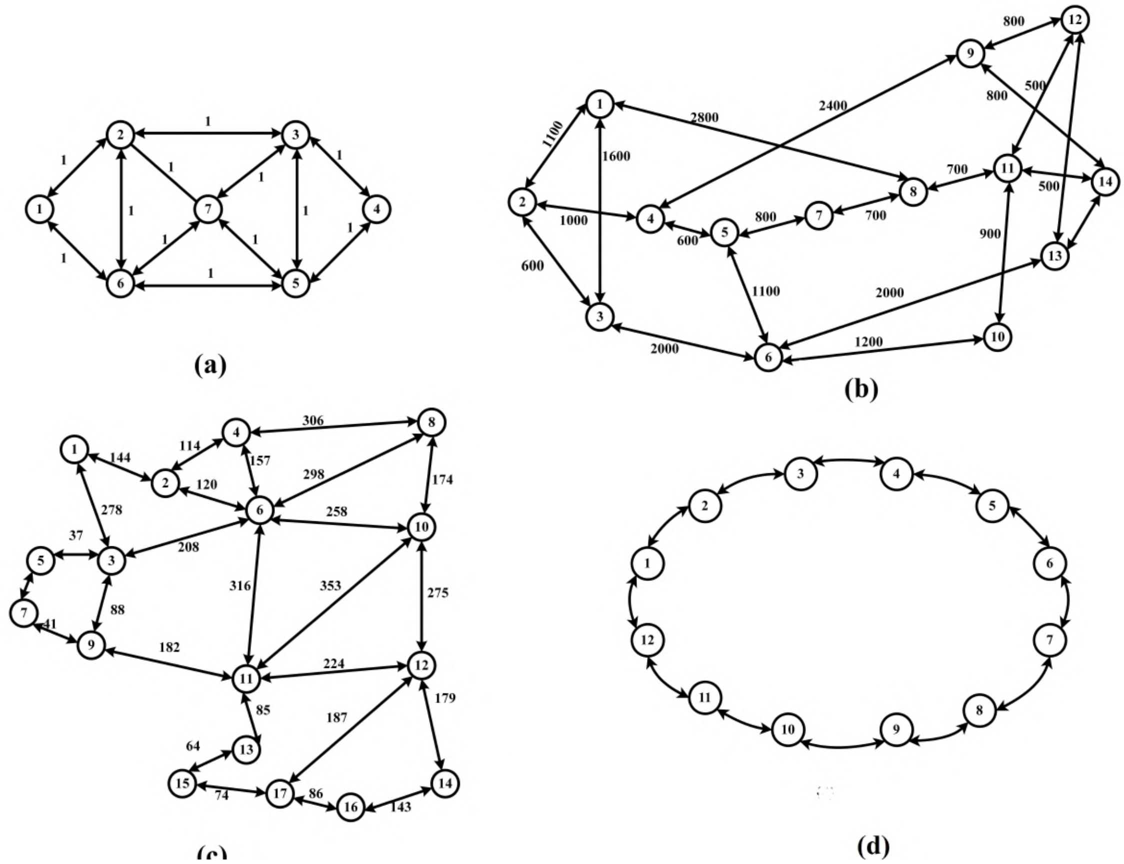

Figure 2.5: (a) Net-A, (b) NSFNET, (c) German network and (d) Ring network topologies.

2.2 Simulation and Analysis

2.2.1 Simulation Setup

To study our proposed metric, we consider four networks: Net-A with 7-nodes 12-bidirectional links, NSF network with 14-nodes 21-bidirectional links, German network with 17-nodes 26-bidirectional links, and Ring network with 12-nodes 12-bidirectional links as shown in Figure 4.2. Each network link has 320 SS (with 12.5 GHz spectrum slice width), providing 4 THz of bandwidth in the C-band. We generate connection requests (or demands) on every node using the Poisson distribution with arrival rate λ and each connection has a holding time with exponential distribution with mean $\frac{1}{\mu}$.The normalized traffic load range is estimated using $\frac{(\lambda/\mu)}{(\lambda/\mu)_{max}}$. We consider a uniformly distributed SS requirement by connection requests, ranging between 1 and 16. We assume no waveband conversion scheme at any intermediate node. We use the Shortest Path-First Fit technique to provide the first contiguously available SS to the connection requests. The PPP selects 12, 20, 22 and 8 paths for $\beta-$ component calculation in Net-A, NSF, German and Ring network, respectively. The single points on the plots are an average of 500000 connection requests over 20 iterations. We obtained all the results with a 95% confidence interval as indicated in the plots.

First, we study the general characteristics of the proposed metric using different network traffic dynamics. We use the AVFM, A-Alpha (1-α), and A-Beta (1-β) to study the fragmentation level. After that, we compare the network performance using several link-based and path-based metrics with AVFM when the metric is used to trigger fragmentation management in a dynamic traffic scenario.

2.2.2 Analysis of adapted vectored fragmentation metric as a fragmentation indicator

The objective of the AVFM analysis in different traffic scenarios is to establish its utility. The AVFM should be able to reflect the network spectrum state in the form of fragmentation level. Fragmentation level depends on the network spectrum status, which depends on the network traffic dynamics. The traffic dynamics can vary with the average arrival rate, average holding time, or heterogeneity in the SS requirement of the incoming connection requests [3]. The observations are taken in the network's steady-state, i.e., in the period after the six times the average holding time from the start of the simulation. The network is observed to reach steady-state roughly in this period.

In Figure 2.6, we first evaluate how fragmentation levels vary with the connection holding time for the given arrival rate. We considered four arrival rates (lambda- 5 per time units (t.u.) , lambda- 10 per t.u, lambda- 25 per t.u, and lambda- 50 per t.u), and the holding time varies from one to ten t.u. We observed that overall AVFM increases with the increase in the load, i.e., increasing holding time and arrival rate. Net-A's steady-state fragmentation level is around 0.75 for a higher arrival rate (lambda-50), which is 7.5 times more severe than the fragmentation at a lower arrival rate (lambda-5) while having the same holding time (1 t.u.). NSFNET, German network and Ring network (Figure 2.6(b)-

[3] using the maximum SS requirement labeled MaxDemand in related plots

(d)) also exhibit similar behavior; however, the networks converge to maximum AVFM level (0.6) much faster in these three networks. When the holding times and arrival rates are both less, the network shows a lower fragmentation level because the utilization of the spectrum slices is also less (only 20-30% of the available spectrum slices are busy).

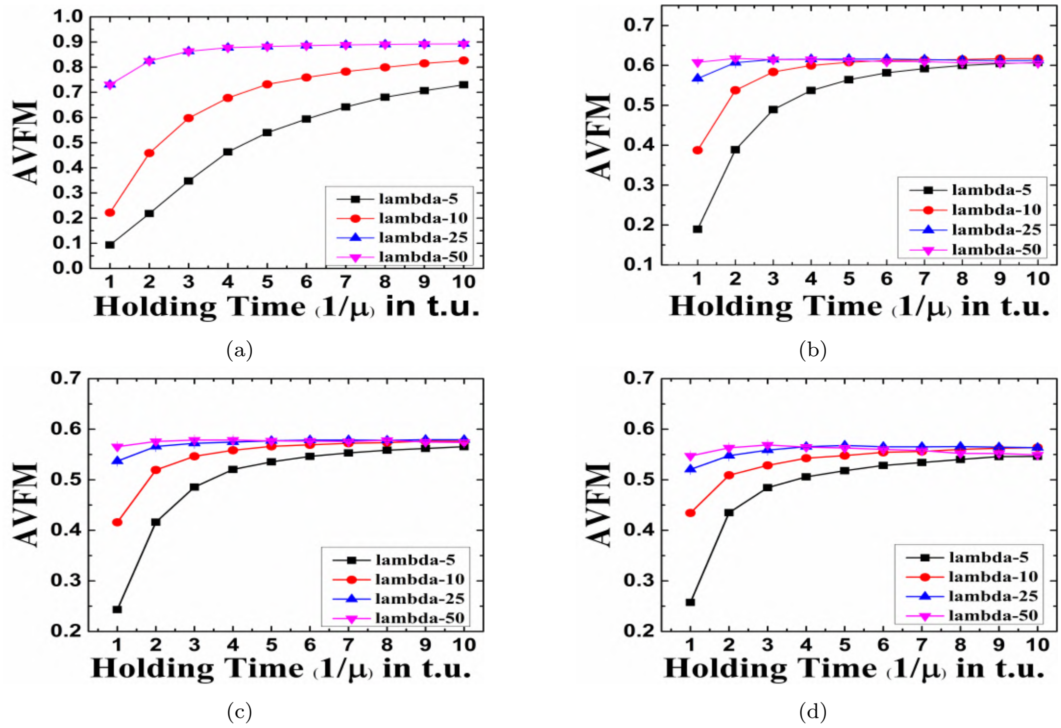

Figure 2.6: AVFM vs holding time in steady-state for (a) Net-A, (b) NSFNET, (c) German network, and (d) Ring network for different arrival rates (lambda)

Next, we observed the AVFM level for different arrival rates for holding times (HT). We considered three holding times (HT-0.1 t.u, HT-1 t.u, and HT-10 t.u) and average arrival rates between 5 and 50 connections per unit time (t.u.). In Figure 2.7(a), (b), (c), and (d), we observe that the fragmentation level increases with the arrival rate when the holding time is 0.1 t.u and 1 t.u. When the holding time is short, the release of connection requests is speedy, and AVFM is comparatively low. Whereas, when the holding time for connection requests is longer (10 t.u.), the AVFM level saturates to its highest value.

In Figure 2.8(a)-(d), we considered four different arrival rates (lambda-5, lambda-10, lambda-25, and lambda-50), each one with increasing holding times to create varying load conditions. We observed that AVFM value increases with the traffic load. Net-A's maximum steady-state fragmentation level is around 0.6, i.e., 60 percent fragmentation,

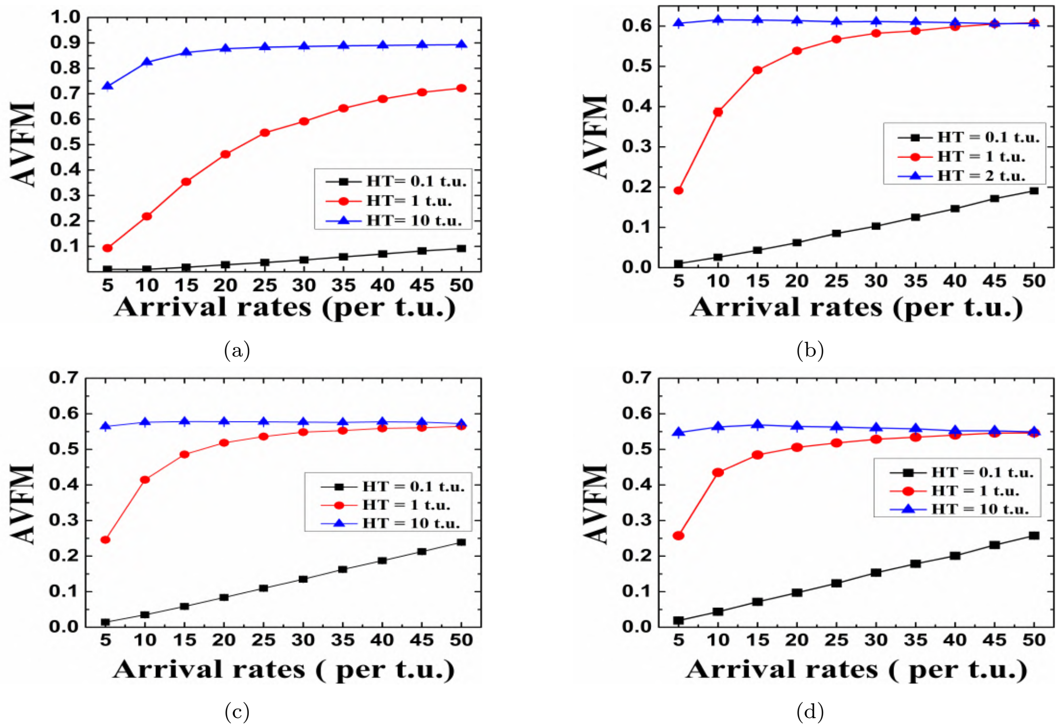

Figure 2.7: AVFM vs arrival rates (lambda) in steady-state for (a) Net-A, (b) NSFNET, (c) German network, and (d) Ring network for different holding times

for the normalized load of up to 1. In NSFNET and German network (Figure 2.8(b)-(c)), the steady-state AVFM value varies from 0.55 to 0.6 from 0.4 to 1 normalized traffic load. The Ring network has maximum fragmentation level of 0.55 for most of the normalized traffic load range (Figure 2.8(d)). We observe that the steady-state AVFM value does not change for a fixed load. So, varying the arrival rate and holding time for a fixed load will result in the same fragmentation level.

We also observe that the maximum permissible slot size or granularity range of the incoming connection requests (MaxDemand) affects the fragmentation level (Figure 2.9(a)-(d)). We consider three MaxDemand values, 4, 8, and 16. The higher granularity range (MaxDemand 8 and 16) indicates more fragmentation (AVFM) compared to the scenario of the MaxDemand 4, as the arriving connection requests are more diverse and leave the spectrum more disorganized. We observed this behavior in all four network topologies. However, at a very high traffic load, the increase in AVFM may restrict to a maximum value due to the unavailability of network slices. It might be because of more connection requests of smaller granularities being accommodated (Figure 2.9(b)-(d)). The high heterogeneity

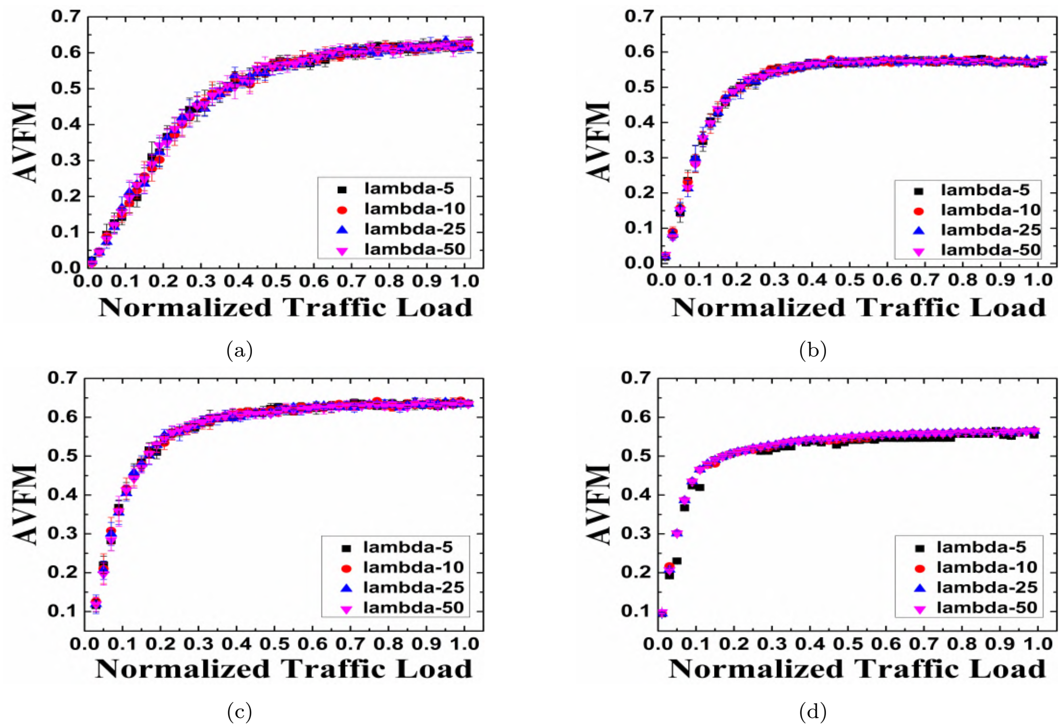

Figure 2.8: AVFM vs normalized traffic load in steady-state for (a) Net-A, (b) NSFNET, (c) German network, and (d) Ring network for different arrival rates

of the demands combined with higher arrival rates indicates a more fragmented network spectrum.

Next, in Figure 2.10(a)-(d), we observed how the influence of A-alpha and the A-beta as fragmentation level indicators vary for different network topologies. In Net-A and Ring network, Figure 2.10(a) and Figure 2.10(d) at low load traffic, A-beta is dominant than the A-alpha (A-alpha/A-beta < 1) for normalized traffic load of up to 0.5. The A-beta influences the Net-A more at lower traffic load, when there is lower spectrum occupancy. The crossover point is when A-alpha becomes more than A-beta. For Net-A, the crossover point occurs at around 0.52. For NSF and German network, it can be seen in Figure 2.10(b)-(c) that A-alpha is the dominant component for a wide range of the normalized traffic loads. One of the reasons could be the number of paths considered in PPP, and the uniform type of connection arrivals. At high traffic load, more SS are occupied, and hence the fragmentation of available SS is less. It implies that link fragmentation is more prominent than the path fragmentation when majority of the spectrum slices in the links are occupied. In this case, the blocking of the connection requests for multi-hop paths

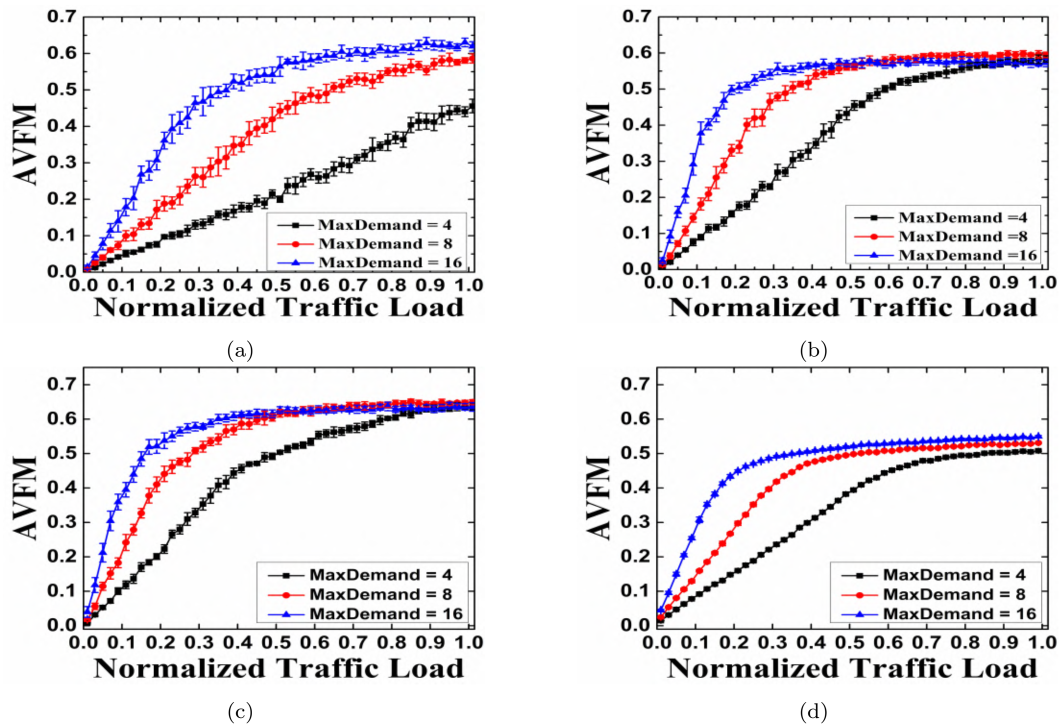

Figure 2.9: AVFM vs normalized traffic load in steady-state for (a) Net-A, (b) NSFNET, (c) German network, and (d) Ring network for different maximum permissible SS requirement

would be due to the unavailability of spectrum resources rather than fragmentation. The chances of single-hop connection paths being accommodated are more in such cases.

In Figure 2.11(a)-(d), AVFM, A-alpha and A-beta are plotted against the Network Spectrum Slices Utilization (NSSU) for four networks. One can observe that AVFM, A-alpha, and A-beta are all smaller for smaller and higher NSSU values. They all achieve their maximum value somewhere between the NSSU value of 0.4 to 0.9.

AVFM is a composite function of A-alpha and A-beta; it always has a higher value than A-alpha and A-beta. A-alpha achieves its peak at a higher value of NSSU as compared to A-beta. It indicates that contiguity fragmentation is significant at higher NSSU while continuity fragmentation is significant at lower NSSU. One can also observe that at higher NSSU there are less number of available SS, and thus continuity fragmentation is low. Contiguity fragmentation is dominant for all networks, especially at higher utilization.

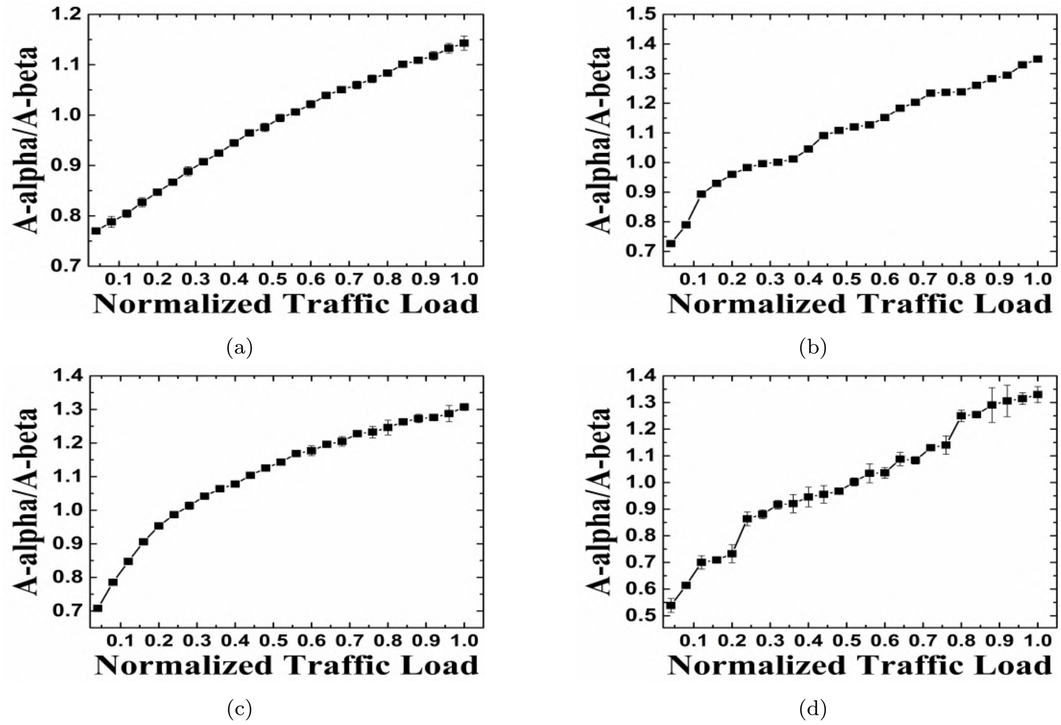

Figure 2.10: Ratio of A-alpha and A-beta vs normalized traffic load in steady-state for (a) Net-A, (b) NSFNET, (c) German network, and (d) Ring network

2.3 Concluding Comments

To the best of our knowledge, there has not been any other proposal for a vectored metric using the resultant of both continuity and contiguity aspects for network-level fragmentation in elastic optical network spectrum. In this chapter, we have proposed a vectored fragmentation metric to estimate the degree of fragmentation in a network. This chapter assessed a vectored fragmentation metric's (AVFM) ability to capture fragmentation levels using continuity (β) and contiguity (α) in real-time network scenarios using simulations. We observed that the fragmentation level evolves with time and network spectrum status. In the AVFM, continuity (β) and contiguity (α) contribute significantly to the overall fragmentation level. We also observed that continuity fragmentation (A-beta) is more than contiguity (A-alpha) in networks at a low traffic load. The A-alpha surpasses it at some cross-over point as load increases. The other network characteristics like arrival rates, holding times, and the connection requests' granularity range may also significantly affect the fragmentation levels. We have also found that both α and β-component can

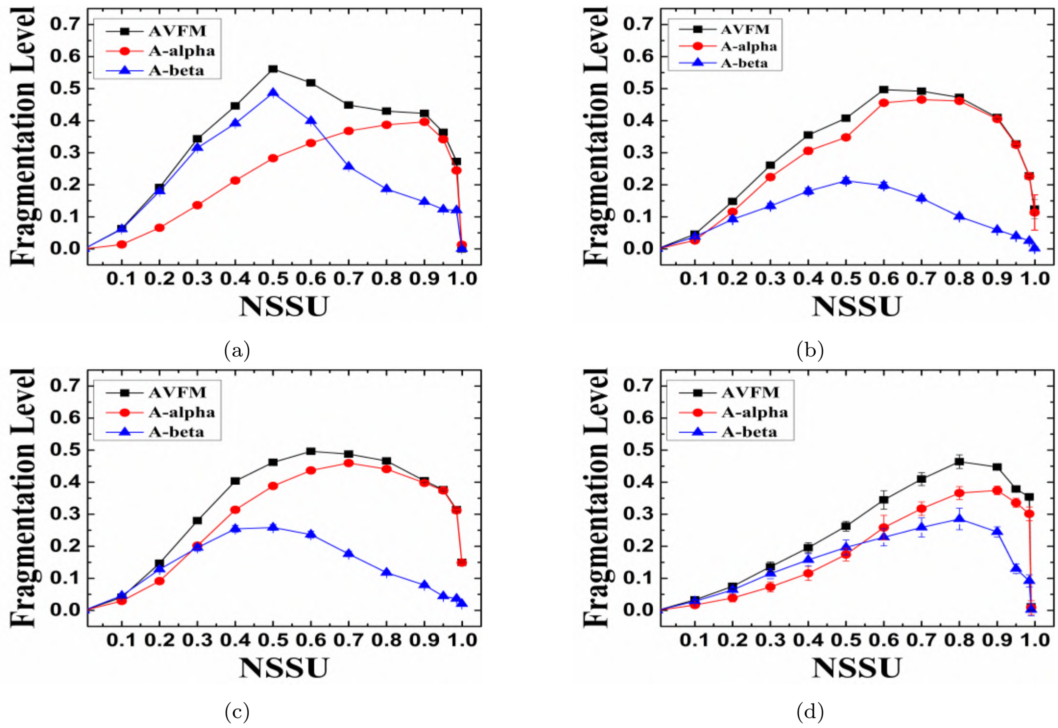

Figure 2.11: Fragmentation level vs NSSU for (a) Net-A, (b) NSFNET, (c) German network, and (d) Ring Network

be accepted as a measure of fragmentation individually. In this work, connectivity of multiple contiguous slices over a path in β-component is not considered. Thus, it is a 1^{st} level metric, as it takes into account only a single slice index for the evaluation of continuity constraint fragmentation. The representation of the fragmentation for single slice connection requests also represents a worst-case scenario for applications with large bandwidth requirements. In the next chapter, we present the resource provisioning techniques in fragmented spectrum scenario using link-state awareness and threshold-based defragmentation using fragmentation metrics.

Chapter 3

Fragmentation Management: Defragmentation Approach

> We occupied canteen seats for twelve people, but only five were present. See fragmentation is useful sometimes! We used fragmentation to our benefit. Tell this to network operator!
>
> *A passing comment during Lab's tea time break*

In the previous chapter, a two-dimensional fragmentation metric, AVFM, was proposed. We studied the impact of traffic characteristics on the behaviour of the fragmentation indicator. However, the important question is how this fragmentation indicator could be used to mitigate fragmentation's deteriorating effects on spectrum utilization efficiency. In this chapter, we use the AVFM fragmentation indicator to trigger defragmentation. The defragmentation process rearranges the network links' spectrum to a compact version.

3.1 Background

The EON's performance depends on the consideration of physical layer impairments and how the connection requests are provisioned in it. When the connection requests with heterogeneous bandwidth requirements arrive dynamically in a network, their random setup as well as dismantling, makes the available network spectrum state scattered. The required spectrum resources (Spectrum Slices, SS) are available but cannot be allocated to arriving connection requests. This condition is called Spectrum Fragmentation. The available spectrum resources' usage is infeasible, as they can not fulfill the RSA constraints. Figure 3.1 shows an example of fragmentation and its effects on future connection requests. We can see that more than 50% of the total SSs are available, yet a connection request demanding two SSs is rejected. The fragmentation leads to more blocking of the connection requests and inefficient use of available spectrum resources. There is unfairness in terms of network inclusivity for the connection requests. When in a fragmented state, the network can only accommodate low bandwidth requests and rejects high bandwidth requests. The probability of finding lesser number of SS confining within RSA constraints is higher than the probability of finding more number of SS. Thus, there is need to operate network in such a state, so that Spectrum Fragmentation is minimized or mitigated. Hence, the Fragmentation management approaches come into play.

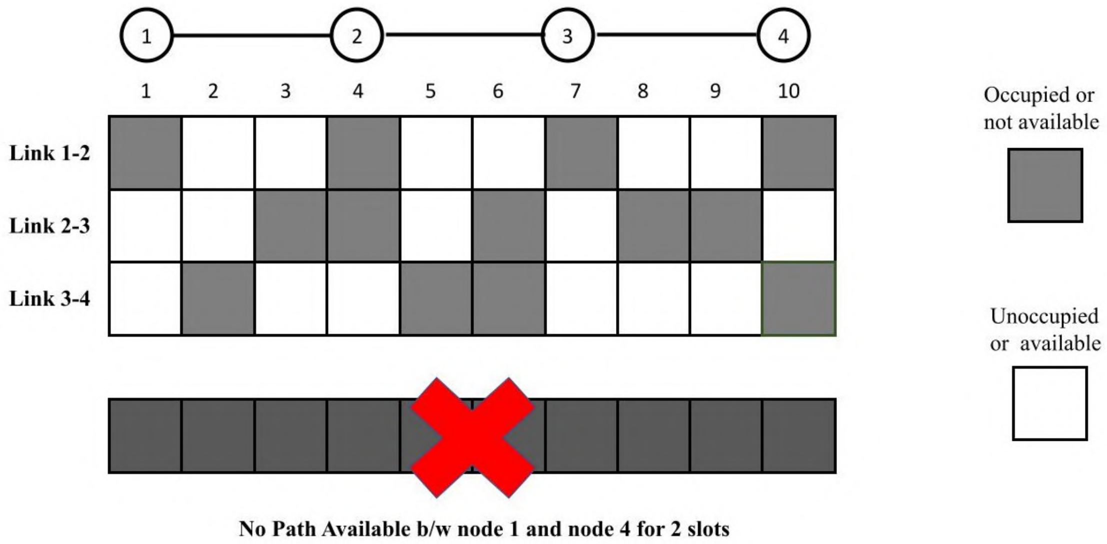

Figure 3.1: An example of Spectrum Fragmentation

Spectrum Fragmentation Management (SFM) in EON is another extensively researched topic that aims to maximize the bandwidth requests intake in the network. There is a need to address the SFM using RSA context and spectrum rearrangements within feasibility. Three approaches could be used to steer the effects of fragmentation: Spectrum Management (SM), Defragmentation, and Non-Defragmentation techniques. We discuss more about them in the following sections.

3.1.1 Spectrum management

When the connection requests arrive in the network sequentially, the SS resources are provided to them using some Spectrum Allocation (SA) techniques. Any usable technique is expected to have low computational complexity and no or limited retention of global information. The selection and release of the SSs in appropriate portions of the spectrum can considerably affect the network's spectrum fragmentation. The works in [45], [46] and [47] used link-based slot contiguity ratios (same as in eqn 3.4) as fragmentation metrics and the blocking ratio of the connection requests in a dynamic traffic scenario to evaluate the different spectrum allocation policies. Different SA techniques as reported in literature are shown in Figure 3.2.

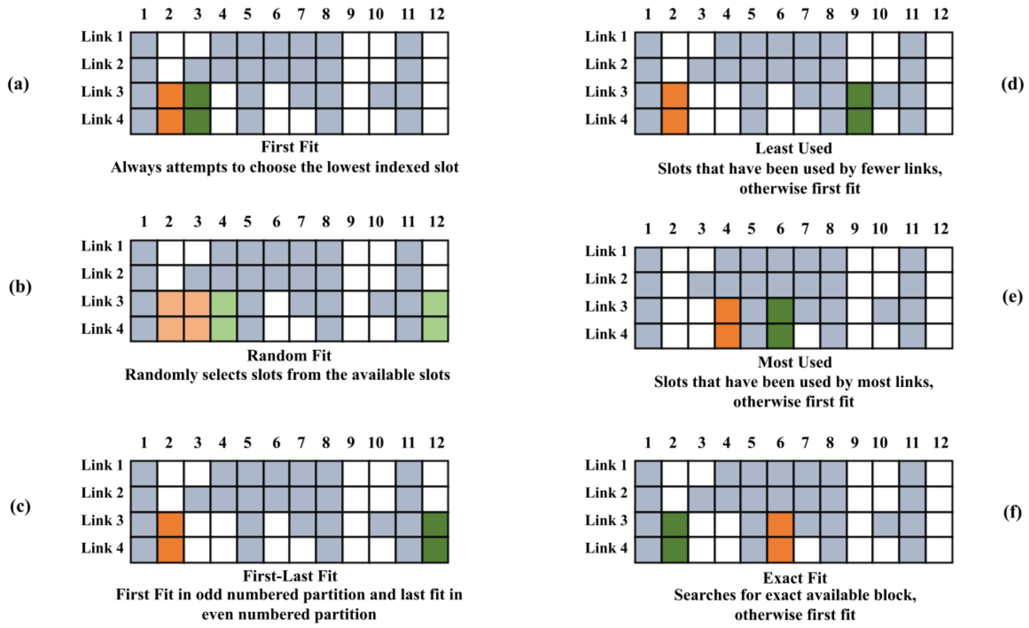

Figure 3.2: Spectrum allocation of two connection requests that want to use Link 3 and Link 4, CR1 (Orange colored) and CR2 (Green colored), following (a) First Fit (FF) technique, (b) Random Fit (RF) technique, (c) First-Last Fit (FLF) technique, (d) Least Used (LU) technique,(e) Most Used (MU) technique and (f) Exact Fit (ExF)technique.

Least Used (LU) and Most Used (MU) techniques have the highest time complexity compared to the other SA techniques, as one need to retain the global information about the spectrum index being least or most used. According to studies in [45], [46], and [47], the First-Last Fit (FLF) technique has the highest link slot contiguity ratio, and the

Random Fit (RF) technique has the least. When using the FLF technique, the connection requests can be grouped based on whether the paths share any links in the path, the granularities of the bandwidth demand, and the path length. Each group is then assigned SSs either from lower-indexed FF or higher-indexed LF.

In [48], a Sliding Fit and Parcel Fit spectrum assignment techniques has been proposed, where a particular set of available SS are selected and then the corresponding connection request which can use it is searched. It promises to perform better than FF but the test scenario is for static traffic, i.e., the set connection requests are already available and they are not changing over time. Appropriate spectrum allocation technique together with routing can lead to fragmentation-less or minimum-fragmentation operation. Authors in [33],[34], [35] and [36] discussed the fragmentation-aware RSAs to accommodate the connection requests only if they do not lead to fragmentation in the future.

3.1.2 Non-Defragmentation Approaches

In the non-defragmentation approach, the objective is to operate the network to keep the fragmentation at a minimum level at every observation point. The active connection requests are not affected in this scheme. However, a 100% fragmentation-less operation is not guaranteed. If a network gets into a fragmented state, the appropriate algorithms must ensure that it comes out of it on its own at the earliest. The main techniques in this approach are spectrum partitioning [29], multipath [30], and multigraph [42].

The spectrum partitioning strategy divides the spectrum into smaller blocks, and different spectrum assignment policies are employed to achieve the desired performance. The connection requests are grouped, and each partition is dedicated to a single group. The partitioning can be of two types depending on the spectrum division boundary: Pseudo Partitioning (PP) and Dedicated Partitioning (DP). When the FLF technique is implemented with no connection groupings, it falls in the PP category. In DP, there are fixed partitions for all groups, which could be greater than two. Spectrum partitioning, with FLF and connection groupings, yields a better fragmentation and blocking ratio performance [31].

In [30], authors have used Multipath Routing with pre-assignment, post-assignment, and fragmentation level assessments to control the fragmentation and lower the blocking ratio for incoming requests. The multigraph technique in [32] uses spectrum availability to make edges of virtual networks for deciding route between source-destination pairs. It then uses a cost function in the virtual network to decide on the final route. It promises to lower the blocking of the connections while maintaining the fairness among different connection requests.

Next we discuss how defragmentation techniques are used for Fragmentation Management in EONs.

3.1.3 Defragmentation Approaches

The defragmentation management technique is primarily reconfiguring the active connection requests to reduce fragmentation. When the network enters into a fragmented state and has started to affect the network performance, the defragmentation process may act on active connection requests' arrangements. The reconfiguration can be in the form of a new spectrum assignment on the same route or a new spectrum assignment on a new alternate path. The reconfiguration allows the availability of more contiguous spectrum slices and makes room to accommodate new connection requests in the network. An example of a defragmentation process by rearranging the allocated spectrum slices following the FF technique is shown in Figure 3.3. It is a Green-field approach where the controller assumes that all the connections are dismantled for defragmentation and need to be set up again. The sequence of connection requests for rearrangements depends on the remaining connection holding time as in the given example.

In literature, the defragmentation process could be categorized as proactive or reactive depending on its triggering mechanism. If the defragmentation process is triggered periodically, we call it a proactive strategy. The parameters deciding periodic defragmentation frequency could be the arrival of some number of connection requests, a specified time period, or fixed threshold-based fragmentation metrics. In reactive strategy, if the controller sees blocking of the arriving connection request, then to avert that, it will reconfigure some minimum number of existing connection requests, and then try to accommodate

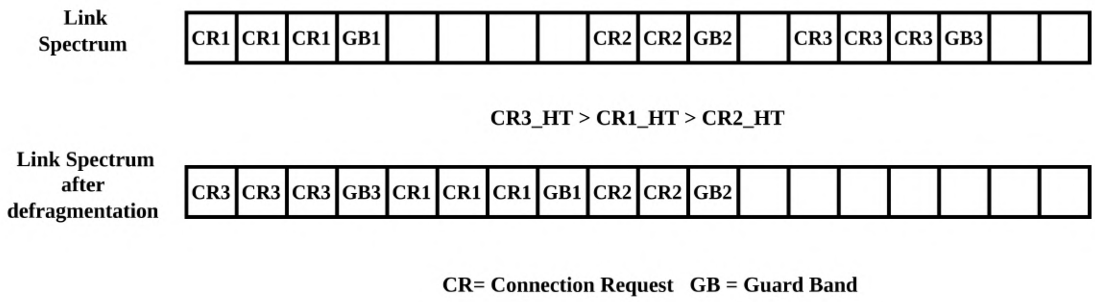

Figure 3.3: An example of Spectrum Defragmentation using remaining Holding Time of the Connection Requests

the blocked connection request. Authors in [62] have studied the conditions in which the two, reactive and proactive, approaches can outperform each other. The number of rearranged connections adds to the defragmentation cost and should be minimized in both approaches. The defragmentation approaches may or may not interrupt the existing connections when rearrangement occurs, [39], [40]. Some of the defragmentation techniques, in both proactive and reactive categories, are re-optimization, make-before-break, push-pull [41], and hop-tuning, [26], [42]. In [56], a path shift based defragmentation strategy is studied where the original route is not changed, but the retuning of transmitter is done to shift the spectrum assignment. The other existing connections are not affected, and this strategy is studied for both Proactive and Reactive defragmentation.
The defragmentation techniques are more reliable in alleviating fragmentation but are computationally complex and complicated. However, the non-defragmentation approach cannot guarantee the 100% fragmentation-less operation of the network. The non-defragmentation approaches, like multipath routing, underestimate the severity of the fragmentation. The use of longer path lengths could adversely affect the availability of the spectral resources as per constraints. Therefore, defragmentation methods could be more reliable in pacifying the fragmentation. Identifying a suitable instant to initiate defragmentation is challenging, and using an appropriate strategy to find these instants is crucial.

Many of the defragmentation strategies uses periodic time interval as triggering mechanism [37], while some use fragmentation indicating metrics. Some of the link-based fragmentation metrics which exploit the spectrum status in links have been discussed in

[42], [43] and [44]; these are External Fragmentation metric [42], Shannon entropy-based metric [42], Access Blocking probability-based metric [42], Utilization entropy [43], High-slot mark [43] and Spectrum Compactness metric [44]. The metrics discussed in the cited works give an abstract treatment to the fragmentation measure. They tend to ignore some crucial aspects of spectrum status, e.g., small fragments. A few of these metrics cannot differentiate between different spectrum scenarios as listed in Chapter 3.

Other than link-based metric, there are path-based metrics as well. Pederzolli *et al.* [49] have proposed one such metric. The authors use the Wasted-Unused-Free ratio as the metric in the RSA to find path-slots combination for a connection request. It should result in a lower overall fragmentation level and accommodation of more future connection requests. So, inappropriate path selection is a precursor to fragmentation, if any. While this metric captures fragmentation due to continuity and contiguity, it is path/connection request specific. In [50], Bonani *et al.* presented the network-level metrics, using the link consecutiveness aspect in all the links at specific observation periods (time-weighted) to decide on a network's fragmentation level. They also gave the idea of unfairness, i.e., high bandwidth requests are more likely to get blocked due to fragmentation at higher loads.

Using defragmentation technique is advantageous, as it is triggered only when absolutely necessary. The cost of defragmentation events is dependent on number of such events and number of rearrangements in each event.

3.2 A Pro-Reactive Defragmentation Approach using Fragmentation Metrics

Defragmentation is a complex and expensive process, and it is necessary to implement it efficiently. The essential considerations for a well-planned defragmentation process are: when and how to defragment the network links' spectrum. The defragmentation cost, i.e., the number of active connection requests affected by this process, is another factor to scrutinize. Firstly, in our study, we assume that the incoming traffic has a uniform connection arrival; that is, the arrival rate does not vary over the considered period.

The fragmentation levels are checked after a unit time interval. If within an interval there is a considerable increase in blocking of the connection requests, in comparison with the previous interval, then the fragmentation level at that instant is set as the Threshold Fragmentation (FM_{th}) level for defragmentation. Then, the defragmentation is performed using the re-optimization approach. The connection requests are arranged according to their remaining holding time and re-assigned SSs using the FF technique. The proactive of the defragmentation management is using threshold-fragmentation level. The reactive part is updating threshold-fragmentation level using blocking performance after every unit interval, and performing defragmentation if required. By combining the proactive and reactive approaches, we intend to use the defragmentation judiciously and only when necessary. The process of fragmentation management using the Pro-Reactive approach is shown as flowchart in Figure 3.4.

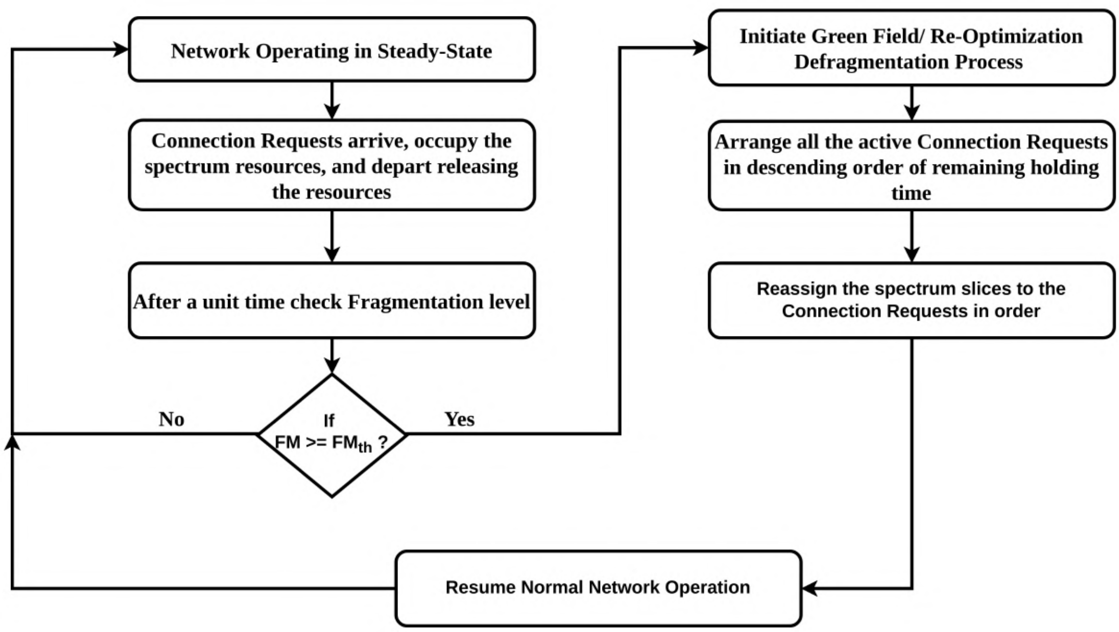

Figure 3.4: A Pro-Reactive Defragmentation Approach

We can use different fragmentation metrics to record and trigger the defragmentation process, after which the available SS are more contiguous and continuous for future connection requests. The link-based metrics used in triggering the defragmentation process are link-external fragmentation metric (L-EFM) [42] as given in eq. 3.4, the compaction-based fragmentation metric (Com-FM) [44] as given in eq. 4.1, and the entropy-based fragmentation metric (Ent-FM) [42] as given in eq. 4.2. We have also used a path-based fragmentation metric (Path-FM) [49] as given in eq.4.3.

$$\text{Com-FM} = \frac{\text{Maximum index of used SSI - Minimum index of used SSI} + 1}{\text{Total used SS * Available Blocks}} \tag{3.1}$$

where SSI is the Spectrum Slice Index. A higher value of Com-FM indicates the occupied spectrum is in compacted form, i.e., a low level of fragmentation, and a lower Com-FM value indicates a more fragmented spectrum.

$$\text{Ent-FM} = -\frac{\text{(Used SS/Unused SS)}}{\text{Total SS}} log \frac{\text{(Used SS/Unused SS)}}{\text{Total SS}} \tag{3.2}$$

The higher Ent-FM value indicates a higher fragmentation level and vice versa in the network spectrum.

$$\text{Path-FM} = \frac{\text{Wasted SS + Unused SS}}{\text{Total SS on the path}} \tag{3.3}$$

Wasted SS indicates a sufficient number of spectrum slices per requirement but is unavailable per RSA constraints on the links. Unused SS cannot be used for a few connection requests as it is an insufficient number of available SS following RSA constraints.

In the next section, we study the role of the above fragmentation metrics in accurately identifying the fragmentation state of the network to trigger defragmentation and compare the performance with the Adapted Vectored Fragmentation Metric (AVFM) discussed in the last chapter.

3.3 Simulation and Analysis

3.3.1 Simulation Setup

We consider the same four networks which were discussed in the last chapter: Net-A with 7-nodes 12-bidirectional links, NSF network with 14-nodes 21-bidirectional links, German network with 17-nodes 26-bidirectional links, and Ring network with 12-nodes

12-bidirectional links (Figure 4.2). The network links have 320 spectrum slices (12.5 GHz spectrum slice width), worth 4 THz of bandwidth in the C-band. We use similar traffic dynamics, where arrival rate λ is Poisson distributed, and holding time is exponentially distributed with mean $\frac{1}{\mu}$. The normalized traffic load range is estimated using $\frac{(\lambda/\mu)}{(\lambda/\mu)_{max}}$. We consider a uniformly distributed bandwidth requirement by connection requests, ranging between 12.5 Gbps to 200 Gbps. We assume no waveband conversion scheme at any intermediate node. We studied in the last chapter that the fragmentation level is considerably high in the network where the heterogeneity in the required SS is high. In simulation, we update the network fragmentation metric after one unit time. After blocking of ten connections within one time interval, the fragmentation level after tenth connection is set as threshold value for future defragmentation triggering. The threshold fragmentation is updated in the similar manner next time. Our current study uses only the BPSK modulation scheme with the Shortest Path-First Fit technique to provide the first contiguously available SS to the connection requests. In pursuit of the most efficient technique, the network tends to use multiple modulation formats to their advantage. However, using only BPSK means the network operates in the worst-case scenario. We want to obtain the best-performing metric in the worst-case scenario. We evaluate the performance of the metrics by considering the Average Blocking Ratio of the arriving connection requests. The single points on the plots are an average of 500000 connection requests over 20 iterations. As indicated in the plots, we obtained all the results with a 95% confidence interval.

3.3.2 Performance Evaluation

We compare the network performance of different fragmentation level indicators using the blocking ratio as a primary parameter. The Blocking ratio (BR) is the ratio of blocked requests to total arrived requests during the simulation time. A connection request is generally blocked if continuous and contiguous resources are unavailable on the selected path. We also observe the percentage of the defragmentation time to total observation time when using the different metrics (Table. 3.1). The triggering of the defragmentation is a threshold-based event. Considering the worst fragmentation case in all the network links, i.e., Figure 2.1, we normalized the fragmentation levels and decided on a threshold value of the rate of the blocking of the connection requests and average fragmentation level in the time intervals for initiating the defragmentation. The different defragmentation processes using different fragmentation metrics are AVFM-DF, L-EFM-DF, Com-FM-DF, Ent-FM-DF, and Path-FM-DF. We also considered the no defragmentation (No-DF) case to compare it with the defragmentation performance of fragmentation metrics.

We take two dynamic traffic scenarios:

- Case-I - the probability of arrival of all connection requests is uniform, and
- Case-II - the likelihood of the arrival of connection requests with longer hop paths is more than the shorter hop paths (considering only the shortest path between the source-destination pair).

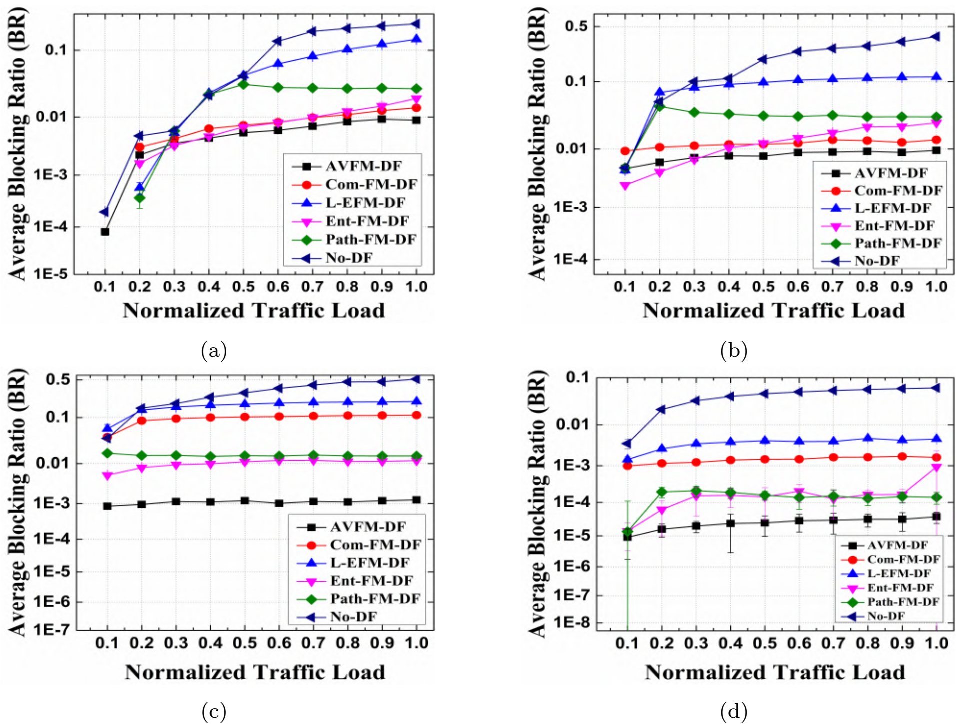

Figure 3.5: BR vs normalized traffic load in Case-I traffic for (a) Net-A, (b) NSF network, (c) German network, and (d) Ring network using threshold-based defragmentation

Figure 3.5(a)-(d) shows the BR as a function of normalized traffic load for the four networks with case-I traffic type. We observe that our proposed metric performs better than the other metrics significantly. The blocking ratio increases with the increase in the

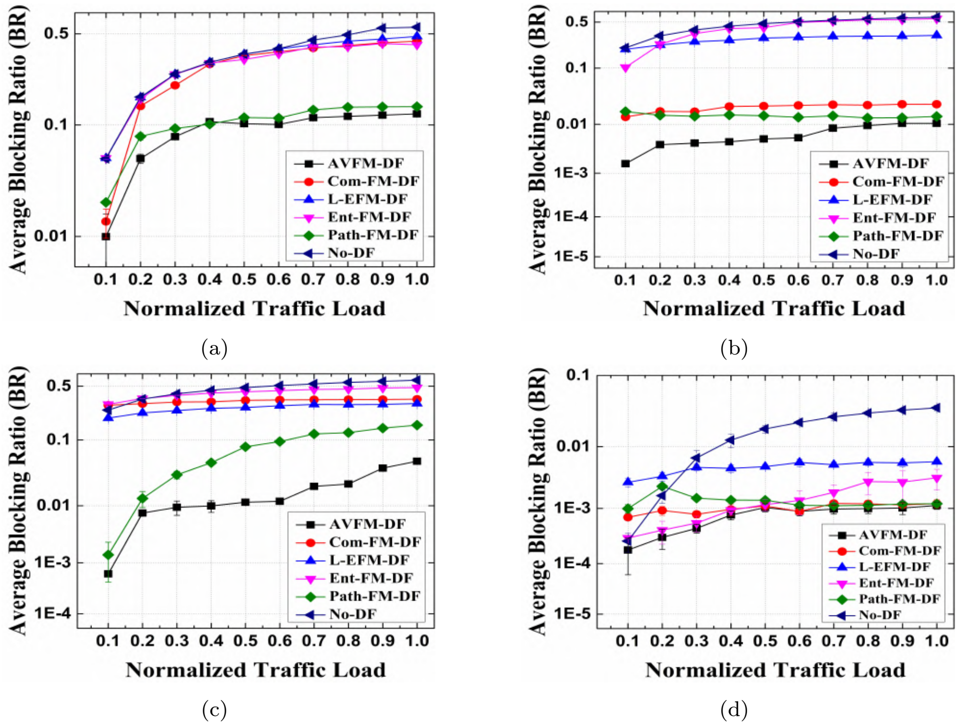

Figure 3.6: BR vs normalized traffic load in Case-II traffic for (a) Net-A, (b) NSF network, and (c) German network using threshold-based defragmentation

network traffic load. We can observe in Figure 3.5(a)-(d) that for all networks, AVFM-DF has less than 1% blocked requests for the considered traffic load range. In Net-A, the L-EFM-DF, Com-FM-DF, and Ent-FM-DF have a maximum of 10%, 2%, and 3% blocked requests, respectively (Figure 3.5(a)). However, in Figure 3.5(b-d), we can observe similar behavior of these three metircs. In Figure 3.5(a-d), Path-FM-DF has a maximum of 5% blocked requests in the considered traffic load range. In Figure 3.5(b)-(d), AVFM-DF has a maximum of 1%, 0.9%, 0.1% and 0.001% of blocked requests in Net-A, NSFNET, German, and Ring networks, respectively for the considered traffic load range. There is more blocking of the connection requests in the no-DF scenario because the network spectrum has fewer contiguously and continuously aligned SS. We conclude that AVFM can better manage the fragmentation than other metrics in the Case-I traffic type for the considered load range.

In Figure 3.6(a)-(d), we plot the BR for the Case-II traffic type as a function of traffic load. In the Case-II traffic type, there are more connection requests with longer path lengths (70%) than connection requests with shorter path lengths (30%). By longer path

Table 3.1: T_d Percentage of total time used for defragmentation for various fragmentation metric use

Networks		Case-I				
		AVFM-DF	Com-FM-DF	L-EFM-DF	Ent-FM-DF	Path-FM-DF
Net-A	Low-Load	0.18	0.08	0.08	0.05	0.04
	High-Load	17.16	6.71	2.21	2.47	19.46
NSFNET	Low-Load	4.94	7.43	5.91	11.16	8.72
	High-Load	11.17	16.25	13.19	23.30	18.77
German	Low-Load	0.26	0.47	0.08	0.15	0.34
	High-Load	17.26	27.91	14.30	15.46	18.17
Ring	Low-Load	1.8	4.8	2.5	3.13	3.18
	High-Load	7.82	15.6	9.1	9.454	6.26
		Case-II				
		AVFM-DF	Com-FM-DF	L-EFM-DF	Ent-FM-DF	Path-FM-DF
Net-A	Low-Load	0.09	0.06	0.01	0.01	0.35
	High-Load	2.31	2.92	0.11	0.09	9.75
NSFNET	Low-Load	5.44	6.09	3.60	1.60	6.86
	High-Load	12.21	13.56	8.29	3.78	15.11
German	Low-Load	0.62	0.58	0.27	0.15	1.04
	High-Load	13.12	10.10	12.69	6.50	34.58
Ring	Low-Load	6.17	5.14	4.8	3.35	6.5
	High-Load	9.17	7.7	8.3	6.26	10.61

length, we mean greater than half of the network diameter and the rest are of shorter path lengths. In Figure 3.6(a) for Net-A, AVFM-DF, and Path-FM-DF, a maximum of 12% connection requests are blocked. The connections with longer paths are more vulnerable to blocking and prone to fragmentation. Therefore, we see overall increased blocking in the case-II traffic type compared to the case-I traffic type. The L-EFM-DF, Com-FM-DF, and Ent-FM-DF may not be able to identify the severity of the continuity fragmentation in the longer paths. Hence, they have more blocked requests than the path-based metrics even after defragmentation. In Figure 3.6(a)-(d), we can see the advantage of using multi-dimensional metrics over link-based metrics. The AVFM-DF keeps the maximum number of blocked connections under 1% in NSF and Ring and under 10% in the Net-A and German network for higher load values. The no defragmentation in the system has worst performance, as the connection requests cannot even find resources on their shortest path because of contiguity and continuity fragmentation. Overall, we can conclude that AVFM has a better performance gain than the link-based metrics and the Path-FM-DF when considering the Case-II traffic type.

Table 3.1 shows the percentage of the total time dedicated for defragmentation operation ($T_d = \frac{\sum_{i=1}^{N} t_d^i}{T_{OB}} \times 100$). The defragmentation time considers the total processing time taken by all the individual defragmentation instances (t_d^i). The defragmentation processing time is the time taken to rearrange the active connections. The processing time may depend on the traffic load (number of active connections) and the defragmentation frequency. Defragmentation frequency (N) is the number of times the defragmentation is triggered per observation time T_{OB}. The most sensitive fragmentation metric would trigger the defragmentation more frequently. We have considered the low traffic load (normalized traffic load ≤ 0.5) and high traffic load (normalized traffic load > 0.5) for Case-I and Case-II traffic types in Table 3.1 for different defragmentation cases.

We observed that both the AVFM-DF and the Path-FM-DF take a significant time for the defragmentation processes in Case -I and Case-II traffic conditions in all four networks. However, the BR of the Path-FM-DF is greater than the AVFM-DF. In most cases, the L-EFM-DF, Com-FM-DF, and ENT-FM-DF take the least defragmentation time, and their BR performance is also not good. It could be due to the inability of the link-based metrics to identify the severity of the continuity fragmentation. In these cases, the metric identifies the fragmentation in the spectrum much later. In some ENT-FM-DF cases, the T_d is the highest in high-load conditions. There is significant defragmentation time, owing to frequent defragmentation and yet higher BR than the AVFM-DF and the Path-FM-DF. We can conclude that the AVFM-DF, which uses the AVFM as a fragmentation indicator, gives better BR performance, but at the cost of time, which is still less than the other path-based metric.

The results show that our metric AVFM improves the network's performance in both traffic types (Case-I and Case-II). The AVFM metric captures the fragmentation level accurately with changing traffic dynamics. Also, it performs better than other considered metrics when used for fragmentation management.

3.4 Concluding Comments

In this chapter, we studied fragmentation management using link-based and path-based fragmentation metrics in a Pro-Reactive defragmentation environment. In real networks, there is significant fragmentation with dynamic arrival and departure of connections. This brings unfairness and inefficiencies in the resource provisioning process. Thus, deploying fragmentation management techniques provides an advantage in network operation. Defragmentation is a costly process but operates more efficiently than other fragmentation management techniques.

In the previous chapter, we studied AVFM as a fragmentation indicator. The effectiveness of the AVFM in actual defragmentation initiating scenarios has been studied in this chapter. We found that threshold-based defragmentation using AVFM as a fragmentation indicator takes more defragmentation time than other link-based metrics; the frequency of the defragmentation operation when using AVFM is low, but the number of rearrangements are more. Nevertheless, AVFM outperforms the other metrics when considering the blocking ratio of the arriving connection requests.

Chapter 4

Fragmentation Management: Non-Defragmentation Approach

> We have, as human beings, a storytelling problem. We're a bit too quick to come up with explanations for things we don't really have an explanation for.
>
> *Malcolm Gladwell, Blink*

In the previous chapters, we studied a Pro-reactive fragmentation management approach. In real life, network service providers strive to have a minimal expenditure per bit successfully transported across the network. The defragmentation process is an effective but still complex and costly process. The performance of any resource provisioning algorithm is relative to the network state and traffic dynamics. So, the Pro-reactive defragmentation approach might not be cost-efficient in all the traffic scenarios. Identifying such traffic scenarios and employing simple resource provisioning techniques could be a better approach considering cost and performance.

In this work, we propose two simple resource provisioning algorithms, RSA-With Penalty (RSA-WP) and Routing and Best Effort Spectrum Assignment (RBESA). In RSA-WP, the penalty is imposed on the links constituting the route if the required number of spectrum slices are unavailable in the fragmented links' spectrum. It ensures less usage of the then-current route by future requests. The links are depenalized after the departure of a few connection requests, i.e., the cost of links is reduced. The reduced weight depends on the availability of considerable-sized blocks of contiguous slices in the link spectrum. In RBESA, a connection request is admitted but assigned a limited spectrum which is less than the requirement. The primary resource assignment uses the most robust modulation configuration, while the limited spectrum assignment means compromising the Quality of Service (QoS) using different modulation configurations. The resource provisioning operations in the fragmented spectrum are considered, but the fragmentation management techniques are not employed, i.e., there is no defragmentation by rearrangement.

The chapter is organized as follows. Section 5.1 discusses the penalty mechanism and RSA-WP. Section 5.2 discusses RBESA, its concept, and its relevancy. In Section 5.3, we present and compare the performance of RSA-WP and RBESA with the shortest path, k-shortest path, and a proactive defragmentation provisioning technique.

4.1 Routing and Spectrum Assignment with Penalty

Before explaining the proposed resource provisioning technique, we represent EON as a graph topology $G(V, L, SS)$, where V is the set of nodes, and L is the set of fiber links. Each link has a set of spectrum slices, SS. When a new connection request arrives at a node, it may require S_r spectrum slices to transmit data to the destination node. The first step in a general provisioning technique is to find the least cost or shortest path. Then, the spectrum slices on all the links of the selected path are searched in the set SS of individual links. At that time, the network can be in a fragmented state. Assignment of S_r slices may not be possible on the shortest path due to unavailable contiguous and continuous spectrum slices. A further practical step would be to look for an alternate path and check for the resources complying with constraints. If the alternate path also fails, the connection request can still be accommodated using constraint relaxation techniques. It may require additional components like waveband converters leading to conversion overhead [1]. The connection request is blocked if an eligible path is still not feasible.

Our proposed RSA-WP technique is very similar to the general provisioning technique. We select the least cost path, but if the spectrum slices are unavailable on the least cost path, we do not use an alternate path. We block the current connection request but update

[1]We do not consider the waveband conversion approach in the present work

the weight/cost of the links on the path. It ensures that future requests could choose a less-fragmented path and, thus, increase traffic admissibility.

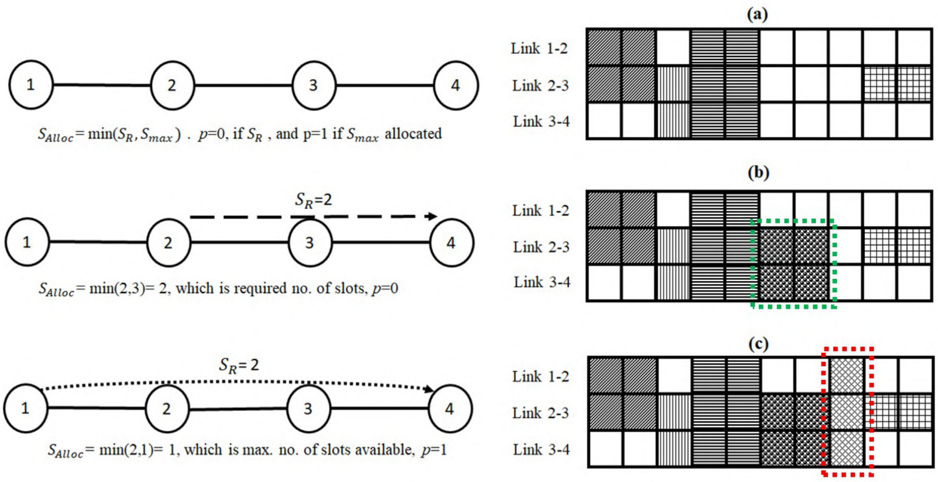

Figure 4.1: An example of RBESA

In algorithm 1, we present the pseudocode of the RSA-WP. The RSA-WP algorithm's overall objective is to find the most suitable paths for the connection requests even in a fragmented network state. Initially the cost of the link is proportional with the distance covered by individual links, $W_i^{t_0}$. The cost is updated as per arrival and departures of the requests. A connection request $CR(o, d, S_r)$ arrives at a source node o. Let the destination node be d. The number of spectrum slices required by the connection request CR is S_r, calculated using available modulation formats and the distance of the routes. p is the binary variable which indicates whether penalty will be imposed on the links or not. A least-cost path $P(o, d)$ is selected based on the link-weights. Then, the S_max is checked on the selected path. If the S_r is available, i.e., $S_r \leq S_{max}$, then it returns the path. As the desired number of spectrum slices are available, no penalty is imposed on the links of the path. It also returns the starting slot index ($SSI(o, d)$) and the last slot index ($LSI(o, d)$) of the range of selected spectrum slices. However, if the S_r can not be accommodated on the least-cost path, then a penalty is imposed on all the links of the path $P(o, d)$. The penalty on the links is dependent on two factors as shown in equation (4.1); first, the difference between the requested slices and maximum contiguously available slices on the path, and second, the total available slices in the i^{th} link of the path. The updated weight of the link, W_i^u, is given by

$$W_i^u = W_i + \frac{S_r - S_{max}^p}{TA_i} \tag{4.1}$$

where, W_i is the current weight of i^{th} link, S_{max}^p is the maximum available continuous and contiguous slices on the path $P(o, d)$, and TA_i is the total available slices on the link i. The penalty is only applied when S_{max}^p is less than the required S_r slices.

The links, where $TA_i < S_r$, are heavily penalized as there are fewer available spectrum slices. The imposed penalty does not severely impact the links that cannot accommodate current requests but have a considerable TA_i value. Future connection requests can use the less fragmented links as per their requirement. The penalty is reduced on the links periodically as explained further. When a certain number of connection requests (NDR) release the occupied resources, the i^{th} link is again checked for the maximum contiguous spectrum slices (CG_{max}^i) and compared with the total available spectrum slices (TA_i). The corresponding fraction is deducted from the link weight as per equation (4.2). That is how the links are depenalized. The updated weights of the links, W_i^u, after removing the penalty is given by

$$W_i^u = max(W_i - \frac{CG_{max}^i}{TA_i}, W_i^{t_0}) \tag{4.2}$$

Where W_i is the current weight of the i^{th} link.

Next, we discuss a modified version of the RSA-WP, which provides the best-effort spectrum assignment based on the availability of spectral resources. It also uses a similar penalizing and depenalizing mechanism.

4.2 Routing and Best Effort Spectrum Assignment for Non-Defragmentation

The current Sliceable Bandwidth Variable Transponders (SBVTs) facilitate modulation level adaptability and give the maximum allowable bandwidth to connection requests. A bit-rate squeezing technique has been discussed in the literature to provide restoration in

Algorithm 1 RSA-WP- To find at least one path and required spectrum slots/slices for a connection request in the network, using link costs with penalties.

procedure RSA-WP
  Input: $G(V, L, SS)$, CR(o, d, S_r)
  Output: $P_{o,d}$, $SSI_{o,d}$, $LSI_{o,d}$
  Find a least cost path $P_{o,d}$ between o and d using G(V,L,SS) status
  Find S_{max} on path $P_{o,d}$
  if $S_r \leq S_{max}$ **then**
    S_r spectrum slices are available on path $P_{o,d}$
    set no penalty and $S_{alloc} = S_r$
    $LSI_{o,d} = SSI_{o,d} + S_{alloc} - 1$
    Return: $P_{o,d}$, $SSI_{o,d}$, $LSI_{o,d}$
  else
    set penalty on links of the path
    Update the link weight with penalty on path $P_{o,d}$.
    Return: the CR connection blocked.
  end if
end procedure

the fiber-link failure scenario using a similar concept [58]. A similar bit-rate squeezing feature could be used, with variable modulation formats, advantageously in provisioning the connection requests and providing a best-effort spectrum assignment. When using higher modulation formats, the required number of SS reduces, but at the cost of compromised QoS, i.e., the signal is affected by noise during transmission for long paths. The best-effort spectrum assignment leverages admission assurance to connection requests with compromised QoS.

In algorithm 2, we discuss a best-effort spectrum assignment on the least cost path. The RBESA is similar to RSA-WP discussed in algorithm 1, with an additional S_{max} assignment step. The main idea is to provide at least half of the required spectrum slices to the new connection request on the least cost path, with some trade-off in Quality of Service, using higher modulation formats irrespective of minimum adaptive distance. This scheme takes advantage of the advanced, versatile capabilities offered by Sliceable Bandwidth Variable Transponders (SBVTs). Such SBVTs enable the adaptation of link parameters according to the number of slices, slot size, data rate, and available spectrum resources.

An example of RBESA is shown in Figure 4.1. S_{alloc} is the number of spectrum slices that can be assigned considering the best available options. If the S_r is available, then

Algorithm 2 RBESA- Finds at least one path and maximum allowable spectrum slices for a connection request in the network.

```
procedure RBESA
Input: G(V, L, SS), CR(o, d, S_r)
Output: P_{o,d}, SSI_{o,d}, LSI_{o,d}

    Find the least cost path between o and d using G(V, L, SS) current status.
    Find S_max on the path P_{o,d}
    if S_r ≤ S_max then
        set no penalty and S_alloc = S_r
        LSI_{o,d} = SSI_{o,d} + S_alloc − 1
        Return: P_{o,d}, SSI_{o,d}, LSI_{o,d}
    else if S_r/2 ≤ S_max < S_r then
        Set penalty on links of the path and S_alloc = S_max
        Update the link weight with penalty on P_{o,d}.
        LSI_{o,d} = SSI_{o,d} + S_alloc − 1
        Return: P_{o,d}, SSI_{o,d}, LSI_{o,d}
    else
        Update the link weight with penalty on P_{o,d}.
        Return: CR connection blocked.
    end if
end procedure
```

$S_{alloc} = S_r$, with no penalties on the link. However, if the initial requirement S_r could not be accommodated, and some $S_{max} \geq \frac{S_r}{2}$) is available, then RBESA should assign it to maximize the admissible traffic. If a compromise in the assigned spectrum slices occurs, the penalty is the same as in Algorithm 1. If $S_{max} \leq \frac{S_r}{2}$), the connection is blocked after applying penalties. In our RBESA study, the incoming traffic with a short holding time is considered, so the possibility of the connection switching to the originally requested slice is not considered for simplicity.

The RBESA is expected to have more traffic admissibility and better network utilization. The possible effect of fragmentation is considerably reduced, as the objective is not to manage fragmentation but to reduce its effect on network performance.

If we talk about the time complexity for simple routing and spectrum assignment technique using a single shortest path, it is $O(V^2 + V.SS)$. The time complexity of the routing and spectrum assignment technique, using a k-shortest path, is $O(k.V.V^2 + k.V.SS)$. The time complexity of RSA-WP is $O(V^2 + 2.V.SS + V)$, using a single shortest path and applying penalties on links of the path. The RBESA has a time complexity of

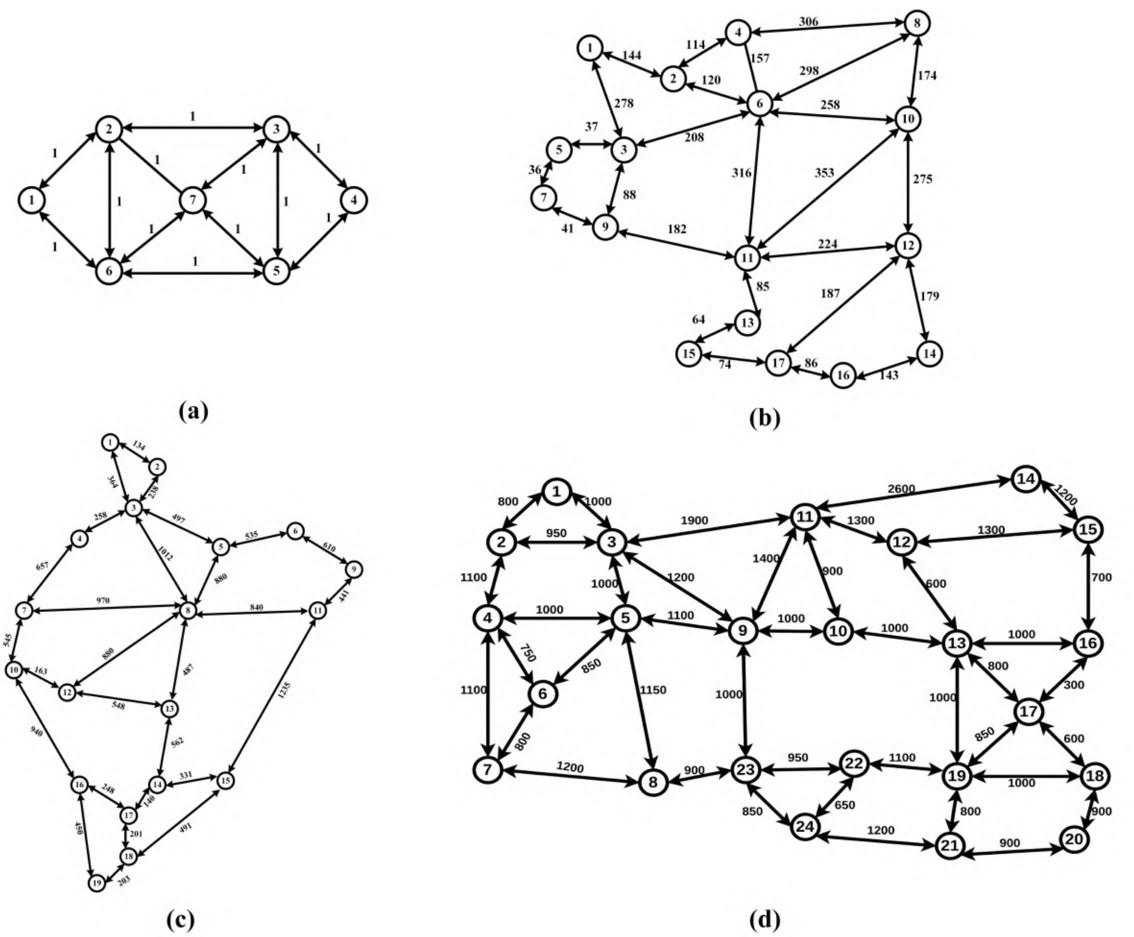

Figure 4.2: (a) Net-A, (b) German network, (c) Indian Network, and (d) US Backbone network topologies.

$O(V^2 + 2.V.SS + V)$. The complexity computation assumes that the centralized controller does all the computations. Here, V is the number of nodes in the network, and SS is the number of spectrum slices in a link between two nodes. Next, we study the simulation performance of the RSA-WP and RBESA to find out their suitability in the fragmented network scenario.

4.3 Simulation and Analysis

4.3.1 Simulation Setup

We simulated the algorithms on four network topologies: 1. 7-nodes 12-bidirectional links Net-A, 2. 17-nodes 26-bidirectional links German network, 3. 19-nodes and 28-bidirectional links Indian network, and 4. 24-nodes and 42 bidirectional links US Backbone Network (UBN). Each fiber link has a capacity of 320 spectrum slices, and each spectrum slice has a spectral width of 12.5 GHz. The arrival of the connection requests at a node is Poisson-distributed with an average arrival rate λ. The holding time of the connection requests is exponentially distributed with an average value of $1/\mu$. We consider a randomly distributed bandwidth requirement (in terms of spectrum slices) ranging from 10 Gbps to 200 Gbps, for connection requests with one slot guard band between adjacent spectrum assignment. We compare RSA-WP, RBESA, simple RSA, K-shortest paths RSA (k-RSA), and periodic defragmentation RSA (PDF-RSA) in the network topologies. The shortest/least cost path selection and first-fit spectrum assignment are considered in the techniques. Three shortest paths are considered in k-RSA. The PDF-RSA uses only spectrum reallocations during the defragmentation step, after every 500 connection requests. The first four techniques are operated in a fragmented network state, while PDF-RSA uses a fragmentation management technique. The waveband conversions are not used. We take Spectrum Slots Blocking Ratio (SBR), Network Spectrum Utilization (NSU), and Link Contiguity Fragmentation (LCF) as the performance parameters in Figure 4.3, Figure 4.4 and Figure 4.5. The LCF is actually an external link fragmentation metric, as mentioned in previous chapters and [63], and covers the spectral fragmentation in links. We obtained all the results in the steady-state scenario. The values in the plots are averaged over multiple simulation results with 95% confidence levels (also shown in plots).

$$SBR = \frac{\text{Number of blocked spectrum slices' (lots)}}{\text{Number of requested spectrum slices}} \tag{4.3}$$

$$NSU = \frac{\text{Total time for which spectrum slices are used}}{\text{Total Simulation Observation Time}} \tag{4.4}$$

$$LCF = 1 - \frac{\text{Largest contiguous free spectrum slices}}{\text{Total number of free spectrum slices}} \tag{4.5}$$

The LCF in equation (4.5) is used under the condition that there is at least one available spectrum slice in the links. Generally, based on the objective type, one desires lower SBR values, higher NSU values, and lower LCF values.

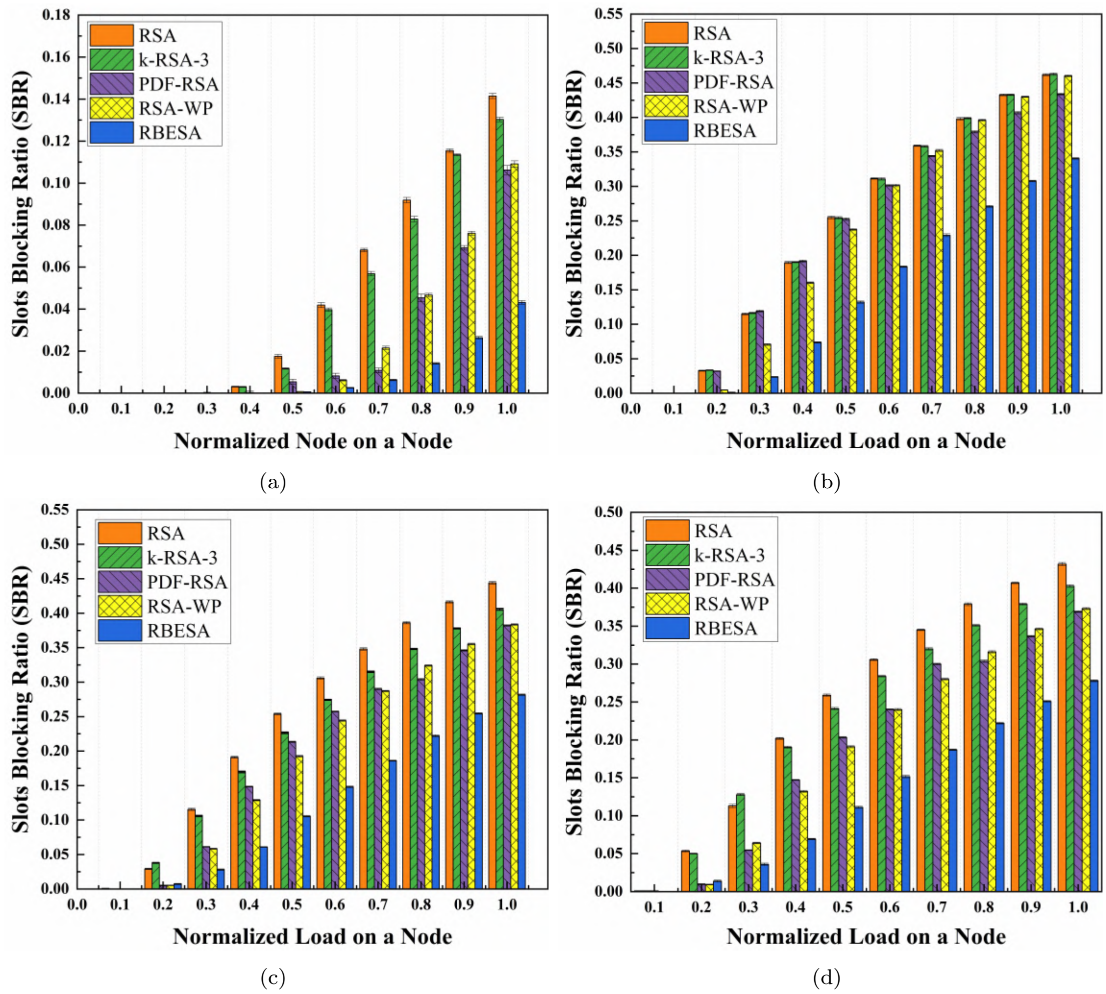

Figure 4.3: Performance of SBR vs normalized traffic load on a node for (a) Net-A, (b) German network, (c) Indian network and (d) UBN network considering five provisioning techniques

4.3.2 Performance Evaluation

The results in the plots are considered for normalized traffic load per node. The connection requests are arriving dynamically in the network. The penalty is applied to the links which cannot accommodate any new incoming connection requests. After checking the link contiguity, the penalty is removed using the (4.2) after every unit time.

First, the SBR performance of the RBESA and RSA-WP is compared with the other three techniques in Figure 4.3. We observe that the RBESA has the lowest SBR than the other four routing techniques, as shown in Figure 4.3(a)-(d). In the N7L24 network, Figure 4.3(a), the RSA-WP also performs better than RSA and k-RSA-3. PDF-RSA performs better SBR than RSA-WP but has added computational and hardware complexity. The

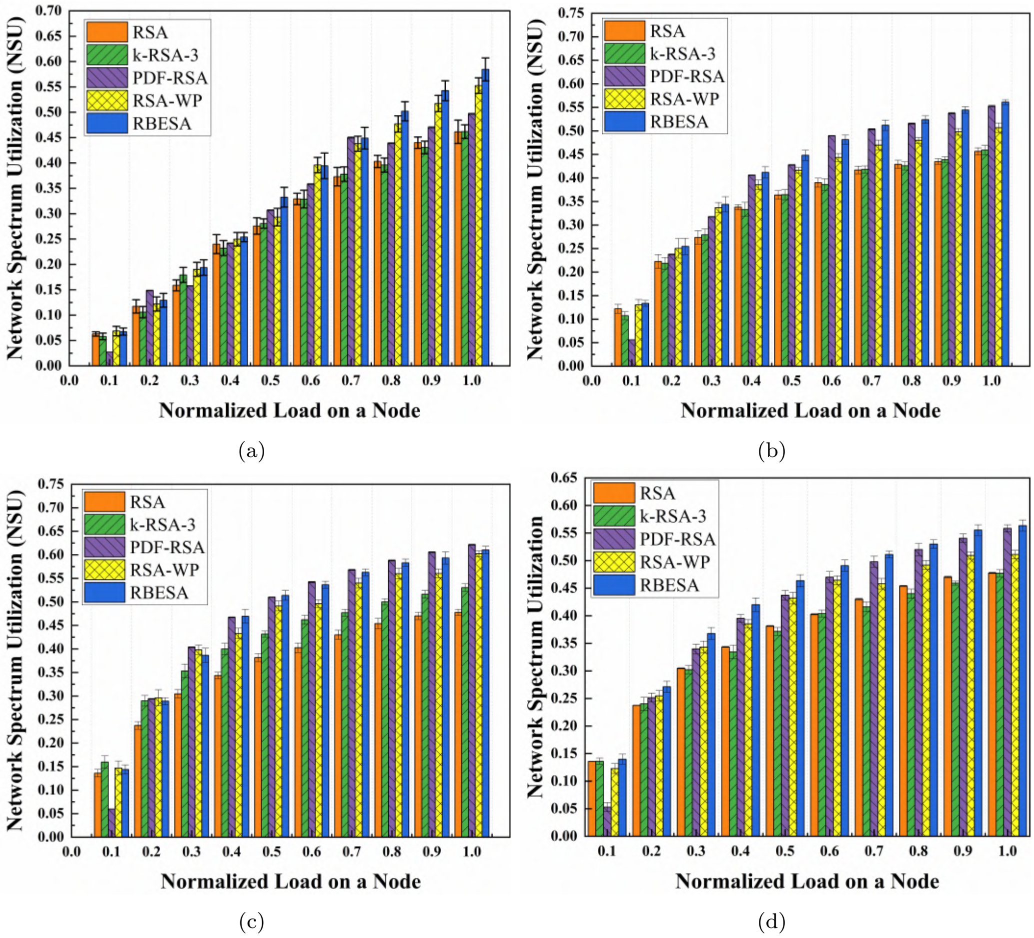

Figure 4.4: Performance of NSU vs normalized traffic load on a node for (a) Net-A, (b) German network, (c) Indian network and (d) UBN network considering five provisioning techniques

RSA-WP could perform equivalent to a periodically defragmented network for low-load traffic conditions, but at higher traffic loads, defragmentation is imperatively necessary. The computational resources could be saved using efficient provisioning techniques such as RBESA and RSA-WP. RSA-WP and RBESAs' SBR advantage over RSA, k-RSA, and PDF-RSA is also seen in the German as well as other network topologies, Figure 4.3(b)-(d). All these plots show that for low-load traffic conditions, RSA-WP and RBESA could be better than PDF-RSA. This advantage of the proposed techniques over PDF-RSA could be due to frequent reconfigurations of active connections on longer paths and since we are using fixed modulation configurations, thus occupying more spectral resources.

Also, the NSU performances of considered networks corroborate with the SBR performance for all the considered techniques. RSA-WP, RBESA, and PDF-RSA have more overall network utilization for all network topologies as these techniques can accommodate

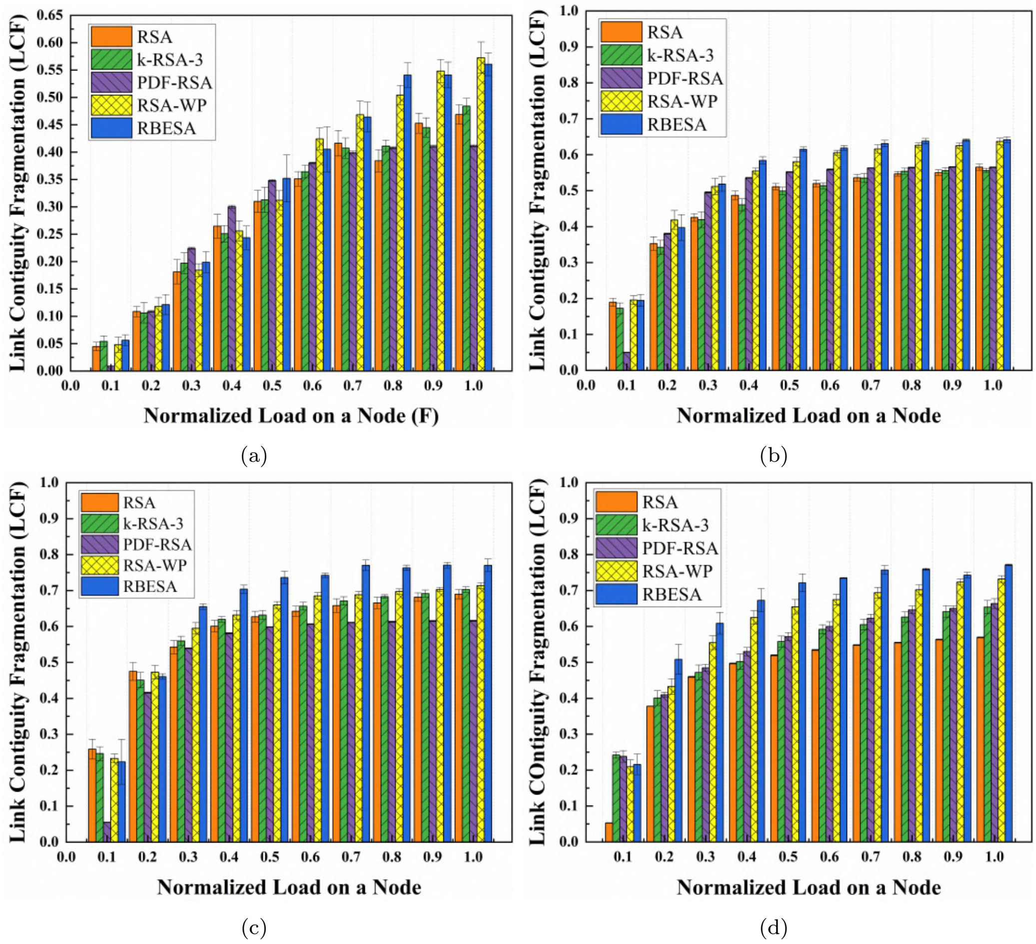

Figure 4.5: Performance of LCF vs normalized traffic load on a node for (a) Net-A, (b) German network, (c) Indian network and (d) UBN network considering five provisioning techniques

more connection requests (Figure 4.4(a)-(d)). In RBESA and RSA-WP, the utilization of the spectrum on the least cost paths after applying penalties on fragmented links increases the overall network utilization. In all the network topologies, for RBESA, the NSU level is more than RSA-WP as it accommodates more bandwidth at compromised QoS, i.e., using higher modulation configurations even for connection requests with the longest pathlengths. The PDF-RSA and k-RSA-3 have higher NSU levels than others, as they must have used longer paths and more spectral resources.

The initial idea was to accommodate more connection requests and provide maximum requested spectrum slices in the network, even in the fragmented environment. Hence, the proposed algorithms, RBESA and RSA-WP, fulfill that criteria but they are not contributing in lowering the fragmentation level. In Figure 4.5(a)-(d), RSA-WP and RBESA have a higher LCF value when compared with RSA, k-RSA-3, and PDF-RSA. It can be attributed to the higher network utilization factor of RBESA and RSA-WP. The higher network utilization can leave small-sized spectrum islands on the links, leading to a significant fragmentation in the overall network. RSA and k-RSA-3 have lower fragmentation levels than the proposed techniques, as there are not enough occupied spectral resources that allow the link to recover from the fragmentation. In N7L24, Figure 4.5(a), PDF-RSA has the lowest fragmentation level, LCF, as it employs fragmentation management. In German, Indian and UBN networks, PDF-RSA has more fragmentation than RSA and k-RSA-3, as they have relatively more connection requests and, thus, heterogeneity in spectrum occupancy. Overall, RBESA and RSA-WP provide better SBR and NSU at the cost of higher LCF. Overall, we can observe that the higher value of LCF for RBESA and RSA-WP can be seen as a cause-effect cycle of spectrum utilization and fragmentation.

We conclude the above section and state that RBESA and RSA-WP can provide the desired performance of lower blocking and better spectral utilization but without additional fragmentation management complexities for low-load traffic conditions.

4.4 Conclusion

In this work, we have proposed a penalty-based routing and spectrum assignment strategy (RSA-WP), where the penalty is imposed on the links of the path that could not admit a request due to the fragmented state. The adaptive link weights based on rejected connection requests' pave the opportunity for future connection requests to select a better path. It gives better traffic admissibility and network spectrum utilization than the fixed- and k-shortest path RSA in a fragmented network state. We also present a best-effort RSA (RBESA), which could use SBVTs' bit-rate variation to its advantage. It admits the connection requests that would have been blocked but with limited spectrum slices. It assigns the maximum available spectrum for that particular request on the selected path. It further improves traffic admissibility and network utilization as compared to RSA-WP. RSA-WP may perform better than the Periodically defragmented resource provisioning (PDF-RSA) for particular network load conditions. Hence, RBESA and RSA-WP could be conveniently used as a replacement to the fragmentation-managed resource provisioning under suitable conditions.

Chapter 5

Adaptive Weights-based Dynamic Resource Provisioning in SDM-EON

Unlearning is a crucial step in a learning process. You can always unlearn things and start again. Unlearn, Learn, Check, and Repeat, if required.

In conversation with Prof. Yatindra Nath Singh

In the previous chapters, we studied different metrics and resource provisioning techniques to manage and mitigate the effects of Fragmentation in Elastic Optical Networks. Space Division Multiplexed systems have been presented as a prospective technology to meet the ever-increasing capacity demand. One of the core research issues in Space Division Multiplexed-Elastic Optical Networks (SDM-EON) is the Routing, Space, and Spectrum assignment (RSSA) to support the maximum possible incoming traffic. Due to the addition of spatial dimension, additional constraints and design issues crop up for the resource provisioning in SDM-EON. There could be severe Fragmentation in the network spectrum along with the crosstalk impairment among cores leading to the unavailability of the resources following RSSA constraints. It limits the efficient utilization of the available capacity in SDM-EON.

This chapter proposes an Adaptive Weights-based Dynamic Resource Assignment (AW-

DRA) technique using SDM-EON's link cost parameters and their respective weights [1]. Each network link periodically adapts the parameter weights, conforming with the link spectral state, using the Teaching-Learning Based Optimization (TLBO) approach.

5.1 Introduction

In Chapter 1, we described the spatial forms (Multiple fibers, MultiCore, and MultiMode fibers) that could enable the spatial dimension in SDM-EON. While selecting the best possible spatial domain scenario, the overall cost plays an important role. MCFs have approximately the same attenuation profile as that of single-core fibers. Thus, using MCF can be efficient from the network design perspective.

In MCF-enabled SDM-EON, there is a Routing, Core, and Spectrum Assignment (RCSA) problem in providing resources to the new service requests. A suitable modulation format can also be used to make the spectrum usage more efficient, making it an RMCSA (Routing, Modulation Level, Core, and Spectrum Assignment) problem. RCSA/RMCSA can be divided into three sub-problems- (1) route selection, (2) core selection, and (3) spectrum assignment. The joint RCSA operation is time-consuming, where the route and the spectrum resources are searched simultaneously, but it promises to provide an optimal result. However, when each sub-problem is implemented independently (decomposed as R+C+SA, RC+SA) or R+CSA), it is a much simpler process as the search space is reduced and is restricted to selective routes only. The objective of any RCSA problem is to find a suitable route and an appropriate set of spectrum slots in a core while complying with the constraints: spectrum contiguity on each link, spectrum continuity on the links of the route, and core continuity (if core switching is not enabled) (See Figure 5.1). The RCSA constraints are followed as per the nodes' switching capabilities [69].

Since each node follows the principle of allocating flexible optical channels to the connection requests in the core, the Fragmentation issue remains in the link spectrum. Moreover, if the cores in MCF are coupled, Inter-core Crosstalk (IXT) is an issue, especially

[1]This chapter is based on the previously published work, refer 'A. Sharma, B. S. Heera, V. Lohani and Y. N. Singh, "Adaptive Weights-based Dynamic Resource Provisioning in Space Division Multiplexed-Elastic Optical Networks (SDM-EONs)," *2022 International Conference on Software, Telecommunications and Computer Networks (SoftCOM)*, 2022, pp. 1-6, doi: 10.23919/SoftCOM55329.2022.9911494.

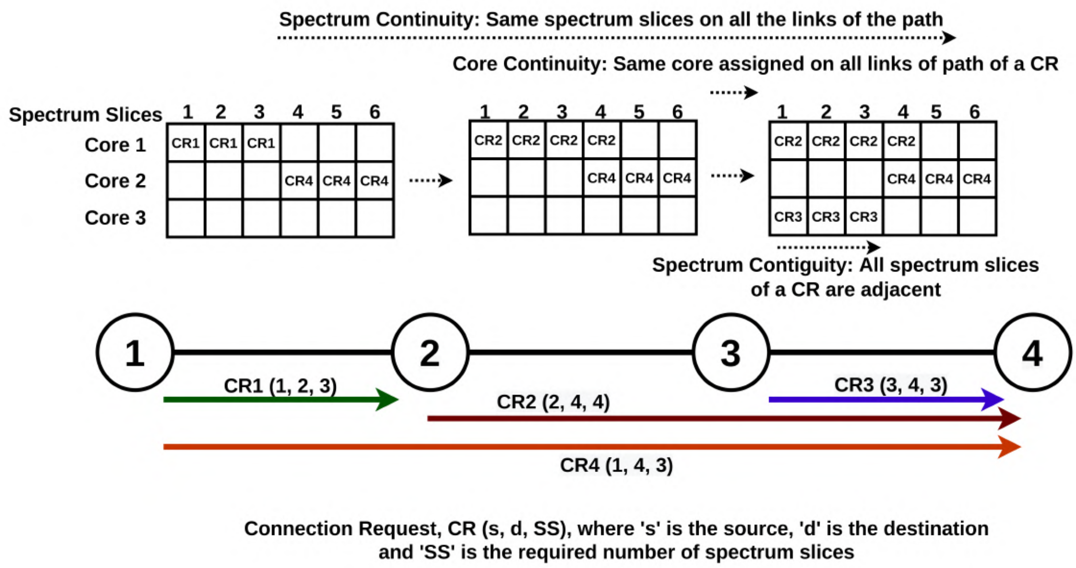

Figure 5.1: Routing, Core and Spectrum Assignment Constraints.

in Strongly Coupled MCF. The IXT impairments limit the excess capacity provided by SDM-EON. The IXT is estimated using an analytical model discussed in chapter 1. If the impairment caused by IXT is significant, it may degrade the quality of transmission (QoT) and limit the reach. Crosstalk-aware (XTA) resource provisioning can help accommodate maximum connection requests while minimizing the possible IXT that may occur, keeping the QoT unaffected.

While managing IXT, assigning the same spectral band to two adjacent cores is prohibited and thus results in Spatial Fragmentation (SpF). However, SpF may bring more Spectral Fragmentation (SF) and, hence inefficiencies in the spectral resource utilization. Spectral and spatial constraints, dynamic allocation, and release of connections, together with crosstalk management, may further intensify the SF. In the SF state of the link, the available spectrum resources become scattered and cannot be used as per constraints, leading to blocked connection requests.

To efficiently use the capacity advantage of SDM-EON, both SF and SpF have been considered at different RCSA steps in the previous works. Rubén Rumipamba-Zambrano *et al.* [70] have optimized using multiple-input multiple-output digital signal processing in optical channels together with resource provisioning to curb the Crosstalk in MCF. Tode and Hirota [71] proposed an RCSA solving technique by using core prioritization to reduce the crosstalk levels, where the core and spectrum slices/slots are selected based on certain unavailable and crosstalk-prohibited states on each route link. Yu Lei *et al.* [72] have proposed a crosstalk-aware dynamic RCSA, where the knowledge of crosstalk levels of adjacent cores and occupied spectrum slots is taken into account while provisioning. Zhang *et al.* [73] have formulated a three-dimensional (spectrum, time, and space) fragmentation metric and used it to allocate resources to minimize future Fragmentation. Lechowicz *et al.* [74] have introduced several Fragmentation metrics to be used in SDM-EONs. They proposed a bordering super-channels concept (a set of spectrum slots adjacent to a busy set of spectrum slots). They used this concept with fragmentation metrics in a fragmentation-aware resource provisioning scheme. Zhao *et al.* [75] proposed a crosstalk-aware spectrum defragmentation technique that uses the spectrum compactness index and crosstalk levels to reassign active connections' spectrum slots. It is a reactive process in response to chosen threshold values of the considered metrics. Trindade and Fonseca [76] used Fragmentation aware route selection and then core and spectrum assignment with core prioritization. It is stated that low crosstalk values maintain lower Fragmentation. We believe this statement holds for low traffic load conditions, but at higher traffic load, both the Crosstalk and the Spectrum Fragmentation could be a menace. Maintaining low Spectrum Fragmentation may lead to more crosstalk and vice versa.

Inspired by the works mentioned above, we presented a simple Fragmentation Aware-resource provisioning in [77] to tackle Fragmentation effects while keeping the crosstalk impairments within threshold values. One question we encountered was, which of the provisioning techniques, i.e., Crosstalk-aware, Fragmentation-aware, link-load based, or distance-based, would be suitable in which conditions? Also, what if, based on traffic and link occupancy status, route selection could be adaptively Fragmentation-aware or Crosstalk-aware?

Also, in the previous works, the core and spectrum selection based on SF and SpF have been performed on fixed shortest or K-shortest routes. To the best of our knowledge, a dynamic route selection and provisioning strategy using multiple link attributes in SDM-EON have not been investigated in the literature. The following section presents our proposed work and studies this aspect in RCSA in a centrally controlled Optical Network scenario.

5.2 Proposed Dynamic Resource Provisioning based on Adaptive Weights

We propose an Adaptive Weights-based Dynamic Resource Assignment (AW-DRA) technique in SDM-EON. Resource assignment involves Route, Core, Modulation format, and spectrum slots selection. The basic idea of this technique is that, between a source-destination pair, the shortest path will not be the same but will keep on changing according to the costs of the links. The cost of the network links will adapt as per changing link spectrum dynamics and the weights of the cost-associated parameters.

The SDM-EON network can be presented as a graph with N nodes (vertices) and L MCF links (edges) to perform the AW-DRA technique by simulations. The nodes primarily act as traffic origin, transit and sink points. Each MCF link has K number of coupled fiber cores, and each core has S number of spectrum slices. The links are the transmission medium, and the route selection depends on a links' characteristics. A link's cost depends on four parameters: one of them is a static, i.e., link length, and the other three are dynamic, i.e., Fragmentation, Crosstalk, and Resource utilization. The cost C_l of the link $'l'$ is calculated using weighted parameters, given by:

$$C_l = \frac{w_h * D_l + w_f * FR_l + w_{xt} * XT_l + w_u * RU_l}{w_h + w_f + w_{xt} + w_u} \tag{5.1}$$

where C_l is the cost of the link, w_h, w_f, w_{xt}, w_u are the weights of the link length parameter, Fragmentation parameter, Crosstalk parameter, and link resource utilization parameter, respectively; D_l is the normalized length of the link l, FR_l is the fragmentation parameter of the link l, XT_l is the crosstalk parameter of the link l, and RU_l is the resource utilization of the link l.

The above link cost parameters are further detailed as follows:

- **Crosstalk in spatial dimension**: Occupying the same spectrum bands in the adjacent cores of a fiber link can deteriorate the transmission quality due to the

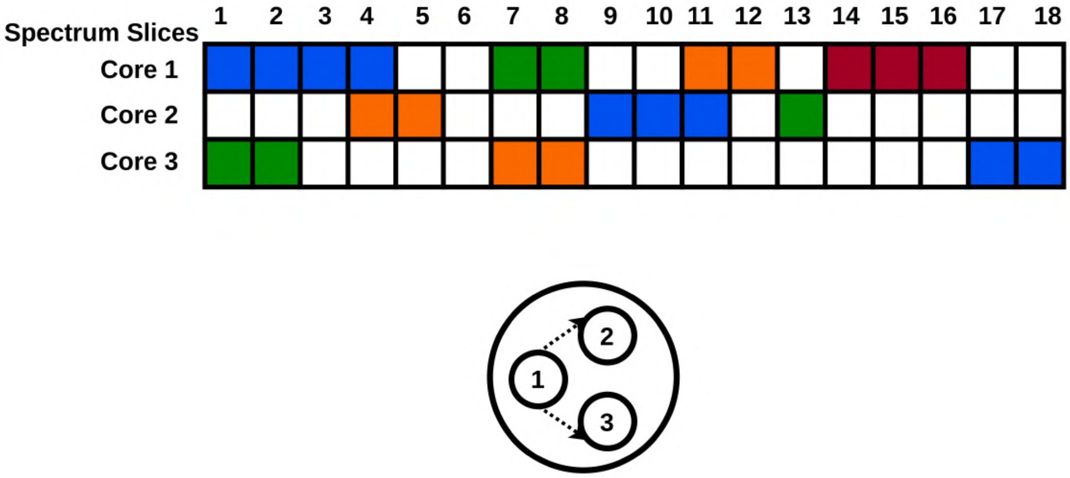

Figure 5.2: An example of the link's spectrum occupancy and core arrangement in the fiber link using 3-cores MCF.

inter-core Crosstalk. $IXT_l^{k_i,k_j}$ [75] is the crosstalk level between adjacent cores k_i and k_j in a link l, calculated using the length of the link, the power-coupling coefficient, bending radius, propagation constant and core pitch.

XT_l in a link is calculated by taking the ratio of Crosstalk based on current spectrum occupancy status and the Crosstalk if all the neighbouring spectrum bands were occupied.

- **Fragmentation in link spectrum of the core**: In this work, we use the ratio of the total number of fragments in a core to the total number of available spectrum slots to indicate the fragmentation level. For example, in Figure 5.2, in core 1, there are four fragments and seven available spectrum slots. The value of $FR_l = mean(\frac{4}{7}, \frac{4}{12}, \frac{2}{12})$, thereby considering all the cores. The range of this parameter is $[1/|S|, 1]$ where $FR_l = 1$ indicates severe Fragmentation in the link.

- **Link-length**: This is a static parameter where the distance (in kilometers) between two nodes is considered. The normalized link lengths (D_l) are considered to scale down the value in the (0,1] range by dividing the link lengths by the longest link length.

- **Resource utilization**: A dynamic parameter, denoted by the ratio of total busy spectrum slots to the total number of spectrum slots. For example, in Figure 5.2, the $RU_l = mean(\frac{11}{18}, \frac{6}{18}, \frac{6}{8})$. The range of this parameter is [0,1], where 1 indicates all the spectrum slots are busy.

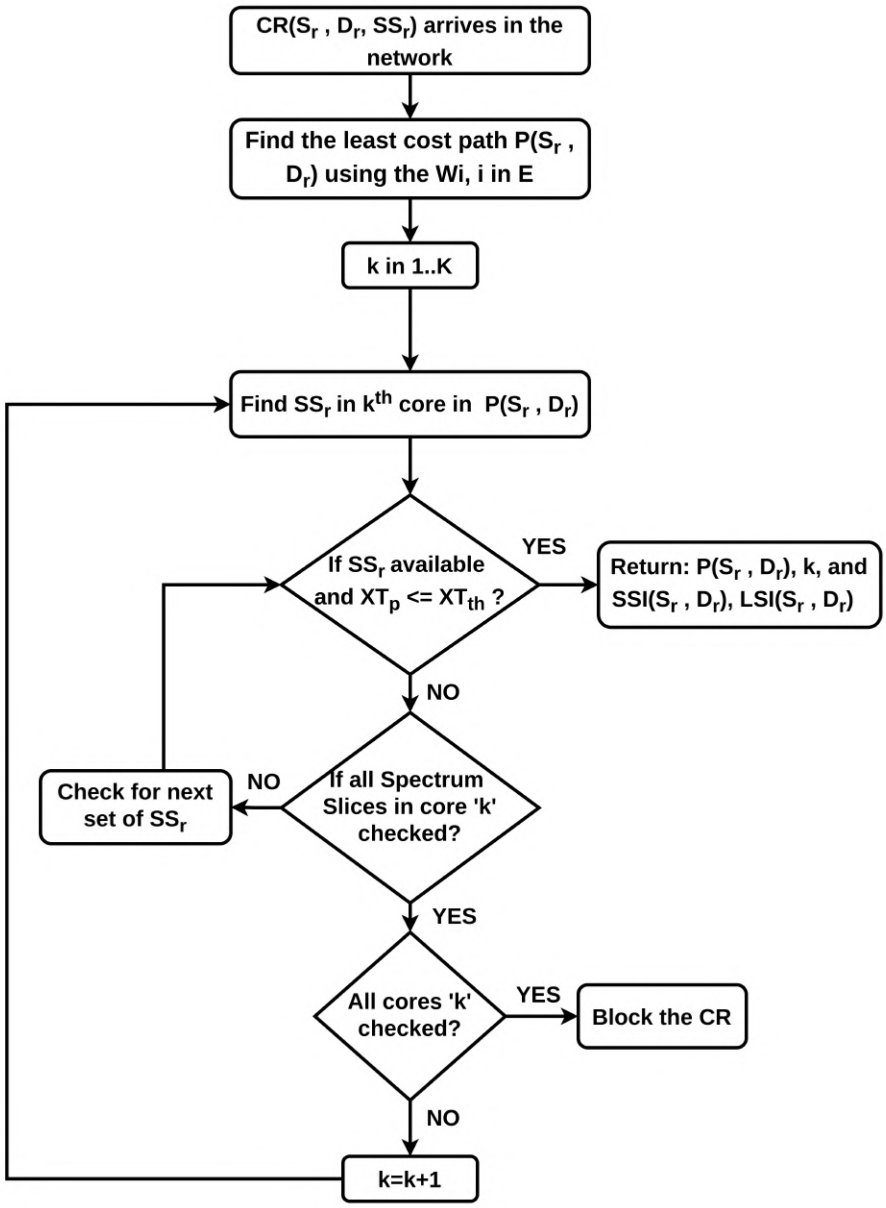

Figure 5.3: Flowchart of the AW-DRA technique when a new connection request (CR) arrives in the network.

When a 'r^{th}' connection request 'CR' arrives at node S_r, the AW-DRA technique checks the requirements, i.e., Destination (D_r), Bandwidth (BW_r) and the required service time (also known as the call holding time). AW-DRA first selects a least-cost route between

S_r and D_r, then select a core, k, using the first-fit strategy. The modulation level, M_r, is selected based on the physical distance of the selected route. The SS_r is calculated using the formulation, $SS_r = \lceil \frac{BW_r}{CW*M_r} \rceil$, where CW is the sub-channel width. Then, in the selected core k, it finds the SS_r, again using the first-fit strategy. The selected spectrum band should maintain the crosstalk level below the predicted threshold. The CR is accommodated if such a spectrum band is available. If not, the next core is searched for the SS_r. If the SS_r is unavailable in any of the cores, then the CR is blocked. The flowchart of the AW-DRA technique is shown in Figure A.2.

5.2.1 Need for the adaptive weights

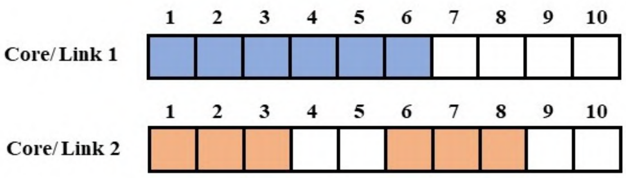

Uniform Weights			Non-Uniform/Adaptive Weights	
Parameters	Link 1	Link 2	Link 1	Link 2
Fragmentation	0.25x(1/4)	0.25x(2/4)	0.40x(1/4)	0.40x(2/4)
Utilization	0.25x(6/10)	0.25x(6/10)	0.20x(6/10)	0.20x(6/10)
Link Length	0.25x(16/20)	0.25x(10/20)	0.20x(16/20)	0.20x(10/20)
Crosstalk	0.25	0.25	0.20	0.20
Total Cost	0.6625	0.65	0.54	0.62

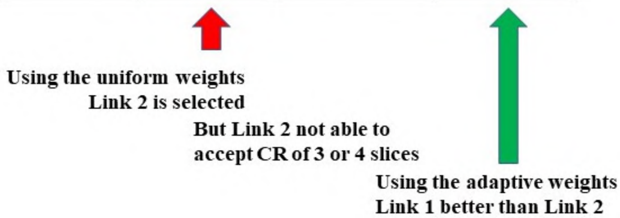

Figure 5.4: An example of fixed weights vs adaptive weights

The parameters mentioned above have been considered independently in many works. However, one thing is clear: all of them affect the choices of least-cost route selection. One interesting question is why one should consider adaptive weights. Why not assign equal weightage to all the parameters?

To answer the questions, let us take an example[2] . We consider two links in Figure 5.4: Link 1 and Link 2. We assumed that both the links have 60% link occupancy state and the highest crosstalk levels, i.e., 1. Next, we assign the fixed weights, 0.25, to all four parameters. The costs of these links using (5.1) make Link 2 a better choice. However, a connection request requiring 3 or 4 spectrum slices could not be accepted. The second best path has to be searched to find resources for such a connection request. However, if we use adaptive weights and the Fragmentation parameter is weighed more, Link 1 is selected with the least overall cost after the weight update calculation. Here, it makes sense to use adaptive weights, as the preference for a particular provisioning technique, i.e., Fragmentation-aware, Crosstalk-aware, or dependent on all of the parameters, will be given as per the network state requirement. The important question is how to find these weights and on what factors they depend. Next, we discuss how the weights are updated using an optimization technique.

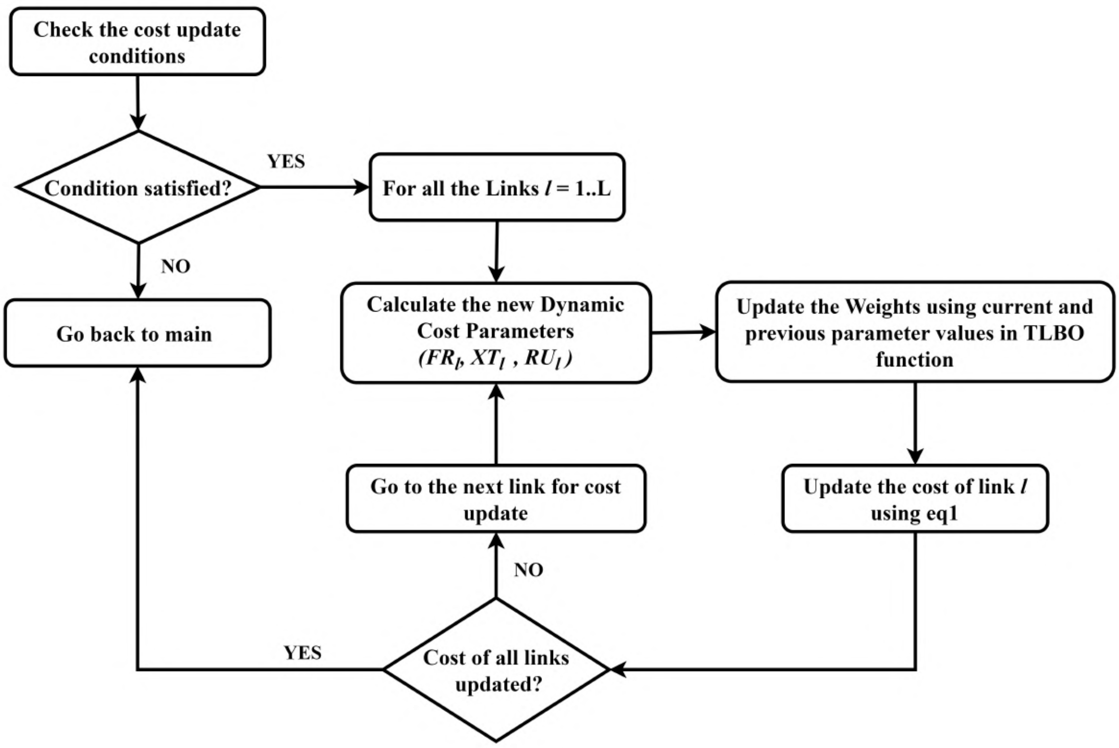

Figure 5.5: Flowchart of Parameter Weights' update process

[2]It is a single core's spectrum status in respective links, but we have used the term link in this example

5.2.2 Teaching-Learning Based Optimization (TLBO)

Resource provisioning issue is a Non-deterministic Polynomial- hard (NP-hard) problem, which means that large instances of such problems can not be solved in a reasonable period. Optimization techniques like heuristics and meta-heuristics find the local and global optimal results in a minimum amount of time and effort by tuning the algorithm's parameters. Meta-heuristics are disassociated from a specific set of problems, thus making it generic, and also, it can avoid getting stuck at local optima. Several meta-heuristic techniques are reported in the literature; for example, Genetic Algorithm, Simulated Annealing, Tabu search Etc. TLBO is another meta-heuristic technique miming the classroom environment where the solution sets learn from the best solution, i.e., the teacher, and then learn amongst themselves to give the best performance. In previous resource allocation studies, TLBO presented a potential for faster convergence and a larger set of global searches than other meta-heuristic techniques [79]. The motivation behind using TLBO in our proposed work is that it can search for many variables (parameter weights) quickly without getting stuck at local optima, with or without using algorithm-specific parameters. Next, we discuss TLBO specific to our problem and explain its functioning.

5.2.3 Calculation of adaptive weights using TLBO

The cost of the links of the network is updated periodically based on the parameters' current values and their adaptive weights, Figure 5.5. We have used TLBO [78] to find the most optimum parameter weights (W_p, where $W_p = w_h, w_f, w_{xt}, w_u$) that capture the network dynamics between the last and current weight updates. The TLBO is shown in Figure 5.6. A random population set of variables, i.e., weights, is obtained first. A fitness function evaluates the optimality of any random solution set W_i. We have used weighted mean square error between the current and previous parameter values as the fitness function. The objective is to minimize the cost of the fitness function, $N - \sum_{i=1}^{N} w_i * \frac{f_i^{prev}}{f_i^{current}}$, where N is the number of link cost parameters, (f_i^{prev}) is the previous parameter value, and ($f_i^{current}$) is the current parameter value. The best solution has a minimum fitness value. Based on the fitness values of the individual variables, the variables are modified

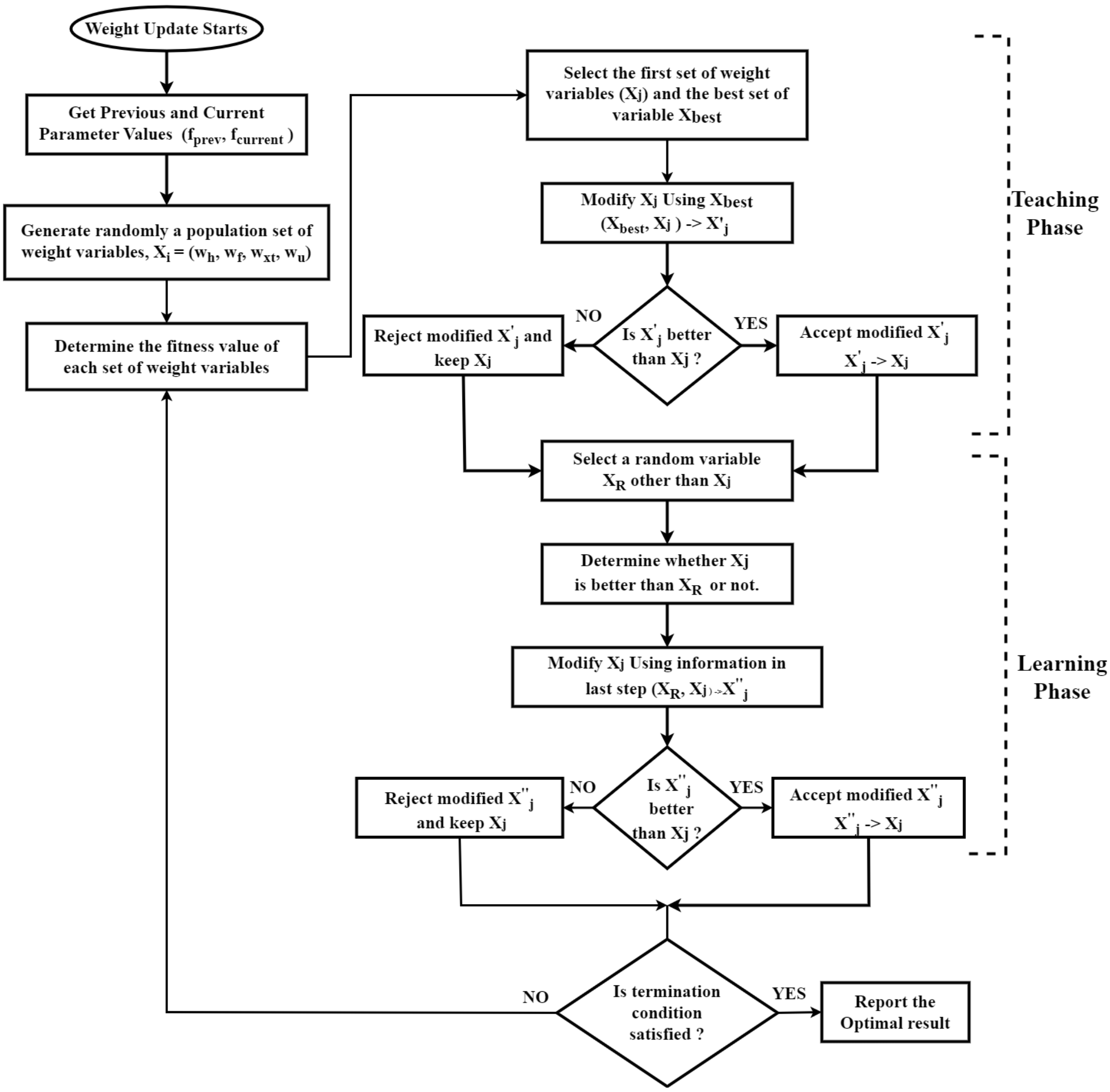

Figure 5.6: Teaching Learning Based Optimization (TLBO)

after learning from the best solution first (teaching phase) and then any random variable (learning phase). We have not included the modification steps specific to the TLBO; however, relevant information can be found in [78] and [79]. The variable (parameter weight set) giving the "learned" solution at the termination condition is considered the optimal result. The parameter weights in the optimization process reciprocate the shift between f_i^{prev} and $f_i^{current}$ to give the best fitness value. In this work, a hundred iterations of the teaching-learning process are the termination condition.

We have used a simple RCSA technique with K-shortest paths (K-RCSA) and a Fragmentation Aware-RCSA [77] (FA-RCSA) techniques to compare our proposed technique in the next section. We used AW-DRA and Fixed Weights-based Dynamic Resource Allocation (FW-DRA) to test our technique. In our technique, we have a single least-cost route (both in AW-DRA and FW-DRA), and then we find suitable core and spectrum slices. The computational complexity is calculated considering V number of nodes,F number of fiber cores, and S number of spectrum slices in each core of the link. K-RCSA technique considers K number of shortest paths. There is an additional space domain, so the computation complexity becomes $O(V^2+F+V.S)$. The computation complexity of K-RCSA and FA-RCSA is $O(K.V.V^2 + K.F + V.S)$. In the next section, we compare the performance of the four techniques using simulations.

5.3 Simulation and Analysis

5.3.1 Simulation Setup

We simulated the proposed and benchmark techniques on the DT-12, UBN-24, and the Indian network (IND-19). The DT-12 comprises 12-nodes and 20-bidirectional MCF links, as shown in Figure 5.7(a). UBN-24 has 24-nodes and 42-bidirectional MCF links, as shown in Figure 5.7(b). MCF links have seven cores, and each core has 320 spectral slots. Spectral slot granularity is 12.5 GHz. The connection arrival is Poisson-distributed, and the connection service time is exponentially distributed. The bandwidth demand ranges from 50 Gbps to 250 Gbps, and the required spectrum slices are calculated accordingly. The simulations are run over 20 iterations for 100000 connection requests in a steady-state scenario. K=3 is used for the K-shortest path route selection for the benchmark techniques. Appropriate modulation levels are considered, ranging from BPSK up to 64-QAM. The weights are updated after departure of 5000 connection requests. All the parameters have a fixed weight of 0.25 in FW-DRA. Request Blocking Ratio (RBR) and Resource Utilization Efficiency (RUE) are primary performance indicators in dynamic simulations. These two

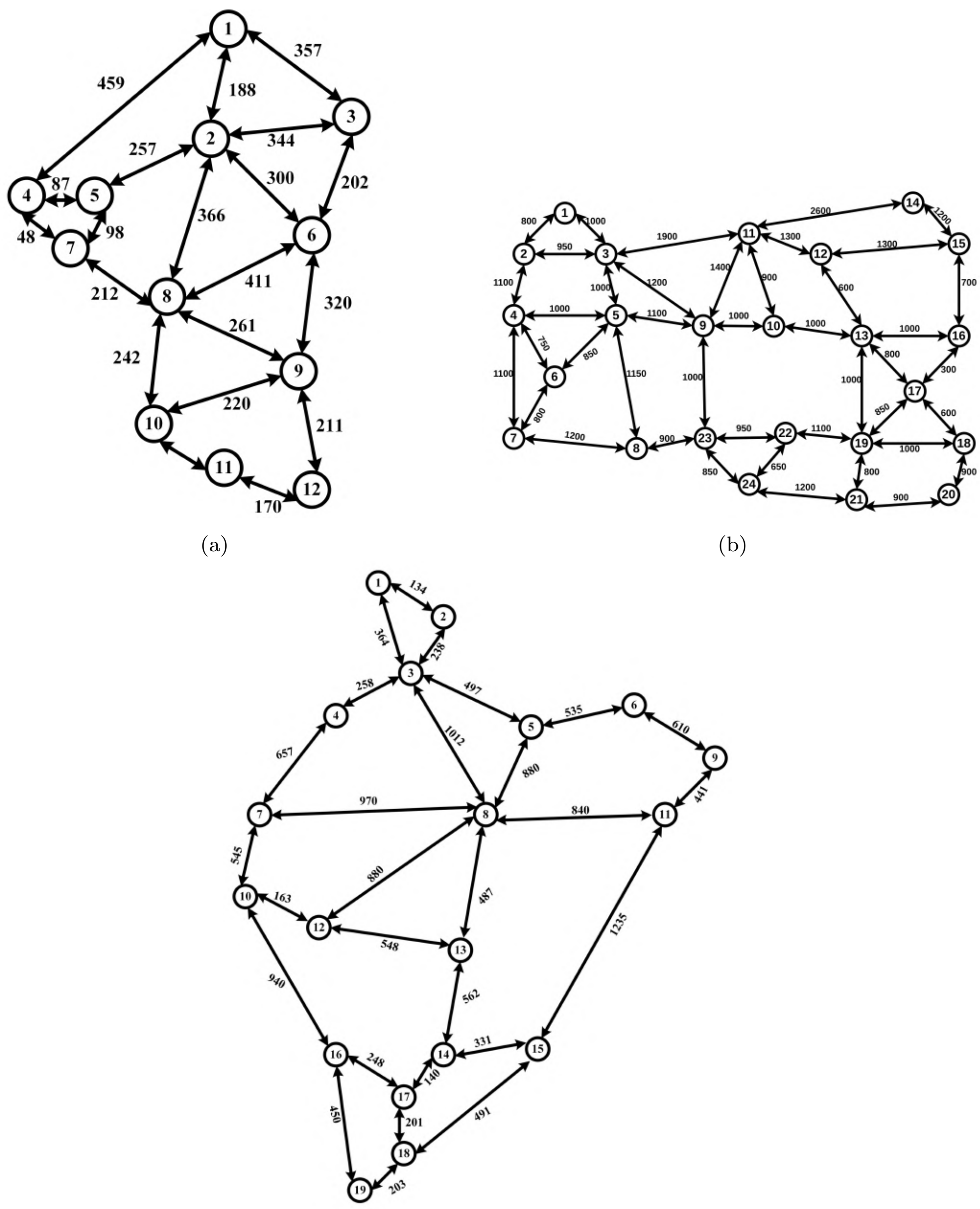

(a) (b)

(c)

Figure 5.7: Network topologies (a) DT-12, (b) UBN-24, and (c) Indian network.

are defined as follows:

$$RBR = \frac{\text{Number of blocked connection requests}}{\text{Total number of arrived connection requests}}, \tag{5.2}$$

$$RUE = \sum_{l=1}^{|L|} \frac{AHT^{*}\ SS_{used}^{l}}{\text{Total Observation Time} * SS^{l}}, \tag{5.3}$$

where AHT is the average holding time of the accepted connection requests, SS^l_{used} is the number of the used spectrum slices by the active connection requests, and SS_l is the total number of the spectrum slices in the link.

5.3.2 Performance Evaluation

The primary results are shown in Figure 5.8 and Figure 5.10. The average weights of the link parameter values are shown in Figure 5.9. The values in the plot are recorded with a 95% confidence interval.

The RBR performance of the AW-DRA technique is better than the FA-RCSA, K-RCSA, and FW-DRA for all the three networks (Figure 5.8). It could be attributed to the consideration of dynamic parameters depending on the link state while deciding on the resources. It selects the route links where the chances of acceptance of the incoming connection requests are higher than the shortest-distance routes. The route selection in FW-DRA also performs better than techniques with multiple available paths, but it could not identify the exact parameter, which may cause performance deterioration. The adaptive weights make it better for AW-DRA to select the most optimum least cost path, which makes it better than the FW-DRA. The FA-RCSA is a special case of AW-DRA and FW-DRA, where w_f is one, and all other weights are zero. With Fragmentation awareness, FA-RCSA performs better than K-RCSA. The reason could be that K-RCSA depends on distance and core availability only and ignores the links' state.

In Figure 5.9(a,b, and c), we can see how the Average Weight of the Parameters varies with different traffic loading conditions. The Fragmentation weight, w_f, increases with the traffic load, which means that the Fragmentation in the link gets severe at the higher traffic load and should be given due consideration. The Resource Utilization in the links does not vary much in a steady state scenario; thus, it has less weight, w_u, than other parameters. Since we are considering crosstalk awareness at the spectrum allocation step, thus crosstalk parameter w_{xt} has less weight at the route selection step. The Fragmentation and Distance related weights parameter, w_f and w_h, are predominantly greater than the w_u and w_{xt} for the given network traffic conditions, which confirms our assertion that uniform weights may not be an optimal solution when considering adaptive route selection in dynamic

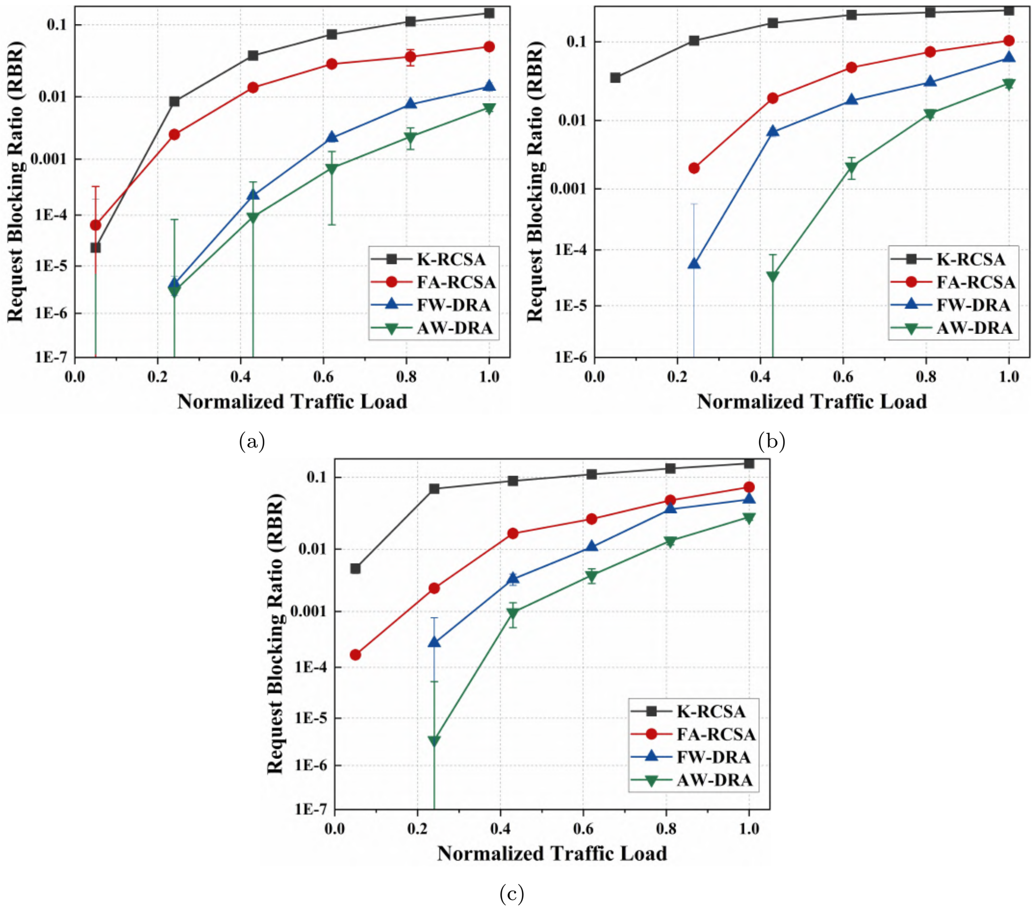

Figure 5.8: Request Blocking Ratio vs Normalized Traffic Load in (a) DT-12, (b) UBN-24 and (c) IND-19.

traffic scenarios.

Also, the AW-DRA has better RUE than other techniques, Figure 5.10(a,b, and c), which indicates that network resources are being used more efficiently by the active connection requests. The higher RUE means more spectrum slices are used over an extended period. This could be due to more active connection requests, the selection of longer routes, or both reasons. We can see in Figure 5.10(a) that the RUE of K-RCSA is more than FA-RCSA at lower load values in the DT-12 network. It could be due to longer path selections in K-RCSA and thus more busy resources, as the RBR is more in K-RCSA at these load values (Figure 5.8(a)). Other techniques like AW-DRA and FW-DRA tend to accept more connection requests, and hence they have adaptive path lengths, they have higher RUE values. It is observed that a maximum RUE goes to 60%, when maximum permissible RBR achieved in AW-DRA. It should be possible to achieve higher RUE, and

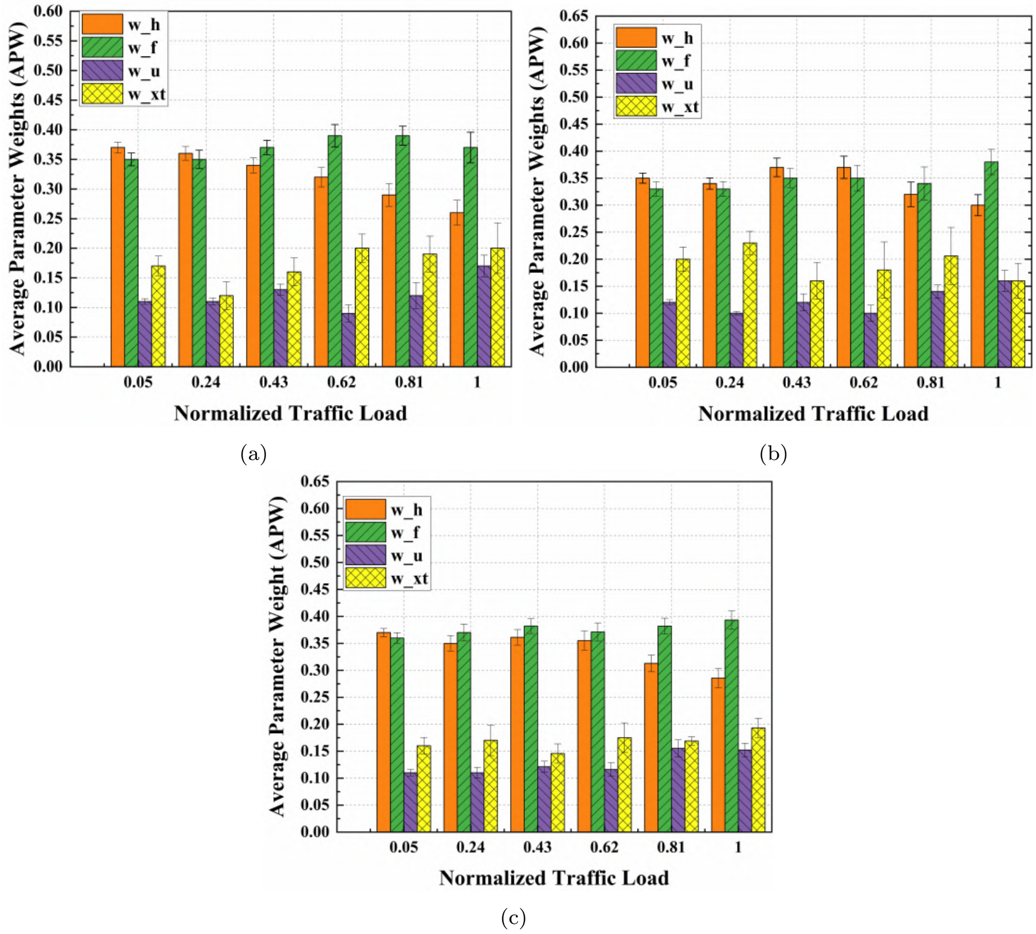

Figure 5.9: Average Parameter Weights of AW-DRA vs Normalized Traffic Load in (a) DT-12, (b) UBN-24 and (c) IND-19.

this is open to further investigation.

The average hop count of the accepted connection requests for the four techniques are shown in Table 6.1. It shows that, on average, the K-RCSA has longer hop lengths than other techniques, so it should utilize more spectrum slices. It, in turn, leads to more blocking of connection requests as the links spectrum state is not considered.

Table 5.1: Comparison of average hop counts of CRs in DT-12, UBN-24 and IND-19 network.

	DT-12	UBN-24	IND-19
AW-DRA	3.148	3.164	2.8
FW-DRA	3.148	3.164	2.89
FAR-CSA	3.2	3.36	2.869
K-RCSA	4.53	5.216	3.37

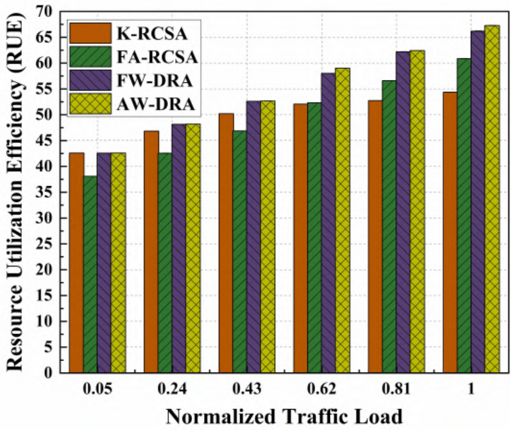

(a)

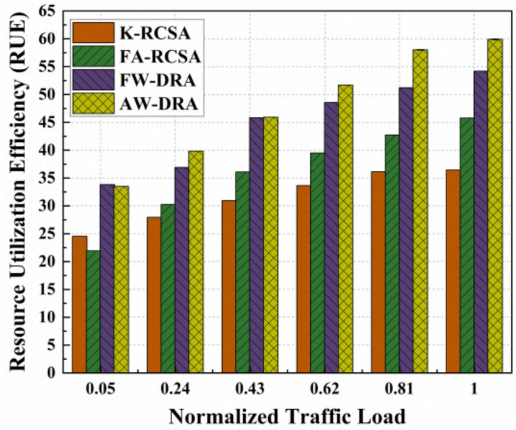

(b)

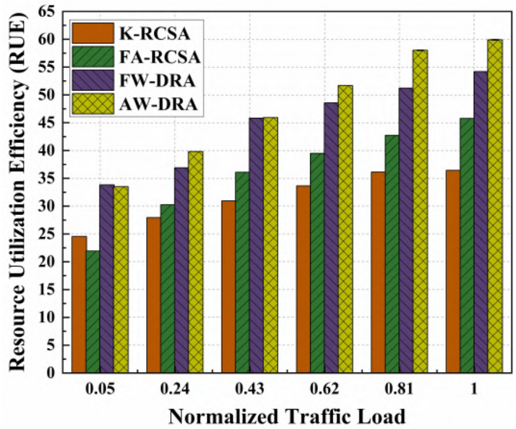

(c)

Figure 5.10: Resource Utilization Efficiency vs Normalized Traffic Load in (a) DT-12, (b) UBN-24 and (c) IND-19.

5.4 Conclusion

In this chapter, we proposed an adaptive weights-based resource provisioning technique, AW-DRA. It uses weighted link parameters' cost while selecting the route. The route can become Fragmentation-Aware, Crosstalk-Aware, or Congestion-Aware based on link spectrum state and weights of paraameters contributing to links' cost. We used Teaching Learning Based Optimization (TLBO) to update the weights of the link parameters conforming with link-state dynamics. We performed simulations on three networks, namely DT-12, UBN-24 and IND-19. Compared to benchmark techniques, the simulation results show that AW-DRA leads to an overall lower blocking ratio (RBR) and better spectral utilization (RUE). Better RBR means the network can accommodate more connection requests, and better RUE signifies that the spectral resources are being used efficiently on least-cost routes by most connection requests. We also presented the variation of adaptive weights for different traffic load conditions and, thus, how considering variable weights could make the overall resource provisioning more efficient and robust.

Chapter 6

Resilient Resource Provisioning in MCF-enabled SDM-EONs

Things we lose have a way of coming back to us in the end, if not always in the way we expect.

Luna Lovegood, in Harry Potter and the Order of the Phoenix.

Space Division Multiplexed- Elastic Optical Networks using Multicore Fibers are a promising and viable solution to meet the increasing heterogeneous bandwidth demands. The extra capacity gained due to spatial parameters in SDM-EONs could encounter detrimental losses if any link failure occurs and timely restoration is not provided. This paper proposes a Protected and Unprotected Working Core Groups assignment (PWCG/ UPWCG) scheme for differentiated connection requests in multicore fiber-enabled SDM-EONs. A PWCG is inherently protected by resources in a Dedicated Spare Core Group (DSCG). First, we divide the cores into three groups using traffic and crosstalk considerations. In the second step, we use the obtained core groups for resource provisioning in dynamic network scenarios. The effectiveness of our proposed technique is compared with a Link Disjoint Path Protection (LDPP) technique, and the simulation study verifies our assertions and the findings.

6.1 Introduction

Recently, Multicore Fibers (MCF) have been the centre of research as they have the same attenuation profile as a single-mode fiber [17]. The need to transmit more information in a single fiber led to significant research in multicore fibers. The transmission capacity can be increased linearly within the existing fibre dimension by increasing the number of spatial parameters or cores resulting in MCF. However, the number of cores or spatial parameters in a single fiber is limited by the core pitch (distance between adjacent cores). The smaller core pitch value leads to more crosstalk impairment, where the power of the signal in one core is leaked into the adjacent cores and deteriorates the performance of the adjacent core's transmission. There is an inherent trade-off between the number of usable spectrum slices in the adjacent cores and the loss of signal quality due to crosstalk accumulation. Crosstalk-aware and crosstalk-avoidance techniques are used when providing resources to connection requests to mitigate the severe effects of crosstalk in Multicore Fibers-based SDM-EONs (MCF-SDM-EON).

When performing the Crosstalk-Avoidance or Crosstalk-Aware Resource provisioning in Route, Core, Modulation and Spectrum Assignment (RCMSA), almost a couple of cores' equivalent bandwidth becomes unusable. The maximum spectral utilization is limited to 60-70% because of intercore-crosstalk considerations in RCMSA. The excess capacity gain of the SDM-EONs can be truly realized by utilizing the crosstalk-affected capacity efficiently. One of the possible techniques is to design such fibers, which only have the usable capacity and are unaffected by the crosstalk impairments. Another technique is to use the available capacity judiciously and effectively. One such efficient and reliable technique is to use the affected capacity to provide resilience to the operating set of connection requests. In that way, the previously unused capacity can be useful, even if for a short duration during the failure time but at the cost of compromised signal quality. The previously proposed protection techniques have also used similar techniques, but we have tried to formulate a much simpler protection technique based on the core utilization and traffic characteristics.

Resilience techniques are employed with provisioning to avoid data losses in the event of failure of the network components. The amount of data that a single MCF fiber can carry is much more than a single-core fiber, and a proportional loss of bandwidth is expected due to the failure. The protection techniques are employed to provide resilience, where the spare capacities are reserved for the backup. The active connections are switched over to spare capacity resources in case of failure [80]. The protection technique could be dedicated-type or shared-type. In shared-type protection, multiple primary routes share the same spare capacity for backup and primary routes need to be link-disjoint. The backup routes are calculated using the spare capacity, and 100% re-establishment of affected connections is possible (in single link failure scenarios). The objective of the resilience techniques is to provide 100% protection with minimum spare capacity and restoration time. The reserved spare capacity creates redundancy and may reduce the effective usable capacity.

Several works have considered crosstalk-aware resource provisioning together with protection techniques. Authors in [81] have used Failure-Independent Path Protecting pre-configured cycles to provide resilience using a PERFECTA algorithm. Using pre-configured cycles give the advantage of shorter restoration time and higher spare capacity efficiency. Authors in [82] and [83] have used Shared Backup Path Protection (SBPP) to provide 100% protection together with minimal crosstalk effects and blocking of the connections. In [84], authors have proposed a Link-disjoint Path Protection (LDPP) technique with crosstalk, blocking and spectrum utilization considerations. Authors in [85] and [86] have used the multipath strategy in combating the losses due to single link failure. Many proposed works have yet to discuss spare capacity redundancy and its associated leverage with crosstalk awareness. In this work, we propose to use the crosstalk-affected core capacities as the reserved spare capacity for protecting connection requests.

6.2 Proposed Resilient Resource Provisioning

In this work, we leverage the unusable capacity due to the crosstalk considerations as the spare capacity needed to protect the prioritized services in SDM-EONs. The concept of the Protected Working Cores (PWC) group has been derived from the Protected Working Capacity Envelope-based protection in WDM to provide link protection. In place of wavelength-level protection switching, we are using Core-level protection as it results in simplified and cost-efficient switching operations and timely restoration, [87]. This resilience model contains three types of resources in the network links: Unprotected, Protected Envelope and Spare Resources. We adopt a similar approach, and the MCF's cores are divided into three groups: Dedicated Spare Cores (DSCG), Protected Working Cores (PWCG), and Unprotected Working Cores (UPWCG) groups. The connection requests in the PWCGs are inherently protected by the protection structures using the DSCGs. When any failure occurs, the connections in the PWCGs are switched to the backup routes in DSCGs. The backup routes are in the form of protection cycles, which can provide better spare capacity efficiency. The protection cycles can protect an on-cycle failed link by providing one backup route and a failed straddling link by providing two backup routes, Figure 6.1. The full waveband and full core switching are assumed here. The connection requests provisioned in the UPWCG require re-routing of the connections using the left-over capacities after PWCG connections are protected in the event of failure. There is no guarantee of restoration, and the time to find backup resources may also keep increasing, leading to the deterioration of the quality of service.

We have used three Service Class Types (SCT) to assign the resources in the mentioned core groups. Table 6.1 shows the type of protection required by each SCT and the core group to which they belong. Considering the cost, the SCT-I are the service type requiring the best and uninterrupted service quality and could be priced more than the other SCTs.

Table 6.1: Service Class Types

Service Class Type (SCT)	**Quality of Protection**	**Provisioning Core Group**
SCT-I	100% Protection	PWC
SCT-II	Best Effort Restoration	UPWC
SCT-III	No Protection	UPWC and DSC based on effective protection

When SCTs' connection requests arrive and depart dynamically in the network, we must find the most relevant resources and accommodate the maximum number of such requests. The whole process of providing resilient resource provisioning requires grouping

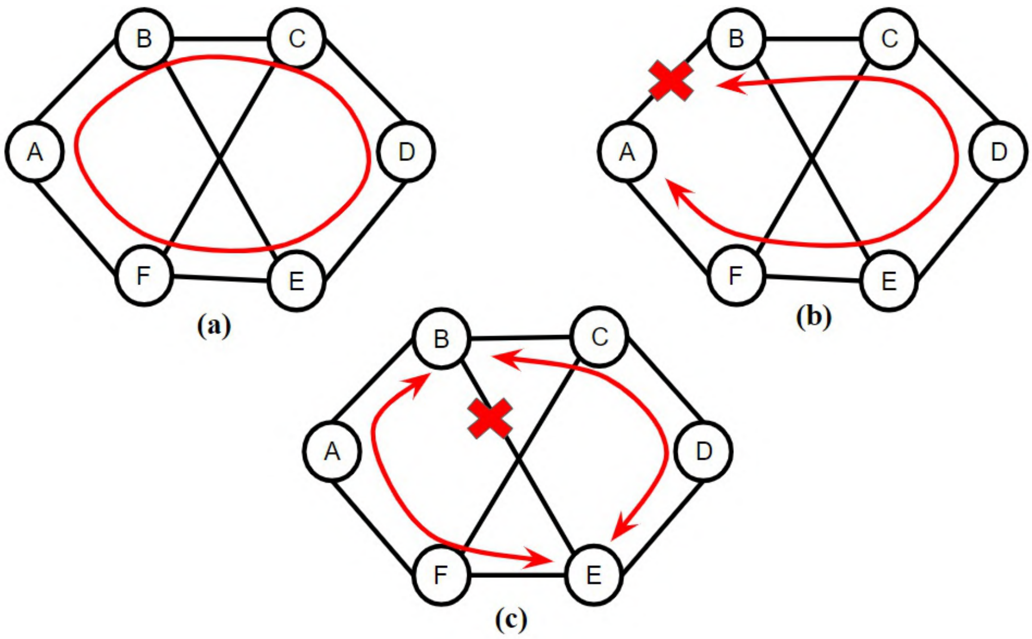

Figure 6.1: (a) Protection Cycle A-B-C-D-E-F-A, (b) when A-B fails (undirected), the services are protected by providing capacity on a single backup route, B-C-D-E-F-A, created by surviving links of the protection cycle, and (c) when B-E fails (undirected), the services are protected by providing capacity on two backup routes, B-A-F-E and B-C-D-E, created by surviving links of the protection cycle.

the cores first. Then the connection requests are assigned to their relevant core groups. We divide the process into three parts: Resource Planning, Resource Provisioning and Reprovisioning after a failure event.

6.2.1 Resource Planning Model

Resource Planning requires prior information on types of arriving connection requests, i.e., the fraction of total arriving connection requests constituting SCT-I, SCT-II and SCT-III individually. The total capacity available in each MCF-link is equivalent to the number of cores as we have considered core-level granularity for the protection structures. We have used an Integer Linear Programming formulation to find the most optimum core group arrangement to provide resilient resource provisioning in the next step.

We model the SDM-EON as a mathematical model using the Integer Linear Programming formulation. The network is modelled as a directed graph with V number of nodes and L number of directional links. In this model, capacity of the links is represented by the

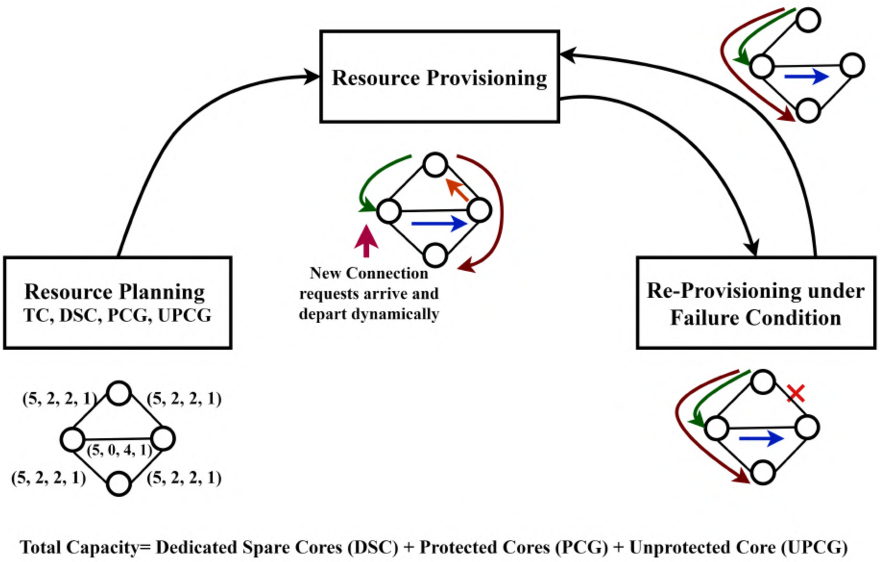

Figure 6.2: Schematic of the resource provisioning with PWC groups

number of cores K. To provide the backup routes/paths, we have used the P number of protection cycles. Table 6.2 lists the sets, parameters and variables needed for the ILP model.

$$\textbf{Minimize} \sum_{i \in L, k \in K} XTC_k * \delta_i^k \tag{6.1}$$

Subject to:

$$S_i = \sum_{p \in P} \pi_i^p * n_p, \forall i \in L \tag{6.2}$$

$$P_i = \sum_{p \in P} X_i^p * n_p, \forall i \in L \tag{6.3}$$

$$UP_i = K - P_i - S_i, \forall i \in L \tag{6.4}$$

$$W_{max} = max(P_i), \forall i \in L \tag{6.5}$$

$$W_{min} = min(P_i), \forall i \in L \tag{6.6}$$

$$\sum_{k \in K} SL_i^k = S_i, \forall i \in L \tag{6.7}$$

$$\sum_{k \in K} PL_i^k = P_i, \forall i \in L \tag{6.8}$$

Table 6.2: List of Parameters and Variables in the ILP model.

Sets	
V	Set of Nodes
L	Set of Links
P	Set of Protection Cycles
K	Set of Cores on each link
Parameters	
CP	Cost of Protected Working Groups
CU	Cost of Unprotected Working Groups
CS	Cost of Dedicated Spare Working Groups
XTC_k	Cost of k^{th} core due to Crosstalk-considerations
W_{max}	Maximum protected core groups required
W_{min}	Minimum protected core groups required
π_i^p	1, if p^{th} protection cycle crosses link i, otherwise 0
X_i^p	1, if p^{th} protection cycle provides on-cycle protection to i^{th} link, 2 for straddling protection, 0 otherwise
Variables	
S_i	Total spare capacity on i^{th} link
P_i	Total protected capacity on i^{th} link
UP_i	Total unprotected capacity on i^{th} link
n_p	Number of copies of p^{th} protection cycle
SL_i^k	1 if k^{th} core on i^{th} link is assigned DSCG, 0 otherwise
PL_i^k	1 if k^{th} core on i^{th} link is assigned PWCG, 0 otherwise
UPL_i^k	1 if k^{th} core on i^{th} link is assigned UPWCG, 0 otherwise
δ_i^k	the cost for k^{th} core in i^{th} link

$$\sum_{k \in K} UPL_i^k = UP_i, \forall i \in L \tag{6.9}$$

$$PL_i^k + UPL_i^k + SL_i^k = 1, \forall i \in L, \forall k \in K \tag{6.10}$$

$$\delta_i^k = (CS * SL_i^k) + (CU * UPL_i^k) + (CP * PL_i^k), \forall i \in L, \forall k \in K \tag{6.11}$$

A connection request requiring 100% protection should be ready to pay extra in terms of cost-per-bit for reliable service. The under-utilized cores are costly to maintain from the service provider's point of view. So, the overall objective is to divide the cores among the three categories to minimize the overall cost, eq 6.1. The constraint in eq. 6.2 assigns the spare capacities (cores) and eq. 6.3 gives the protected capacities on each link of the network. Eq. 6.4 gives the total capacity combination on each link. Eq. 6.5 and Eq. 6.6 gives the variation of the protected working capacity on each link. Eq. 6.7, Eq.

6.8 and Eq. 6.9 gives the assignment of each core on the links for spare, protected and unprotected capacities, respectively. Constraint in Eq. 6.10 ensures that each core is assigned to exactly one core group during the group assignments. Finally, Eq. 6.11 gives the core cost status after grouping them on each link.

6.2.2 Resource Provisioning

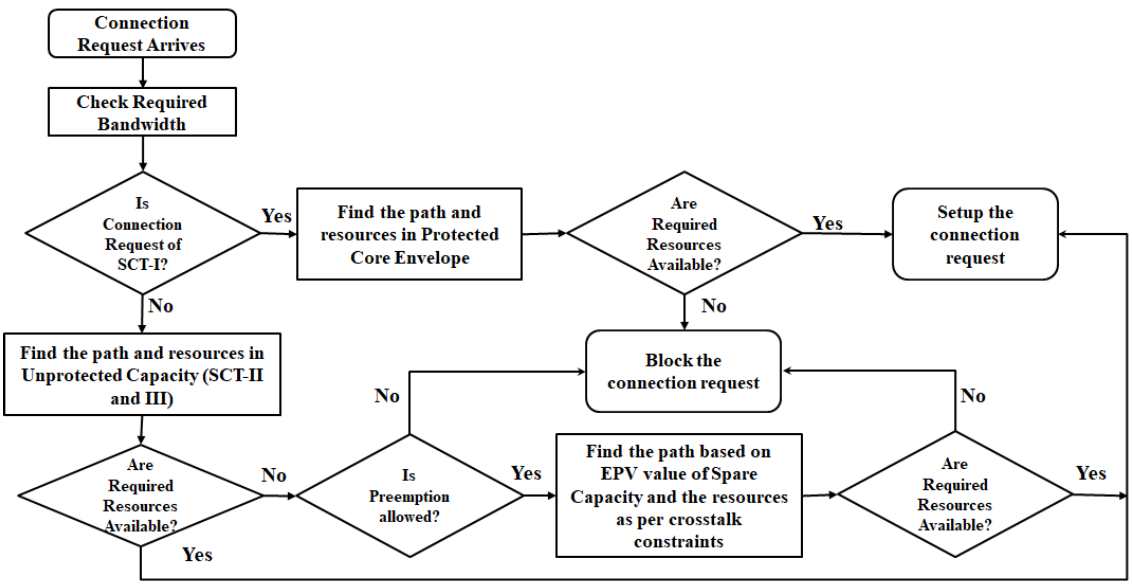

Figure 6.3: Resilient resource provisioning with PWC groups

In the resource provisioning step, the connection requests arrive and depart dynamically. The shortest route is selected using the distance as the cost. On the selected route, the resources are provided in the relevant core groups using first-fit spectrum slices and crosstalk considerations, if available; if not, the connection requests are blocked. If the arrived connection request is of type SCT-I, then the resources are searched in PWCG. If the arrived connection request is of type SCT-II, then the resources are searched in UPWCG. If the resources are available in the PWCG and UPWCG for SCT-I and SCT-II, respectively, then the connection is provisioned and if not, then blocked. For connection requests of type SCT-III, when the connection request arrives, the resources are searched for in UPWCG. If available, a connection request is provisioned. If not, the Effective Protection Values (EPV) of the cores in the DSCG are calculated. EPV is the ratio of the spectrum slices used to provide resilience and the total number of slices in the core.

If the EPV is less than 25% of A-priori protection value (spare capacity reserved for protected capacities), we provision the SCT-III in the DSCG. If not, the connection request is blocked. The flowchart of the resource provisioning is shown in Figure 6.3.

If a single link failure occurs, the active connections on the failed links are reconfigured according to their protection type. At first, all the SCT-III occupying DSCG gets released and relinquishes the resources. The SCT-III are not protected; hence, all the affected requests of this type are blocked. The connection requests of SCT-I are switched to the same spectrum slices in the DSC protection structure, which will be configured at that time to make the backup path. The connection requests of type SCT-II are provided backup resources on the fly, i.e., the backup resources are calculated using the UPWCGs of the surviving links to provide link protection.

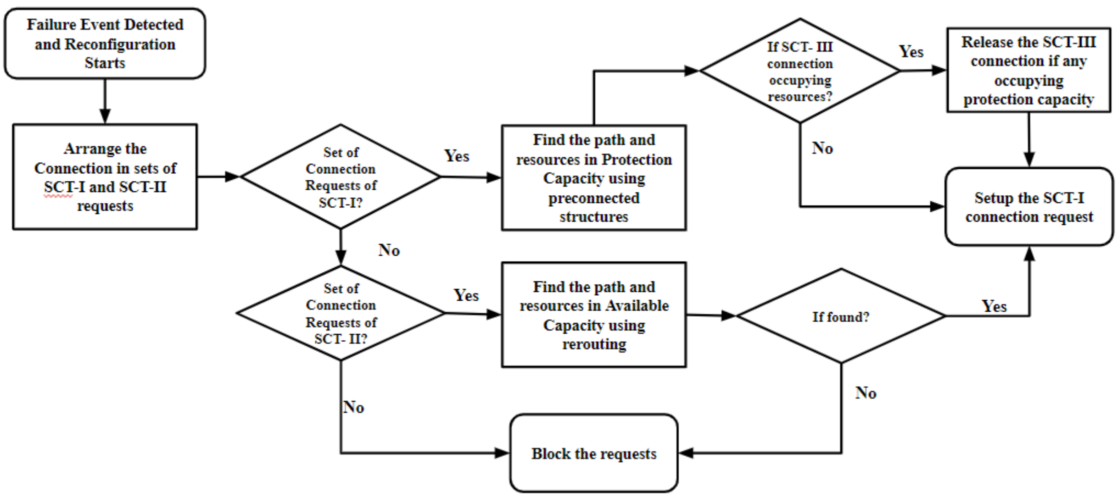

Figure 6.4: Resilient resource provisioning using groups after failure

The computational complexity of the proposed technique involves only the routing and spectrum assignment steps, $O(V^2 + K + V.S)$, where V is the number of nodes in the network, K is the number of cores, and S is the number of spectrum slices on each core of the link. The ILP is performed only once in the offline scenario, which is why the computation time of ILP is neglected.

6.3 Simulation and Analysis

6.3.1 Simulation Setup

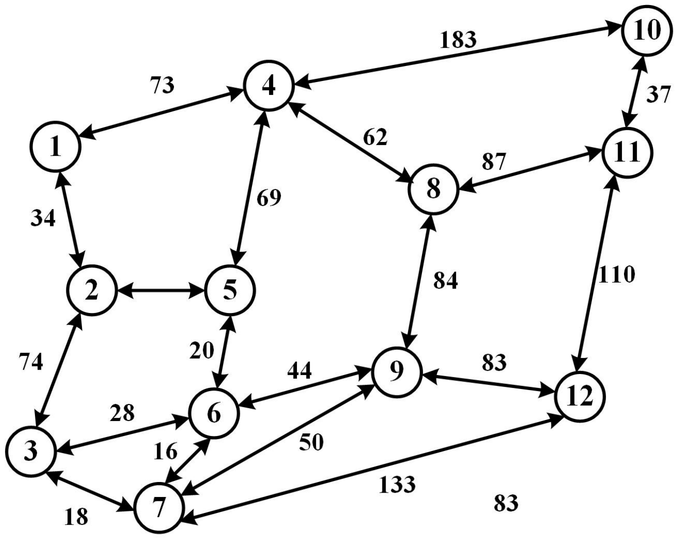

Figure 6.5: Test Network

We simulated the proposed and benchmark techniques on a Finland-12 network. The network comprises 12 nodes and 19 bidirectional MCF links, as shown in Figure 6.5(a). Each MCF link has seven cores, and each core has 320 spectral slots. Here also, the spectral slice granularity is 12.5 GHz. The connection arrival is Poisson-distributed, and the connection service time is exponentially distributed. The bandwidth demand ranges from 50 Gbps to 250 Gbps, and the required spectrum slices are calculated accordingly. Appropriate modulation levels are considered, ranging from BPSK up to 64-QAM. The probability of the arrival of SCT-I, SCT-II and SCT-III are equal. The simulations are run over 20 iterations for 100000 connection requests in a steady-state scenario. A single link failure event is considered, and the time of failure is estimated using the individual link's Mean Time to Failure (MTTF) values.

We have compared the proposed resilient resource provisioning technique with a Link-Disjoint Path Protection (LDPP). In the LDPP, a connection request is provisioned with two routes, primary and backup routes, using the shortest paths and spectral resources available on it.

Connection Blocking Ratio (CBR), Bandwidth Blocking Ratio (BBR), Affected Connec-

Table 6.3: ILP model Parameter Values

CP	CU	CS	W_{max}	W_{min}
3	2	1	2	1

tion Requests (ACR), Affected Bandwidth (ABW), Protection Level and Redundancy are the performance indicators for the proposed technique (PWCG) and the benchmark technique. BBR is the ratio of the amount of blocked bandwidth to total arrived bandwidth requests in the network during simulation. ACR is the average number of connection requests being affected after the occurrence of failure and requiring reprovisioning. ABW gives the total affected bandwidth in (in spectrum slices) active connection requests due to a single link failure. The Protection Level is the percentage of active connection requests protected after the single link failure and given the reconfigured backup routes. Redundancy is the ratio of the reserved spare capacity to the working capacities during the simulation.

6.3.2 Performance Evaluation

Figure 6.6 shows the network performance in different measures. Figure 6.6a and Figure 6.6b record the traffic admissibility of the two techniques using CBR and BBR, and the proposed group-based protection performs better than the LDPP technique. The LDPP technique occupies resources on two routes, the shortest route and the second shortest route, with spectrum slices calculated using appropriate modulation levels. Thus, more blocking is witnessed in the LDPP technique due to the unavailability of spectral resources due to higher redundancy. The blocked services (requests and bandwidth) are within 5% of the total arrived connections in the proposed technique. Figure 6.6c and Figure 6.6d record the protection level and the redundancy required by two protection techniques. LDPP has almost 50% more redundancy than PWCG, which means backup routes use more resources than the primary working route in LDPP. At higher traffic load values, many connection requests are provisioned without protection due to higher redundancy

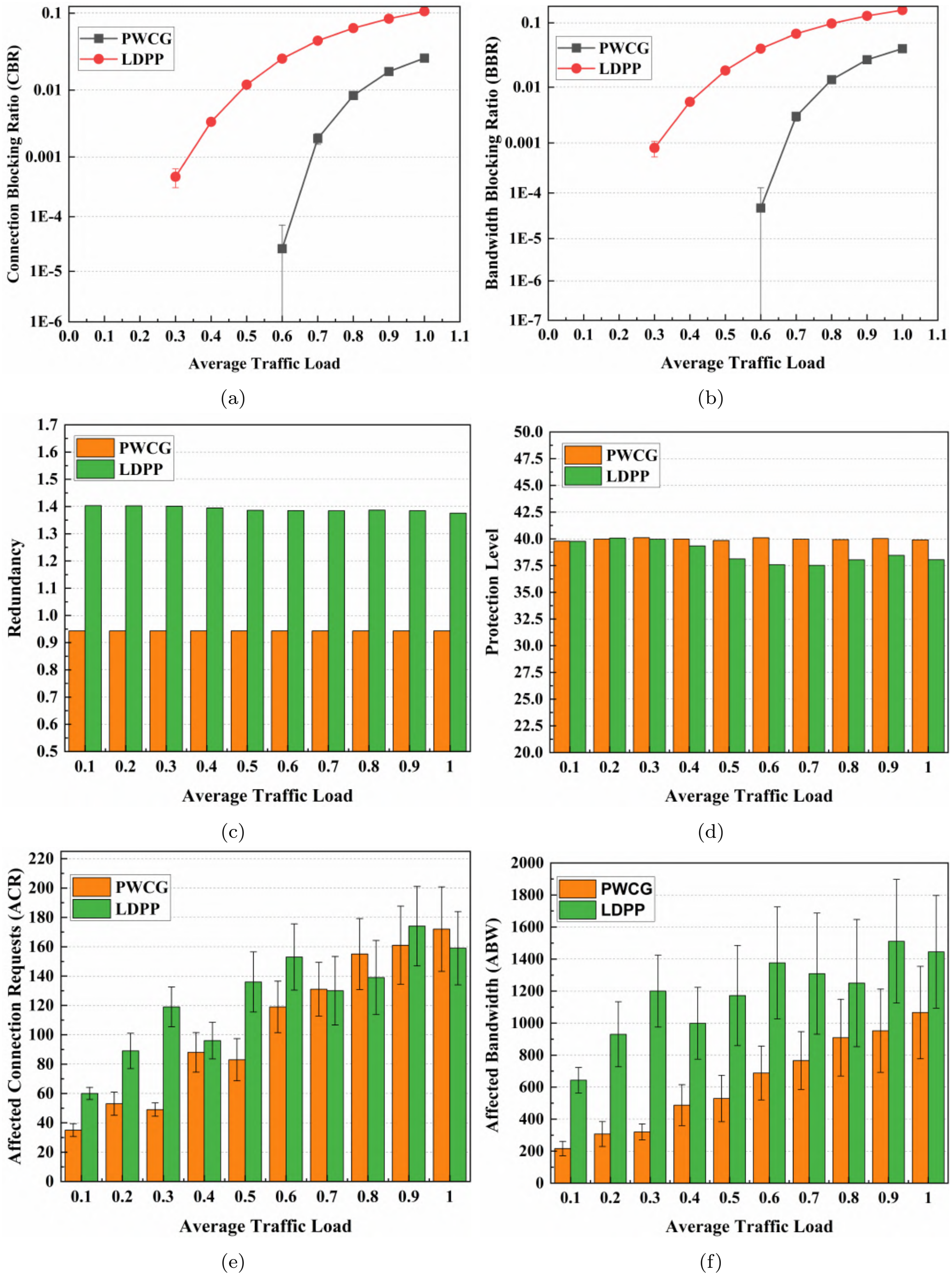

Figure 6.6: Performance Parameters

caused by protected services in LDPP (Figure 6.6c). Due to proper resource grouping, the protection level is more in the PWCG technique.

Figure 6.6e and Figure 6.6f record the impact of single link failures. After the single link failure, the protected connection requests are restored by signalling and switching to backup routes. The unprotected connections of SCT-II, find the backup resources on the fly using complex signalling steps and surviving spectral resources. But, the unprotected connections of SCT-III lose the resources throughout the working route. ACR and ABW values of the LDPP technique are more than the PWCG technique, as most of the active connections are left unprotected due to redundancy.

6.4 Conclusion

In this work, we have considered under-utilized resources due to crosstalk considerations in the MCF of SDM-EONs to provide resilient resource provisioning. The centre-most cores in the circular core arrangement of MCF are the worst affected. We divide the cores into three groups depending on their survivability characteristics using ILP model: Protected, Unprotected and Spare Core Groups. These groups can provide provisioning to three classes of services.

We compared the performance of our Protection Cycles-based PWCG with a Link-disjoint dedicated path protection. The simulation results support our assertions that the proposed technique provides better protection levels and survivability in the event of a single link failure. It also achieves lower blocking of the arriving connection requests than the benchmark technique, making it a resilient provisioning technique.

Chapter 7

Conclusion and Future Scope

7.1 Summary of Research

The optical network capacity is nearly approaching its theoretical limits, despite various efforts to delay it. Capacity-efficient measures are imperative to meet the demands of future bandwidth applications. Over the last two decades, extensive research has been done to improve the spectral and spatial efficiency of the available optical network spectrum. Elastic Optical Networks and Space Division Multiplexed-Elastic Optical Networks are the scions of the existing fixed grid WDM core networks. While these next-generation optical networks scale up the capacity manifolds, they also suffer from a few constraints, which limit their performance to some degree. One such issue is fragmentation in EONs and SDM-EONs. Appropriate management approaches are required to mitigate the effects of fragmentation. It is vital to have information about the level of fragmentation and the network spectrum state to trigger the fragmentation management schemes. **Chapter 2** investigates a Vectored Fragmentation Metric based on two routing constraints in EON. The α-component captures the contiguity of the available spectrum slices in the links, and the *beta*-component captures the continuity of the path segments for a spectrum index. The two-dimensional metric cover the orthogonal aspect of the routing constraints. The proposed metric varies with the network traffic load. It can capture the changes in fragmentation level due to variations in traffic dynamics, like holding time, arrival rate, and bandwidth requirement granularities. Also, the α-component dominates in high traffic load conditions, and the β-component dominates in low traffic conditions. A detailed analysis of all the traffic parameters is presented in this chapter.

Defragmentation is one of the most reliable techniques in curbing performance deterioration due to fragmentation. It is efficient because it is triggered only when required, using Proactive (threshold-based) or Reactive approaches (blocking event-based). Nevertheless, finding the conditions that fulfil the "required " benchmark is crucial. In **Chapter 3**, we proposed a Pro-reactive defragmentation approach. Defragmentation is triggered either when the threshold is crossed or when a connection blocking occurs. The fragmentation level is calculated using the fragmentation-indicating metrics, and the threshold is updated whenever a connection blocking occurs. We evaluated the performance of the proposed defragmentation technique with existing link-based (External Fragmentation, Compactness and Entropy-based) and path-based (Wasted-Unusable-Free Spectrum Ratio) metrics together with our proposed Vectored Fragmentation Metric (AVFM). The proposed defragmentation technique with AVFM as a fragmentation indicator also identifies the fragmentation due to continuity constraints. It helps better fragmentation management in traffic conditions where the probability of arrival of connection requests with longer hop lengths is more than the shorter hop length. We observed that the proposed defragmentation technique using AVFM takes more defragmentation time than other link-based metrics. The frequency of the defragmentation operation when using AVFM is low, but the number of rearrangements is more. Nevertheless, AVFM outperforms the other metrics when considering the blocking ratio of the arriving connection requests.

Since defragmentation is costly, in **Chapter 4**, we proposed penalty-based resource provisioning in EON. Our proposed Routing and Spectrum Assignment with Penalty (RSA-WP) and another Routing and Best Effort Spectrum Assignment (RBESA) technique work well for low-load traffic conditions and improve spectrum utilization. If the appropriate resources are unavailable as per the constraints, the link weights are increased proportionally to the difference between required and available spectrum slices. The main idea is to avoid the links which do not have available spectrum slices for future connection requests. The RBESA admits the connection requests with limited spectral resources, which would have been blocked otherwise. It assigns the maximum available spectrum for that particular request on the selected route and imposes a proportional penalty on the links of the route. The simulation results show that resource provisioning with penalty may perform better than Periodically defragmented resource provisioning (PDF-RSA) for particular network load conditions. Hence, RBESA and RSA-WP could be conveniently used to replace fragmentation-managed resource provisioning under suitable conditions.

Even after using all the fragmentation management techniques and using the available resources most efficiently, the EON can only provide 30% additional capacity in the network link. The rate at which the bandwidth requirement is increasing even this much capacity will seem insufficient. To meet the further capacity demands, the next phase of network upgradation requires enabling the spatial dimension. In this thesis, we discussed Multicore Fibers as the mode of spatial dimension. When the spatial dimension, i.e., Multicore, is introduced in the EON, the usable capacity is scaled up but with the additional constraint of Inter-core Crosstalk. The resource provisioning in SDM-EON requires managing spectral and spatial fragmentation to efficiently utilize the available scaled-up capacity. Next, in **Chapter 5**, we proposed an Adaptive Weights-based resource provisioning technique (AW-DRA), which could become fragmentation aware, crosstalk aware or link congestion aware, according to the link spectrum state. Four critical parameters are identified, Distance, Fragmentation, Crosstalk and Spectral Utilization efficiency, and their corresponding weightage contribute in finding the most appropriate route. A single least-cost route is selected, and the suitable modulation level, core and spectral resources are searched in steps to follow. The parameter weights are updated using the Teaching Learning-based Optimization method to capture the state of the network optimally. The proposed AW-DRA technique is better than the exhaustive K-RCSA and the other specific impairment-aware resource provisioning techniques regarding traffic admissibility and spectral utilization.

The crosstalk avoidance or awareness leads to a considerable wastage of the usable capacity in the SDM-EON. Survivability being an essential contributor to Quality of Service, we have tried to leverage the unusable capacity with the spare capacity needed for protection. In the **Chapter 6**, we have used the equivalent of this crosstalk-affected capacity as

Dedicated Spare Cores to protect a fraction of the remaining cores. The cores are grouped as Unprotected, Protected and Dedicated Spare using an ILP model. The objective of the ILP is to assign the cores to relevant groups cost-efficiently. The resource provisioning in the dynamic traffic scenario provides resources in these groups to three Service Class types. The proposed technique (PWCG-based) provides link protection with more admission of connection requests, spare capacity efficiency and better protection levels than robust link-disjoint path protection.

7.2 Scope of Future Work

- Currently, the α -component of VFM uses the ratio of contiguous spectrum slices to total available spectrum slices. There are many link fragmentation indicators, like the number of fragments. The variations of VFM using these indicators could be used to check the efficacy of the link vs path approach.
- Fragmentation Management on Demand (FMoD) could be a possible investigation area. In the current thesis work, we showed how the Penalty-Based approach works better at low-load traffic, and Pro-reactive defragmentation works better at high-load traffic.
- The network management system and the changes required in the signalling protocols to test the suitability of the proposed techniques need investigation.
- A feasible switch architecture for EON and SDM-EON could be a viable research area.
- The optimization models for the proposed resource provisioning and fragmentation management techniques should be investigated for optimal results.

Bibliography

[1] H. Hopkins, and N. KAPANY, "A Flexible Fibrescope, using Static Scanning," Nature 173, 39–41 (1954). https://doi.org/10.1038/173039b0

[2] Kao K.C., Hockham G.A. Dielectric-fibre surface waveguides for optical frequencies. Proc. IEEE. 1966;113:1151–1158.

[3] Borner, M. "Electro-optical transmission system utilizing lasers." U.S. Patent 3,845,293, issued October 29, 1974.

[4] Kapron FP, Keck DB, Maurer RD (1970) Radiation losses in glass optical waveguides. Appl Phys Lett 17:423–425

[5] Miya T, Terunuma Y, Hosaka T, Miyoshita T (1979) Ultimate low-loss single-mode fiber at 1.55 mm. Electron Lett 15:106–108

[6] C.A. Brackett. "Dense Wavelength Division Multiplexing Networks: Principles and Applications," *IEEE Journal on Selected Areas in Communications*, 8(6):948-964, August 1990.

[7] Chraplyvy A.R., Gnauck A.H., Tkach R.W., Derosier R.M. 8 x 10 Gb/s transmission through 280 km of dispersion-managed fiber. IEEE Photon. Technol. Lett. 1993;5:1233–1235.

[8] Taylor M.G. Coherent detection method using DSP for demodulation of signal and subsequent equalization of propagation impairments. IEEE Photon. Technol. Lett. 2004;16:674–676.

[9] S. Chandrasekhar, X. Liu, B. Zhu, and D.W. Peckham, Transmission of a 1.2-Tb/s 24-carrier no-guard-interval coherent OFDM superchannel over 7200-km of ultra-large-area fiber, in Proc. European Conf. Optical Communication (ECOC) 2009, Sept., paper PD2.6

[10] Winzer P.J., "Energy-efficient optical transport capacity scaling through spatial multiplexing," IEEE Photon. Technol. Lett. 2011;23:851–853

[11] Spectral grids for WDM applications: DWDM frequency grid. https://www.itu.int/rec/T-REC-G.694.1/

[12] See, e.g., press release Huawei's ON2.0 Leads the Commercial Use of All-Optical Networks ... (tagitnews.com/en/article/36282), 2019.

[13] Peter J. Winzer, David T. Neilson, and Andrew R. Chraplyvy, "Fiber-optic transmission and networking: the previous 20 and the next 20 years [Invited]," Opt. Express 26, 24190-24239 (2018)

[14] Uzunidis, Dimitris, Michael Logothetis, Alexandros Stavdas, David Hillerkuss, and Ioannis Tomkos, "Fifty Years of Fixed Optical Networks Evolution: A Survey of Architectural and Technological Developments in a Layered Approach," Telecom 3, no. 4: 619-674, 2022. https://doi.org/10.3390/telecom3040035

[15] The Global Internet Phenomena Report January 2022:Sandvine. https://www.sandvine.com/phenomena

[16] M. Jinno et al., "Demonstration of novel spectrum-efficient elastic optical path network with per-channel variable capacity of 40 Gb/s to over 400 Gb/s," *2008 34th European Conference on Optical Communication*, 2008, pp. 1-2, doi: 10.1109/ECOC.2008.4729581.

[17] G. M. Saridis, D. Alexandropoulos, G. Zervas and D. Simeonidou, "Survey and Evaluation of Space Division Multiplexing: From Technologies to Optical Networks," in *IEEE Communications Surveys & Tutorials*, vol. 17, no. 4, pp. 2136-2156, Fourthquarter 2015, doi: 10.1109/COMST.2015.2466458.

[18] B. J. Puttnam, G. Rademacher, and R. S. Luís, "Space-division multiplexing for optical fiber communications," *Optica*, vol. 8, no. 9, pp. 1186–1203, 2021.

[19] T. Hayashi et al., "Field-Deployed Multi-Core Fiber Testbed," *2019 24th Opto-Electronics and Communications Conference (OECC) and 2019 International Conference on Photonics in Switching and Computing (PSC)*, 2019, pp. 1-3, doi: 10.23919/PS.2019.8818058

[20] Cisco Annual Internet Report (2018-2023). https://www.cisco.com/c/en/us/solutions/collateral/executive-perspectives/annual-internet-report/white-paper-c11-741490.html

[21] Masahiko Jinno, "Elastic Optical Networking: Roles and Benefits in Beyond 100-Gb/s Era," *Journal of Lightwave Technology*, vol. 35, no. 5, pp. 1116-1124, March 2017.

[22] Masahiko Jinno, Hidehiko Takara, Bartlomiej Kozicki, Yukio Tsukishima, Yoshiaki Sone, and Shinji Matsuoka, "Spectrum-efficient and scalable elastic optical path network: Architecture, benefits and enabling technologies", *IEEE Communications Magazine*, vol.47, no. 11, pp.66-73, Nov. 2009.

[23] O. Gerstel, M. Jinno, A. Lord and S. J. B. Yoo, "Elastic optical networking: a new dawn for the optical layer?," *IEEE Communications Magazine*, vol. 50, no. 2, pp. s12-s20, February 2012, DOI: 10.1109/MCOM.2012.6146481.

[24] B.C. Chatterjee, N. Sarma, and E. Oki, "Routing and spectrum allocation in elastic optical networks: a tutorial", *IEEE Commun. Surveys Tuts.,* Vol.17, no.3, pp. 1776-1800, 2015.

[25] Velasco, L., Klinkowski, M., Ruiz, M. et al., "Modeling the routing and spectrum allocation problem for flexgrid optical networks," *Photon Netw Commun* 24, 177–186 (2012). https://doi.org/10.1007/s11107-012-0378-7.

[26] I. Tomkos, S. Azodolmolky, J. Solé-Pareta, D. Careglio, and E. Palkopoulou, "A tutorial on the flexible optical networking paradigm: State of the art, trends, and

research challenges," *in Proceedings of the IEEE*, vol. 102, no. 9, pp. 1317-1337, Sept. 2014, DOI: 10.1109/JPROC.2014.2324652.

[27] S. Yan, J. Kim, X. Wang, and A. Fumagalli, "Spectrum Fragmentation Analysis in a Two-Rate Elastic Optical Link," *in Advanced Photonics 2015*, OSA Technical Digest (online) (Optical Society of America, 2015), paper NeM2F.4.

[28] J. Kim, S. Yan, A. Fumagalli, E. Oki, and N. Yamanaka, "An Analytical Model of Spectrum Fragmentation in a Two-Service Elastic Optical Link," *2015 IEEE Global Communications Conference (GLOBECOM)*, San Diego, CA, 2015, pp. 1-6, DOI: 10.1109/GLOCOM.2015.7417243.

[29] P. D. Choudhury, N. Agarwal and T. De, "A Clique Partitioning Based Spectrum Allocation Strategy in Elastic Optical Networks," *2019 21st International Conference on Transparent Optical Networks (ICTON)*, 2019, pp. 1-3, DOI: 10.1109/ICTON.2019.8840530.

[30] Faezeh Yousefi, Akbar Ghaffarpour Rahbar, Mohsen Yaghubi-Namaad, "Fragmentation-aware algorithms for multipath routing and spectrum assignment in elastic optical networks", *Optical Fiber Technology*, Volume 53, 2019, 102019, ISSN 1068-5200, https://doi.org/10.1016/j.yofte.2019.102019.

[31] H. -L. Liu, L. Lv, Y. Chen and C. Wei, "Fragmentation-Avoiding Spectrum Assignment Strategy Based on Spectrum Partition for Elastic Optical Networks," *in IEEE Photonics Journal*, vol. 9, no. 5, pp. 1-13, Oct. 2017, Art no. 7906413, doi: 10.1109/JPHOT.2017.2739750.

[32] P. M. Moura, N. L. S. d. Fonseca and R. A. Scaraficci, "Fragmentation aware routing and spectrum assignment algorithm," *2014 IEEE International Conference on Communications (ICC)*, 2014, pp. 1137-1142, doi: 10.1109/ICC.2014.6883474.

[33] Bórquez-Paredes, D., Beghelli, A., Leiva, A. et al., "Does fragmentation avoidance improve the performance of dynamic spectrum allocation in elastic optical networks?," *Photon Netw. Commun.*, 35, pp. 287–299, 2018.

[34] Y. Yin, H. Zhang, M. Zhang, M. Xia, Z. Zhu, S. Dahlfort, and S. Yoo, "Spectral and spatial 2D fragmentation-aware routing and spectrum assignment algorithms in elastic optical networks [invited]," *IEEE/OSA J. Opt. Commun. Netw.,* vol. 5, no. 10, pp. A100–A106, 2013.

[35] R. Zhu, Y. Zhao, H. Yang, X. Yu, J. Zhang, A. Yousefpour, N. Wang, and J. P. Jue, "Dynamic time and spectrum fragmentation-aware service provisioning in elastic optical networks with multi-path routing," *Opt. Fiber Technol.,* vol. 32, pp. 13–22, 2016.

[36] Huanlin Liu, Jie Ren, Yong Chen, Junling Hu, Chang Tang, Mingming Tang, "Spectrum slicing-based fragmentation aware routing and spectrum allocation in elastic optical networks", *Optical Switching and Networking*, Volume 45, 2022, 100673, ISSN 1573-4277, https://doi.org/10.1016/j.osn.2022.100673.

[37] Comellas, J., Vicario, L. and Junyent, G., "Proactive defragmentation in elastic optical networks under dynamic load conditions," *Photon Netw Commun* 36, 26–34 (2018).

[38] Amar, D., Le Rouzic, E., Brochier, N. et al. "Spectrum fragmentation issue in flexible optical networks: analysis and good practices," *Photon Netw. Commun.* 29, pp. 230–243, 2015.

[39] T. Takagi et al., "Disruption minimized spectrum defragmentation in elastic optical path networks that adopt distance adaptive modulation," *in Proc. 37th Eur. Conf. Exhibit. Opt. Commun.*, Sep. 2011. (Repeated)

[40] X. Wang, I. Kim, Q. Zhang, P. Palacharla, and M. Sekiya, "A hitless defragmentation method for self-optimizing flexible grid optical networks," *presented at the Eur. Conf. Exhibit. Opt. Commun.*, 2012.

[41] F. Cugini et al., "Push-pull defragmentation without traffic disruption in flexible grid optical networks," *J. Lightw. Technol.*, vol. 31, no. 1, pp. 125-133, Jan. 1, 2013.

[42] B. C. Chatterjee, S. Ba, and E. Oki, “Fragmentation Problems and Management Approaches in Elastic Optical Networks: A Survey,” in *IEEE Communications Surveys and Tutorials*, vol. 20, no. 1, pp. 183-210, Firstquarter 2018, doi: 10.1109/COMST.2017.2769102.

[43] M. Quagliotti, D. Cifuentes Arango, M. Schiano, A. Carena, M. Cantono and V. Curri, “Spectrum fragmentation metrics and their use in optical channel allocation algorithms,” *19th Italian National Conference on Photonic Technologies (Fotonica 2017)*, Padua, 2017, pp. 1-4, DOI: 10.1049/cp.2017.0187.

[44] X. Yu and J.Zhang and Y. Zhao and T. Peng and Y. Bai and D. Wang and X. Lin, “Spectrum Compactness based Defragmentation in Flexible Bandwidth Optical Networks”, *OFC/NFOEC 2012*, paper OTh1A.2, Los Angeles.

[45] A. Rosa, C. Cavdar, S. Carvalho, J. Costa, and L. Wosinska, “Spectrum allocation policy modeling for elastic optical networks,” *High Capacity Optical Networks and Emerging/Enabling Technologies*, Istanbul, 2012, pp. 242-246, DOI: 10.1109/HONET.2012.6421472.

[46] B. C. Chatterjee and E. Oki, “Performance evaluation of spectrum allocation policies for elastic optical networks,” *2015 17th International Conference on Transparent Optical Networks (ICTON)*, Budapest, 2015, pp. 1-4, DOI: 10.1109/ICTON.2015.7193485.

[47] B. C. Chatterjee, N. Kitsuwan and E. Oki, “Performance evaluation of first-last-exact fit spectrum allocation policy for elastic optical networks,” *2017 19th International Conference on Transparent Optical Networks (ICTON)*, Girona, 2017, pp. 1-4, DOI: 10.1109/ICTON.2017.8024851.

[48] J. Bermúdez, A. Lozada, R. Olivares and N. Jara, “Fragmentation-aware spectrum assignment strategies for elastic optical networks with static operation,” *2020 39th International Conference of the Chilean Computer Science Society (SCCC)*, 2020, pp. 1-8, doi: 10.1109/SCCC51225.2020.9281223.

[49] Federico Pederzolli, Domenico Siracusa, Andrea Zanardi, Gabriele Galimberti, Domenico La Fauci, and Giovanni Martinelli, “Path-Based Fragmentation Metric and

RSA Algorithms for Elastic Optical Networks," *Journal of Optical Communications and Networking*, Vol. 11, Issue 3, pp. 15-25, 2019.

[50] L. H. Bonani, M. Forghani-elahabad, and M. L. F. Abbade, "Network Fragmentation Measure in Elastic Optical Networks," *2019 SBFoton International Optics and Photonics Conference (SBFoton IOPC)*, Sao Paulo, Brazil, 2019, pp. 1-5, doi:10.1109/SBFoton-IOPC.2019.8910225.

[51] http://www.opennetworking.org

[52] K. Wen, Y. Yin, D. J. Geisler, S. Chang and S. J. B. Yoo, "Dynamic on-demand lightpath provisioning using spectral defragmentation in flexible bandwidth networks," *2011 37th European Conference and Exhibition on Optical Communication*, 2011, pp. 1-3.

[53] T. Takagi, H. Hasegawa, K. Sato, Y. Sone, A. Hirano and M. Jinno, "Disruption minimized spectrum defragmentation in elastic optical path networks that adopt distance adaptive modulation," *2011 37th European Conference and Exhibition on Optical Communication*, 2011, pp. 1-3.

[54] A. N. Patel, P. N. Ji, J. P. Jue and Ting Wang, "Defragmentation of transparent Flexible optical WDM (FWDM) networks," *2011 Optical Fiber Communication Conference and Exposition and the National Fiber Optic Engineers Conference*, 2011, pp. 1-3.

[55] F. Cugini et al., "Push-pull technique for defragmentation in flexible optical networks," *OFC/NFOEC*, 2012, pp. 1-3.

[56] Rui Wang and Biswanath Mukherjee, "Provisioning in Elastic Optical Networks with Non-Disruptive Defragmentation," *J. Lightwave Technol.*, 31, 2491-2500 (2013).

[57] M. Jinno *et al.*, "Spectrum-efficient and scalable elastic optical path network: Architecture, benefits and enabling technologies", *IEEE Communications Magazine*, vol.47, no. 11, pp.66-73, Nov. 2009.

[58] Paolucci, F., Castro, A., Cugini, F. *et al.*, "Multipath restoration and bitrate squeezing in SDN-based elastic optical networks [Invited]". *Photon Netw Commun* 28, 45–57 (2014). https://doi.org/10.1007/s11107-014-0444-4.

[59] B. C. Chatterjee and E. Oki, "Performance evaluation of spectrum allocation policies for elastic optical networks," *2015 17th International Conference on Transparent Optical Networks (ICTON)*, Budapest, 2015, pp. 1-4, doi: 10.1109/ICTON.2015.7193485.

[60] B. C. Chatterjee, N. Kitsuwan and E. Oki, "Performance evaluation of first-last-exact fit spectrum allocation policy for elastic optical networks," *2017 19th International Conference on Transparent Optical Networks (ICTON)*, Girona, 2017, pp. 1-4, doi: 10.1109/ICTON.2017.8024851.

[61] Forough Shirin Abkenar and Akbar Ghaffarpour Rahbar, "Study and Analysis of Routing and Spectrum Allocation (RSA) and Routing, Modulation and Spectrum Allocation (RMSA) Algorithms in Elastic Optical Networks (EONs)," *Optical Switching and Networking*, Volume 23, Part 1, 2017, Pages 5-39, ISSN 1573-4277, https://doi.org/10.1016/j.osn.2016.08.003.

[62] Sergio Fernández-Martínez, Benjamín Barán, Diego P. Pinto-Roa, "Spectrum defragmentation algorithms in elastic optical networks," *Optical Switching and Networking*, Volume 34, 2019, Pages 10-22, ISSN 1573-4277, https://doi.org/10.1016/j.osn.2019.04.001.

[63] S. Behera and G. Das, "Dynamic Routing and Spectrum Allocation in Elastic Optical Networks with Minimal Disruption," *2020 National Conference on Communications (NCC)*, Kharagpur, India, 2020, pp. 1-5, doi: 10.1109/NCC48643.2020.9056071.

[64] A. N. Khan, H. Yousif Ahmed, M. Zeghid, W. A. Imtiaz and Z. H. Khan, "Link Congestion Aware Proactive Routing for Dynamic Traffic in Elastic Optical Networks," in *IEEE Photonics Journal*, vol. 13, no. 1, pp. 1-15, Feb. 2021, Art no. 7900815, doi: 10.1109/JPHOT.2021.3052650.

[65] Neha Mahala, Ujjwal, Jaisingh Thangaraj, "Weight distributed spectrum allocation in flexible-grid optical networks," *Optik*, Volume 228, 2021, 166171, ISSN 0030-4026, https://doi.org/10.1016/j.ijleo.2020.166171.

[66] Erricson Mobility Report, Q2 2021. https://www.ericsson.com/4a4cd9/assets/local/reports-papers/mobility-report/documents/2021/emr-q2-2021-update.pdf .

[67] Dan M. Marom, Roland Ryf and David T. Neilson, "Chapter 16- Networking and routing in space-division multiplexed systems, " *in Optical Fiber Telecommunications VII*, Editor- Alan E. Willner, Academic Press, Cambridge, Massachusetts, 2020, DOI: 10.1016/B978-0-12-816502-7.00018-X.

[68] P. S. Khodashenas et al., "Comparison of Spectral and Spatial Super-Channel Allocation Schemes for SDM Networks," in *Journal of Lightwave Technology*, vol. 34, no. 11, pp. 2710-2716, 1 June, 2016, DOI: 10.1109/JLT.2016.2551299.

[69] Rubén Rumipamba-Zambrano, Francisco-Javier Moreno-Muro, Jordi Perelló, Pablo Pavón-Mariño and Salvatore Spadaro, "Space continuity constraint in dynamic Flex-Grid/SDM optical core networks: An evaluation with spatial and spectral super-channels," *Computer Communications*, vol. 126, pp. 38-49, 2018, DOI. 10.1016/j.comcom.2018.05.013

[70] Rubén Rumipamba-Zambrano, Jordi Perelló and Salvatore Spadaro, "Route, Modulation Format, MIMO, and Spectrum Assignment in Flex-Grid/MCF Transparent Optical Core Networks," *Journal of Lightwave Technology*, 36, no. 16, pp. 3534-3546, 2018, DOI. 10.1109/JLT.2018.2848199.

[71] H. Tode and Y. Hirota, "Routing, Spectrum, and core and/or mode assignment on space-division multiplexing optical networks [invited]," *in Journal of Optical Communications and Networking*, vol. 9, no. 1, pp. A99-A113, Jan. 2017, DOI: 10.1364/JOCN.9.000A99.

[72] Y. Lei, B. Chen, M. Gao, L. Xiang and Q. Zhang, "Dynamic Routing, Core, and Spectrum Assignment with Minimized Crosstalk in Spatial Division Multiplexing Elastic

Optical Networks," *2018 Asia Communications and Photonics Conference (ACP)*, 2018, pp. 1-3, DOI: 10.1109/ACP.2018.8595895.

[73] J. Zhang, B. Bao, Q. Yao, D. Ren, J. Hu and J. Zhao, "3D Fragmentation Metric and RCSA Scheme for Space Division Multiplexing Elastic Optical Networks," *in IEEE Access*, vol. 8, pp. 201595-201605, 2020.

[74] P. Lechowicz, M. Tornatore, A. Wlodarczyk and K. Walkowiak,"Fragmentation metrics and fragmentation-aware algorithm for spectrally/spatially flexible optical networks," *in Journal of Optical Communications and Networking*, vol. 12, no. 5, pp. 133-145, May 2020, DOI: 10.1364/JOCN.382838.

[75] Y. Zhao, L. Hu, R. Zhu, X. Yu, X. Wang and J. Zhang,"Crosstalk-Aware Spectrum Defragmentation Based on Spectrum Compactness in Space Division Multiplexing Enabled Elastic Optical Networks With Multicore Fiber," *in IEEE Access*, vol. 6, pp. 15346-15355, 2018, DOI: 10.1109/ACCESS.2018.2795102.

[76] S. Trindade and N. L. S. da Fonseca, "Proactive Fragmentation-Aware Routing, Modulation Format, Core, and Spectrum Allocation in EON-SDM," *ICC 2019 - 2019 IEEE International Conference on Communications (ICC)*, 2019, pp. 1-6, DOI: 10.1109/ICC.2019.8762005.

[77] A. Sharma, B. S. Heera, V. Lohani and Y. N. Singh, "Fragmentation-Aware Routing, Core and Spectrum Assignment in Multi-Core Fiber based SDM-EON," *2022 IEEE Workshop on Recent Advances in Photonics (WRAP)*, 2022, pp. 1-2, DOI. 10.1109/WRAP54064.2022.9758155.

[78] R. V. Rao, V. J. Savsani and J. Balic, "Teaching–learning-based optimization algorithm for unconstrained and constrained real-parameter optimization problems," *Engineering Optimization Taylor & Francis*, vol. 44, no. 12, pp. 1447-1462, 2012, DOI. 10.1080/0305215X.2011.652103.

[79] Y.-K. Chen, S.-X. Weng, and T.-P. Liu, "Teaching–Learning Based Optimization (TLBO) with Variable Neighborhood Search to Retail Shelf-Space Allocation," *Mathematics*, vol. 8, no. 8, p. 1296, Aug. 2020, DOI: 10.3390/math8081296

[80] R. Asthana and Y. N. Singh, "Protection and restoration in optical networks," *IEEE Journal of Research*, vol. 50, no. 5, pp. 319-329, Sep-Oct 2004.

[81] Oliveira H, M.N.S., da Fonseca, N.L., "Protection, routing, modulation, core, and spectrum allocation in SDM elastic optical networks," *IEEE Commun. Lett.*, 22(9), 1806–1809 (2018)

[82] MNS Oliveira, H., da Fonseca, N.L., "Routing, spectrum and core assignment algorithms for protection of space division multiplexing elastic optical networks," *J. Netw. Comput. Appl.*, 128, 78–89 (2019)

[83] Tang, F., Shen, G., Rouskas, G.N., "Crosstalk-aware shared backup path protection in multi-core fiber elastic optical networks," *J. LightWave Technol.*, 39(10), 3025–3036 (2021)

[84] Yuanlong Tan et al., "Crosstalk-aware provisioning strategy with Dedicated Path Protection for elastic multi-core fiber networks," *2016 15th International Conference on Optical Communications and Networks (ICOCN)*, 2016, pp. 1-3, doi: 10.1109/ICOCN.2016.7875849.

[85] Zhu, R., Aretor, S., Wang, P., Li, S., Li, L., Lv, P., Xu, M., " Survival multipath energy-aware resource allocation in SDM-EONs during fluctuating traffic," *J. Lightwave Technol.*, (2020), https://doi.org/10.1109/JLT.2020.3043271

[86] Halder, J., Acharya, T., Bhattacharya, U., "On Crosstalk Aware Energy and Spectrum Efficient Survivable RSCA Scheme in Offline SDM-EON," *J Netw Syst Manage*, 30, 6 (2022), DOI: doi.org/10.1007/s10922-021-09614-8

[87] Arun K. Somani, Mani Mina and Ling Li, "On Trading Wavelengths With Fibers: A Cost-Performance Based Study," IEEE/ACM Transactions on Networking, Vol.12., 944 - 951, October 2004.

[88] Zhenrong Zhang, W. . -D. Zhong and S. K. Bose, "Dynamically survivable WDM network design with p-cycle-based PWCE," in IEEE Communications Letters, vol. 9, no. 8, pp. 756-758, Aug. 2005, doi: 10.1109/LCOMM.2005.1496606.

Appendices

Appendix A

Flowcharts for the proposed algorithms (Chapter 4)

A.1 Flowchart I: Routing and Spectrum Assignment with Penalty in Elastic Optical Networks

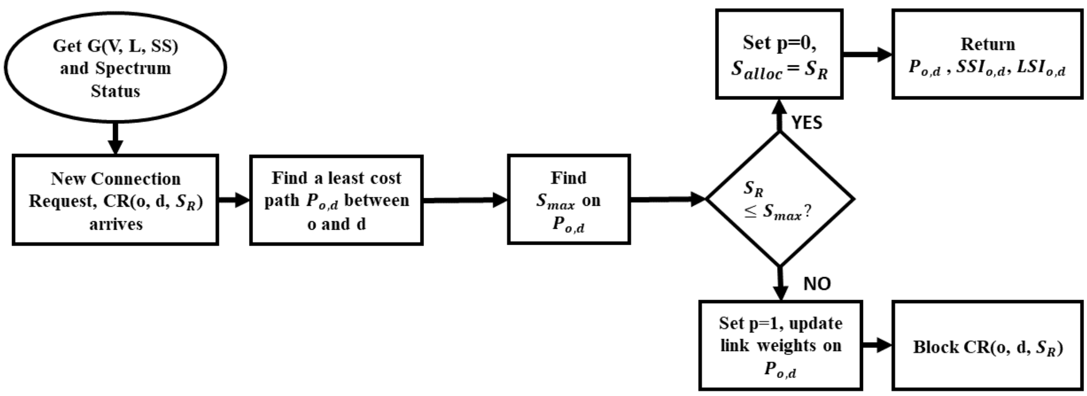

Figure A.1: Flowchart of the RSA-WP technique when a new connection request (CR) arrives in the network.

Description: The flowchart of Algorithm I- RSA-WP, shown in Figure A.1, presents the resource provisioning with penalty technique in Elastic Optical Networks. The RSA-WP algorithm aims to find a path for a connection request even in a fragmented network state. The RSA-WP starts with the arrival of a connection request $CR(o, d, S_r)$, where o is the source node, d is the destination node, and S_r is the number of spectrum slices required by the connection request, calculated using available modulation formats and the length of the paths.

A least-cost path $P(o, d)$ is selected based on the weights of the link. Then, the S_max is checked on the selected path. It returns the path if the S_r is available ($S_r \leq S_{max}$). As the desired number of spectrum slices are available, no penalty is imposed on the links of the path. It also returns the starting slot index ($SSI(o, d)$) and the last slot index ($LSI(o, d)$) of the range of selected spectrum slices. However, if the S_r can not be accommodated on the least-cost path, then a penalty is imposed on all the links of the path $P(o, d)$. p is the binary variable indicating whether a penalty will be imposed on the links. After applying the penalties, the CR is blocked. This technique ensures that future connection requests can use the less fragmented links as required. The penalty is reduced on the links periodically when a certain number of connection requests (NDR) depart and release the occupied resources.

A.2 Flowchart II: Routing and Best Effort Spectrum Assignment in Elastic Optical Networks

Description: The flowchart of Algorithm II- RBESA, shown in Figure A.1, presents the Routing and Best-Effort Spectrum Assignment with penalties in Elastic Optical Networks. The RBESA algorithm aims to find a path with minimum acceptable spectrum resources available for a connection request, even in a fragmented network state. The RSA-WP starts with the arrival of a connection request $CR(o, d, S_r)$, where o is the source node, d is the destination node, and S_r is the number of spectrum slices required by the connection request, calculated using relevant modulation formats and the path lengths.

A least-cost path $P(o, d)$ is selected based on the weights of the link. Then, the S_max is checked on the selected path. It returns the path if the S_r is available ($S_r \leq S_{max}$). As

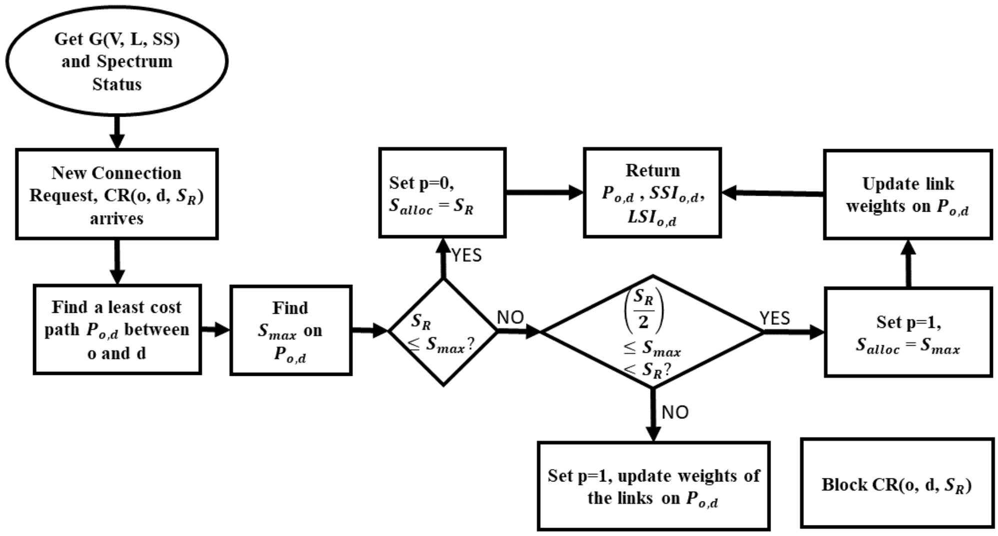

Figure A.2: Flowchart of the RBESA technique when a new connection request (CR) arrives in the network.

the desired number of spectrum slices are available, no penalty is imposed on the links of the path. It also returns the starting slot index ($SSI(o,d)$) and the last slot index ($LSI(o,d)$) of the range of selected spectrum slices. However, if $S_r > S_{max}$, but some $S_{max} \geq \frac{S_r}{2}$ is available, then RBESA should assign it to maximize the admissible traffic. If a compromise in the assigned spectrum slices occurs, the penalty is still applied. In our RBESA study, the incoming traffic with a short holding time is considered, so the possibility of the connection switching to the originally requested slice is not considered for simplicity. If $S_{max} \leq \frac{S_r}{2}$, CR is blocked after applying penalties.

List of Publications

Journals

1. **Anjali Sharma**, Varsha Lohani, and Yatindra Nath Singh, "A Vectored Fragmentation Metric for Elastic Optical Networks," ***Photonic Network Comunications***, 2022.

Conferences

1. **Anjali Sharma**, Baljinder Singh Heera, Varsha Lohani, and Yatindra Nath Singh, " Adaptive Weights-based Dynamic Resource Provisioning in Space Division Multiplexed-Elastic Optical Networks (SDM-EONs)," ***30th International Conference on Software, Telecommunications and Computer Networks***, Split, Croatia, 2022.

2. **Anjali Sharma**, Baljinder Singh Heera, Varsha Lohani, and Yatindra Nath Singh, "Fragmentation-Aware Routing, Core and Spectrum Assignment in Multi-Core Fiber based SDM-EON," ***5th IEEE Workshop on Recent Advances in Photonics***, pp. 01-02, Mumbai, India, 4-6 March, 2022, doi: 10.1109/WRAP54064.2022.9758155.

3. **Anjali Sharma**, Varsha Lohani, and Yatindra Nath Singh, "A Penalty-Based Routing and Spectrum Assignment in Fragmented Elastic Optical Network Spectrum," ***2021 National Conference on Communications (NCC)***, pp. 1-6, 2021, doi: 10.1109/NCC52529.2021.9530071.

4. **Anjali Sharma**, Varsha Lohani, and Yatindra Nath Singh, " Immediate Request vs Book Ahead Request Allocation in Elastic Optical Network," ***ICEIT MCNC-2019***, pp. 1-5, 2019.

List of Publications in Collaboration with Other Group Members

Journals

1. Varsha Lohani, **Anjali Sharma**, Yatindra Nath Singh, "Dynamic Routing and Spectrum Assignment based on the Availability of Consecutive Sub-channels in Flexi-grid Optical Networks," *in IEEE Access*, December 2022. doi: 10.1109/ACCESS.2022.3227438.

Conferences

1. Varsha Lohani, **Anjali Sharma**, Yatindra Nath Singh, "Zone-based Head-Tail Spectrum Allocation in Elastic Optical Network," In ICEIT MCNC 2019, 2019.

2. Varsha Lohani, **Anjali Sharma**, Yatindra Nath Singh, "Routing, Modulation and Spectrum Assignment using an AI based Algorithm," *In 11th International Conference on Communication Systems and Networks (COMSNETS)*, pp. 266-271, Jan 2019.

3. Baljinder Singh Heera, **Anjali Sharma**, Varsha Lohani, Yatindra Nath Singh, "Crosstalk Compliant Routing, Modulation, Core and Spectrum Assignment Techniques in SDM-EON," *presented at IEEE ANTS 2022*, December 2022.

Arxiv Preprint

1. Varsha Lohani, **Anjali Sharma**, Yatindra Nath Singh, "Optimal Slot Size under Various Bandwidth Distributions in the Flexible-grid Optical Networks," *In arXiv preprint arXiv:2112.07831*, Dec 2021. (submitted)

2. Varsha Lohani, **Anjali Sharma**, Yatindra Nath Singh, "Availability-Aware Dynamic RSA with Protection using Consecutive Sub-Channels," *In arXiv preprint arXiv:2206.04933*, June 2022.

Book Chapter

1. Lohani, V., **Sharma, A.**, Singh, Y.N. (2022). Sub-graph p-Cycle Formation for Span Failures in All-Optical Networks. In: Kumar Jain, P., Nath Singh, Y., Gollapalli, R.P., Singh, S.P. (eds) Advances in Signal Processing and Communication Engineering. Lecture Notes in Electrical Engineering, vol 929. Springer, Singapore. https://doi.org/10.1007/978-981-19-5550-110

About the Author

Anjali Sharma received the Bachelor of Engineering (B.E.) degree in Electronics and Communication Engineering from *Chandigarh College of Engineering and Technology, Chandigarh* (Panjab University in 2014). She has completed the Master of Technology (M. Tech.) degree in Electronics and Communication Engineering from *Harcourt Butler Technical University, Kanpur* (Formerly Harcourt Butler Technological Institute), Kanpur, India in December, 2016. She has joined the Doctor of Philosophy (Ph.D.) program in July, 2017. Her current research interests include Design Issues, Resource Provisioning and Resilience Issues in Optical Networks.